

This file is part of the following work:

Greenspan, Sasha Eden (2017) *Thermal thresholds in the amphibian disease chytridiomycosis*. PhD thesis, James Cook University.

Access to this file is available from:

<https://doi.org/10.4225/28/5ac3fc2922b93>

Copyright © 2017 Sasha Eden Greenspan.

The author has certified to JCU that they have made a reasonable effort to gain permission and acknowledge the owner of any third party copyright material included in this document. If you believe that this is not the case, please email researchonline@jcu.edu.au

Thermal thresholds in the amphibian disease chytridiomycosis



Thesis submitted by

Sasha Eden Greenspan

For the degree of Doctor of Philosophy in the
College of Science and Engineering at
James Cook University

November 2017

Title page photographs: *Litoria serrata* outfitted with temperature-sensitive radio-transmitters

Photo credits: Richard Duffy

For my parents, with love and gratitude

Acknowledgments

I am grateful for the support of my supervisory team (Ross Alford, Lin Schwarzkopf, David Pike, and Deborah Bower) and my family and friends. It was a privilege to work with Wayne Morris and Russell Warburton on the fluctuating-temperature incubators; thank you for making this project possible. I am indebted to Lexie Edwards and Richard Duffy for taking on leadership roles in building the incubators and radio-tracking frogs. I could not have done this project without the support of many other research assistants who helped with laboratory and field work, including Jodie Nordine, Kaitlin Creamer, Jenny Cocciardi, Lorenzo Bertola, Nitya Simard, Marnie Smith-Bessen, Brittany Dewdney, Arthit Singtothong, Donald McKnight, Katrin Schmidt, Rachel Duffy, Donna Simmons, Becca Brunner, and Stephen Zozaya. Rebecca Webb was a generous mentor in the lab and faced all the challenges of Chapter 3 alongside me. Betsy Roznik and Lisa Stevenson were generous in allowing me to include their data in my thesis. Gerry Marantelli supplied frogs for infection trials. Dusty Dowse devoted many hours to teaching me time series analyses. Joe Holtum shared his laboratory space with me. Reiner Schuler offered field accommodation at Lamin's Hill Farm. Betsy Roznik and David Pike welcomed me to Australia and introduced me to field work in the Wet Tropics. I am grateful for advice from Sara Bell, Laura Brannelly, Megan Higgie, Natkunam Ketheesan, Smriti Krishna, Alex Roberts, Nadiah Roslan, Yvette Williams, Karen Gerber, Jeffrey Warner, Maria Forzan, Tiffany Kosch, Conrad Hoskin, Doug Woodhams, Heather Neilly, Eric Nordberg, Kiyomi Yasumiba, and Jamie Voyles. I am thankful for technical support from Sue Reilly, Savita Francis, Richard Freeman, Helen Long, Laurie Reilly, and Brynn Greenhill. I would like to acknowledge the financial support of the Australian government, Holsworth Wildlife Research Endowment, and Wet Tropics Management Authority. Finally, I would like to extend special thanks to Deborah Bower for joining my supervisory team and investing so much time, energy, and care into my research and for her many words of encouragement.

Contributions of others

This project was co-supervised by Ross Alford, Lin Schwarzkopf, Deborah Bower, and David Pike. My supervisory team contributed substantially to experimental design and statistical analyses and offered helpful editorial and financial support. The International Postgraduate Research Scholarship program of the Australian Government provided tuition and stipend support. The Australian Research Council provided substantial financial support for my research via grant DP 130101635 to Ross Alford, Lin Schwarzkopf, David Pike, and Rob Puschendorf. The Wet Tropics Management Authority and the Holsworth Wildlife Research Endowment provided additional funding. In addition to my supervisors, Lee Berger, Donna Rudd, Betsy Roznik, Gerry Marantelli, Brett Scheffers, Rebecca Webb, Lexie Edwards, Richard Duffy, Wayne Morris, Russell Warburton, and Lisa Stevenson are co-authors on my published thesis chapters. Their contributions include assistance with experimental design, procurement of research materials, data collection, research infrastructure, data analysis, and editing. Donald McKnight, Steward McDonald, Scott Parsons, and Kiyomi Yasumiba, provided additional statistical support. Wayne Morris provided engineering support and Russell Warburton provided coding support for the fluctuating-temperature chambers that made this project possible. Lexie Edwards, Richard Duffy, and Jodie Nordine provided outstanding technical support for the fluctuating-temperature chambers and field support for frog radio-tracking. Rebecca Webb was a close collaborator on Chapter 3 and devoted many hours to frog blood sampling and molecular analyses. Betsy Roznik, David Pike, Richard Duffy, and Todd Campbell helped with field work for the Appendix. Cesar Australia completed molecular analyses for Chapters 4 and 5. Many people offered technical assistance and advice; they are named in the acknowledgments.

Ethics statement

All research involving live animals was carried out under James Cook University ethics permits A1991 (chapter 3), A2234 (chapter 4 & 5), A2121 (chapter 6), and A2023 (Appendix I). Fieldwork was carried out under Queensland Department of Environment and Heritage Protection permits WITK1526214 (chapter 6) and WITK14585514 (Appendix I).

Copyright statement

Every reasonable effort has been made to gain permission and acknowledge the owners of copyright material. I would be pleased to hear from any copyright owner who has been omitted or incorrectly acknowledged.

General abstract

Recent emergences of fungal diseases have caused catastrophic global losses of biodiversity and temperature strongly influences many host-fungus associations. Ectothermic host body temperatures fluctuate diurnally, seasonally, and annually, but our understanding of the effects of host temperature variability on disease development remains incomplete. My thesis focuses on the effects of host temperature variation on interactions between frog hosts and the widely distributed fungal parasite *Batrachochytrium dendrobatidis* (Bd), which causes the disease chytridiomycosis. I first designed and validated a set of economical, fluctuating-temperature chambers (Chapter 2) that forms the core research infrastructure for four laboratory experiments (Chapters 3–6). Chapter 3 compares frog immune responses after **temperature shifts** (increases and decreases). Cold-acclimated frogs treated with a dose of Bd and a temperature increase had active immune systems before and after treatment. In contrast, hot-acclimated frogs treated with a dose of Bd and a temperature decrease had active immune systems only after treatment and had higher Bd burdens than the cold-acclimated frogs. My results suggest that cold acclimation may prime the immune system for some challenges of infection and help to explain the observation that susceptibility to Bd tends to be lower after temperature increases than after temperature decreases. In Chapter 4, I demonstrate that heavy Bd infections increased the **heat sensitivity** of frog hosts. In ectotherms, behaviors that elevate body temperature may decrease parasite performance or increase immune function, thereby reducing infection risk or the intensity of existing infections. My results suggest that increased heat sensitivity from infections may at times discourage these protective behaviors, tipping the balance in favor of the parasite. Chapters 5–6 center on effects of **diurnal temperature variability** on Bd growth and the course of Bd infections. In the Australian Wet Tropics species *Litoria serrata*, daily body temperatures may regularly exceed the thermal optimum of the fungus, so I focus on effects of these ‘heat spikes.’ In Chapter 5, I exposed Bd cultures and Bd-infected frogs to thermal regimes representing **population medians of** body temperatures and of daily heat spikes experienced by *L. serrata*. Compared to cool constant-temperature control treatments, Bd grew more slowly in the heat spike treatments and frogs that experienced heat spikes developed Bd infections more slowly, were less likely to exceed lethal infection intensities, and were more likely to clear infections. In Chapter 6, I examined the field body temperature regimes of **individual** *L. serrata* and exposed Bd cultures to heat spike treatments representing individual frogs. My data revealed evidence that *L. serrata* appear to thermoregulate. In uplands in

summer and in lowlands in winter, most frogs regularly elevated their body temperatures above the thermal optimum range for Bd. In contrast, frogs appeared unable to reach such elevated temperatures in uplands in winter. These results are consistent with the previous finding that prevalence of Bd in the Wet Tropics tends to be highest in winter at elevations above 400 m, but for the first time, I linked population-level seasonal and elevational patterns in infection prevalence to host body temperature at the scale of the individual frog. In addition, growth of Bd cultures was highly responsive to temperature regimes reproducing the fluctuating body temperatures of individual frogs. Overall, this thesis highlights the direct effects of temperature variability on the course and outcome of Bd infections and underscores the importance of *individual* body temperatures and thermoregulatory behaviors, in addition to population averages, in predicting climate-dependent chytridiomycosis dynamics. Understanding the effects of temperature variability on host-pathogen interactions will remain critical as we continue to confront the realities of the effects of anthropogenic climate change on biodiversity.

Table of contents

Acknowledgments	iii
Contributions of others	iv
Ethics statement.....	v
Copyright statement	vi
General abstract	vii
Table of contents.....	ix
List of tables	xii
List of figures	xiv
Chapter 1 General introduction	1
1.1 Amphibian chytridiomycosis	1
1.2 Temperature and Bd	2
1.3 Aims of thesis	5
1.4 Structure of thesis	6
Chapter 2 Low-cost fluctuating-temperature chamber for experimental ecology.....	7
2.1 Abstract	8
2.2 Introduction.....	9
2.3 Methods	9
Chamber	9
Microcontroller	10
Modifications.....	10
Operation	13
Validation	17
2.4 Results	23
2.5 Discussion	23
2.6 Highlights.....	27
Chapter 3 White blood cell profiles in amphibians help to explain disease susceptibility following temperature shifts.....	28
3.1 Abstract	29
3.2 Introduction.....	30
3.3 Methods	32
Study animals	32
Bd cultures and inoculations	33
Experimental treatments	33
Frog husbandry and infection monitoring	36

Blood collection.....	36
Statistical analysis.....	38
3.4 Results	38
3.5 Discussion	46
3.6 Highlights.....	49
Chapter 4 Infection increases vulnerability to climate change via effects on host thermal tolerance	50
4.1 Abstract	51
4.2 Introduction.....	52
4.3 Methods	53
Acclimation temperature treatments	53
Bd cultures and inoculations	56
Frog disease monitoring and husbandry.....	57
CT _{max} measurement and statistical analysis.....	57
4.4 Results	59
4.5 Discussion.....	65
4.6 Highlights.....	73
Chapter 5 Realistic heat pulses protect frogs from disease under simulated rainforest frog thermal regimes	74
5.1 Abstract	75
5.2 Introduction.....	76
5.3 Methods	78
Temperature treatments	78
Bd cultures.....	81
In vivo experimental infection trial	81
In vitro Bd population growth trial.....	83
Predicting Bd growth potential	84
Statistical analysis.....	87
5.4 Results	87
5.5 Discussion.....	97
5.6 Highlights.....	100
Chapter 6 Experimental evidence that field body temperatures influence disease dynamics in an ectotherm.....	101
6.1 Abstract	102
6.2 Introduction.....	103

6.3 Methods	105
Radio-tracking frogs	105
Bd growth trial.....	106
6.4 Results	113
Frog body temperature variation in nature	113
Performance of Bd in individual frog temperature regimes	116
6.5 Discussion	116
6.6 Highlights.....	120
Chapter 7 General summary	121
References.....	125
Appendix Robust calling performance in frogs infected by a deadly fungal pathogen	145
A.1 Abstract	146
A.2 Introduction	147
A.3 Methods.....	148
Study Species and Site.....	148
Field sampling.....	149
DNA extraction and PCR.....	150
Call attributes and statistical analysis	150
A.4 Results.....	152
A.5 Discussion.....	160

List of tables

Table 2.1 Example of a fluctuating-temperature scheme (a) and schedule (i.e., real-time version of the scheme; b) used to program an economical, Arduino-based, fluctuating-temperature chamber..... 16

Table 4.1 Summary of analyses of covariance on the effects of *Batrachochytrium dendrobatidis* infection status, infection intensity, elevation, (high [15°C] vs. low [18°C] acclimation treatments), heat exposure (pulse [26°C or 29°C for four hours per day] vs. constant acclimation treatments) and the interactions between infection and acclimation on two metrics of the critical thermal maximum (temperature at onset of spasms and temperature at loss of righting response) for the model amphibian host *Litoria spenceri*, with frog snout-urostyle length as a covariate. 60

Table 4.2 Average critical thermal maxima for the model amphibian host *Litoria spenceri* with and without infections by the fungus *Batrachochytrium dendrobatidis* and average infection intensities of the infected individuals. 62

Table 4.3 Review of studies on the effects of infections on upper thermal tolerance in animal hosts. 67

Table 5.1 Summary of the results of linear mixed effects models. We modelled the effects of elevation (high [15°C] vs. low [18°C] elevation treatments), heat exposure (heat pulse temperature treatments [26°C or 29°C for four hours per day] vs. constant cool temperature treatments [15°C or 18°C]), and their interactions on log-transformed *Batrachochytrium dendrobatidis* infection loads (number of zoospore genome equivalents detected on swabs) in the model host *Litoria spenceri*. We included day of swabbing event (4 d, 12 d, 20 d, 28 d, 36 d) as an additional interactive fixed effect and replicate (1–6) as well as frog (1–3) within temperature-controlled chamber (1–4) as random effects. We also modelled the effects of elevation, duration of daily heat exposure (0 h, 1 h, 4 h, 7 h), and their interactions on four in vitro population growth parameters for *Batrachochytrium dendrobatidis*, including replicate (1–3) as a random effect. The four population growth parameters were lag duration (time preceding the exponential growth phase), maximum slope of the exponential growth phase, maximum height of the growth curve, and area under the curve..... 89

Table 5.2 Mean (\pm SD) and maximum *Batrachochytrium dendrobatidis* infection loads (zoospore genome equivalents detected on swabs) on individuals of the model host *Litoria spenceri* after 36 days of exposure to four temperature treatments: low elevation constant

(18°C), low elevation heat pulse (18°C with daily 4-h heat pulses of 29°C), high elevation constant (15°C), and high elevation heat pulse (15°C with daily 4-h heat pulses of 26°C)..... 91

Table 6.1 Summary of body temperature regimes of *Litoria serrata* in the Australian Wet Tropics. 115

Table A.1 Call attributes, body temperatures, body sizes, and body condition indexes of common mistfrogs, *Litoria rheocola*, with and without infections by the fungus *Batrachochytrium dendrobatidis*. 153

Table A.2 Candidate models of the effects of frog body temperature and body (snout-urostyle) length on the advertisement call attributes of common mistfrogs, *Litoria rheocola*..... 154

Table A.3 Summary of the importance of components and axis loadings in a principal component analysis of adjusted advertisement call attributes of common mistfrogs, *Litoria rheocola*. We adjusted the data by removing the effects of frog body temperature and body (snout-urostyle) length from the 157

Table A.4 Summary of multivariate analysis of covariance and canonical correlation analysis of the effects of *Batrachochytrium dendrobatidis* infections on adjusted advertisement call attributes of common mistfrogs, *Litoria rheocola*. We adjusted the data by removing the effects of frog body temperature and body (snout-urostyle) length from the data for each frog. The adjusted call attributes included in each analysis as dependent variables were call duration, pulse rate, dominant frequency, call rate, and inter-call interval..... 159

List of figures

Figure 2.1 Schematic of Arduino UNO microcontroller and electronic components for an economical fluctuating-temperature chamber..... 12

Figure 2.2 Outline of temperature control task sequence for an economical fluctuating-temperature chamber operated with an Arduino UNO microcontroller. 14

Figure 2.3 For an economical fluctuating-temperature chamber operated with an Arduino UNO microcontroller, (a) the temperature scheme used to measure maximum rates of heating and cooling and (b) maximum rates of heating and cooling over 5°C temperature intervals..... 18

Figure 2.4 For an economical fluctuating-temperature chamber operated with an Arduino UNO microcontroller, (a) a target temperature scheme used to measure reliability of temperature control for exact, real-world temperature regimes recorded in the field, (b) the actual chamber temperatures during the reliability trial, logged once per minute for seven days, and (c) the linear regression comparing actual chamber temperatures to target temperatures during the seven-day reliability trial. Gray dots = actual temperatures. Solid line = slope of 1. Dashed line = regression line. 19

Figure 2.5 For an economical fluctuating-temperature chamber operated with an Arduino UNO microcontroller, (a) a target temperature scheme used to measure reliability of temperature control for arbitrarily fluctuating temperature regimes, in this case a sine wave fluctuating between 10-25°C over 24 hours, (b) the actual chamber temperatures during the reliability trial, logged once per minute for 30 days (only the first ten days are shown), and (c) the linear regression comparing actual chamber temperatures to target temperatures during the 30-day reliability trial. Gray dots = actual temperatures. Solid line = slope of 1. Dashed line = regression line. 21

Figure 2.6 For an economical fluctuating-temperature chamber operated with an Arduino UNO microcontroller, (a) the target temperature schemes used to measure reliability of temperature control for constant temperature regimes, (b) the actual chamber temperatures during the reliability trials, logged once per minute for 30 days, and (c) boxplots summarizing actual chamber temperatures during the 30-day reliability trials. We used a unique chamber/microcontroller setup for each constant target temperature trial..... 22

Figure 2.7 Laboratory setup with 48 economical, fluctuating-temperature chambers, each operated by an Arduino UNO microcontroller. 26

Figure 3.1 Configuration of temperature-controlled chambers. 35

Figure 3.2 Representative micrographs of each WBC type (marked with arrowheads). Lymphocyte (a), neutrophil (b), basophil (c), monocyte (d), eosinophil (e). Bar = 10 μm 37

Figure 3.3 (a) Average of logged Bd zoospore equivalents (\pm SD) in *Litoria caerulea* housed at 21°C but acclimated to 26°C (pink) or 16°C (blue) prior to inoculation. (b) Actual zoospore equivalents for reference. 40

Figure 3.4 Bootstrapped descriptive statistics for the white blood cell profiles of 16°C-acclimated, 26°C-acclimated, and free-ranging (Young et al. 2012) *Litoria caerulea*. 41

Figure 3.5 Relative percentages of circulating lymphocytes, neutrophils, and basophils for *Litoria serrata* at baseline (housed at 16°C or 26°C) and at three time intervals post-treatment (shifted to 21°C). A treatment group was inoculated with *Batrachochytrium dendrobatidis* after baseline white blood cell profiles were recorded (a-c). A control group was sham-inoculated and remained uninfected (d-f). 43

Figure 3.6 Number of microscope fields examined to identify 200 white blood cells (WBC) in blood smears from *Litoria serrata* housed at 21°C from four infection status (*Batrachochytrium dendrobatidis* [Bd]-infected vs. uninfected) X thermal history (16°C vs. 26°C) treatments at two time intervals post-inoculation. We used this metric as an estimate of the relative concentration of WBCs in the blood; the higher the number of microscope fields, the lower the concentration of WBCs. 45

Figure 4.1 Daily acclimation temperature regimes for experiment investigating the effects of *Batrachochytrium dendrobatidis* infection status, infection intensity, and thermal acclimation on the upper thermal tolerance of the model amphibian host *Litoria spenceri*. (A) daily rectangular wave with trough at 15°C and crest at 26°C for four hours, (B) constant 15°C, (C) daily rectangular wave with trough at 18°C and crest at 29°C for four hours, (D) constant 18°C. 55

Figure 4.2 Average critical thermal maxima (\pm SE) for the model amphibian host *Litoria spenceri* acclimated to four temperature treatments, with and without infections by the fungus *Batrachochytrium dendrobatidis*. Metrics of the critical thermal maximum were (A) body temperature at onset of spasms and (B) body temperature at loss of righting ability. 61

Figure 4.3 *Batrachochytrium dendrobatidis* infection intensities at the time of measuring the critical thermal maxima of infected *Litoria spenceri* acclimated to four temperature treatments. Dashed line indicates an infection intensity threshold above which frogs were estimated to be at high risk for morbidity and/or mortality from infection. 64

Figure 4.4 The tolerance mismatch hypothesis predicts that infection risk will decrease as the difference in the thermal tolerance of the host and pathogen (tolerance mismatch) increases. This schematic illustrates the potential effects of parasitic infection on tolerance mismatch for disease systems in which the thermal tolerance of hosts exceeds that of the parasite. Consider a host with a thermal tolerance represented by the gray dotted line. If it becomes infected, its upper thermal tolerance may be reduced (blue dotted line), decreasing tolerance mismatch (blue bar). The host is now more likely to occupy microhabitats (blue performance curve) that are favorable for the parasite, at the expense of protective thermoregulatory behaviors. In rare cases, infections might increase (red dotted line) or have no effect (gray dotted line) on thermal tolerance, thus expanding (red bar) or maintaining (gray bar) the magnitude of thermal mismatch. 70

Figure 5.1 Daily temperature treatments for experiment investigating effects of daily heat pulses on in vitro growth of *Batrachochytrium dendrobatidis* (Bd; a–h) and on in vivo Bd infection dynamics in a model amphibian host (b, d, f, h). We generated temperature treatments with body temperature data from *Litoria serrata* in high-elevation (blue gradient; a–d) and low-elevation (red-orange gradient; e–h) rainforests of the Australian Wet Tropics. 80

Figure 5.2 In vitro population growth potential for *Batrachochytrium dendrobatidis* (Bd) under experimental temperature treatments. We generated thermal performance curves for three Bd isolates (a) based on published constant-temperature population growth curves (Stevenson et al. 2013). Solid lines (b–g) indicate growth potential based on the hourly temperatures of our treatments (cumulative thermal performance for each hourly temperature). Dashed lines (B–G) indicate growth potential for hypothetical constant-temperature treatments representing the average daily temperature of each heat pulse treatment. 86

Figure 5.3 *Batrachochytrium dendrobatidis* infection loads (log-transformed zoospore genome equivalents detected on swabs) on the model host *Litoria spenceri* over 36 d of exposure to four temperature treatments. Heavy lines in each box indicate the median value, boxes indicate the 1st and 3rd quartiles, and whiskers indicate the range of the data. The dashed line marks an infection level at which odds predicted morbidity or mortality from chytridiomycosis. Note that over time most frogs gradually exceeded the threshold for morbidity or mortality except those from the low elevation heat pulse treatment, and both low and high elevation heat pulse treatments took longer to approach or exceed this threshold. 90

Figure 5.4 Survival probabilities of groups of *Batrachochytrium dendrobatidis*-infected *Litoria spenceri* exposed to four temperature treatments, estimated with a Cox Proportional Hazards

analysis. In this analysis, time until death is the typical response. Instead, we used number of days until frogs reached a threshold infection intensity of 13,700 ZGE as a proxy for death. A receiver operating characteristic (ROC) analysis (Stockwell et al. 2016) for the first 43 days of the experiment (1 frog died and 14 frogs had shown signs of chytridiomycosis by this time) indicated that frogs with infection loads >13,700 zoospore genome equivalents (ZGE) had a 63% chance of dying or showing signs of chytridiomycosis. This level of infection has also been linked to development of lethal chytridiomycosis in other species (Briggs et al. 2010;

Vredenburg et al. 2010; Kinney et al. 2011). 93

Figure 5.5 Average population growth over 7 d for *Batrachochytrium dendrobatidis* exposed to experimental temperature treatments. Treatments represent body temperature regimes of *Litoria serrata* in high-elevation rainforests (blue gradient) and low-elevation rainforests (red-orange gradient) of the Australian Wet Tropics. 95

Figure 5.6 Characteristics of population growth curves for *Batrachochytrium dendrobatidis* exposed to experimental temperature treatments. Treatments represent body temperature regimes of *Litoria serrata* in high-elevation rainforests (blue gradient) and low-elevation rainforests (red-orange gradient) of the Australian Wet Tropics and differ in the duration of heat pulses (0 h, 1 h, 4 h, 7 h; darker colours correspond to longer heat pulses). The growth curve parameters were lag duration (time preceding the exponential growth phase), maximum slope of curve, maximum height of curve, and area under curve. Each symbol represents the least square mean of the population growth parameter calculated with linear mixed effects models. Different symbols indicate statistically significant pairwise differences determined with general linear hypothesis tests (glht function in Program R)..... 96

Figure 6.1 In vitro *Bd* growth trial. (a–c) Temperature treatments. (d) Predicted growth for each treatment. (e) Average observed growth for each treatment. (f) Frequencies of temperatures for each treatment. (g–j) Characteristics of *Bd* population growth curves for each treatment. Growth curve parameters were (g) lag duration (time preceding the exponential growth phase), (h) maximum slope of curve (representative of the maximum rate of exponential growth), and two measures of total growth: (i) maximum height of the curve and (j) area under the curve. Each symbol represents the least square mean of the population growth parameter calculated with linear mixed effects models. Different symbols indicate statistically significant pairwise differences determined with general linear hypothesis tests.

..... 107

Figure 6.2 Representative temperature regimes for *Litoria serrata* recorded with temperature-sensitive radio-transmitters in the Australian Wet Tropics. Regimes are grouped by season, elevation, and tracking period. Within tracking periods, preliminary non-metric multidimensional scaling analyses ordinated the thermal regimes by maximum temperature, so for the purposes of describing variation in the individual thermal regimes that we recorded, we grouped regimes according to four temperature categories relevant to Bd growth: maximum temperature 15.1–20°C, 20.1–25°C, 25.1–29°C, and >29°C. Each plot corresponds to a line in Table 6.1. Up to three representative regimes are displayed for each group and the total sample size of each group is given at the bottom right of each plot. Gray polygons delineate the temperature categories relevant to Bd growth, with darker shades indicating higher growth rates. Green (air temperature) and blue (water temperature) represent ambient conditions recorded with waterproofed temperature dataloggers (Roznik and Alford 2012) at each site. 108

Figure A.1 Relationships between frog body temperature or frog body (snout-urostyle) length and advertisement call attributes for the common mist frog, *Litoria rheocola*. Intercall interval values were log₁₀-transformed..... 155

Figure A.2 Biplot showing the relationships between adjusted advertisement call attributes of common mistfrogs, *Litoria rheocola*, and illustrating the location of each individual data point in principal component space. We adjusted the data by removing the effects of frog body temperature and body (snout-urostyle) length from the data for each frog. Principal components 1 and 2 accounted for 70% of the variability in call attribute data (Table 3). The length and direction of each arrow correspond to the loading of each adjusted call attribute on the first two principal axes (Table 4). Symbols indicate frog infection status (infected [+] or uninfected [o]). Interspersion of the symbols suggests that infected and uninfected frogs do not differ in call attributes commonly linked to mate choice..... 158

Chapter 1 General introduction

1.1 Amphibian chytridiomycosis

Disease-induced extinctions and population collapses of bats, bees, corals, frogs, salamanders, and snakes have driven emerging fungal pathogens to the forefront of conservation science worldwide (Fisher et al. 2012; Cabañes et al. 2014). One of the most widely pervasive wildlife mycoses is chytridiomycosis, which is caused by fungi in the genus *Batrachochytrium* (Nichols et al. 1998; Longcore et al. 1999; Pessier et al. 1999).

Chytridiomycosis is a principal causal factor in contemporary global declines and extinctions of hundreds of amphibian species, the majority of which are anurans (Laurance et al. 1996; Daszak et al. 2003; Skerratt et al. 2007; Wake and Vredenburg 2008). In the 1970s–2000s, epidemic outbreaks of chytridiomycosis led to mass amphibian mortalities and extinctions in the Australian Wet Tropics (Laurance et al. 1996; Woodhams and Alford 2005), the Pyrenees of Spain (Bosch et al. 2001), the Andes of South America (Ron and Merino 2000; Bonaccorso et al. 2003; Catenazzi et al. 2011), the Cordillera Central of Central America (Berger et al. 1998; Lips 1999; Brem and Lips 2008), and the Sierra Nevada of California (Fellers et al. 2001; Fellers et al. 2007; Vredenburg et al. 2007). The causal agent of these mortality events is *B. dendrobatidis* (hereafter 'Bd'; Longcore et al. 1999). First described in 1999, Bd has been detected in more than 500 amphibian species from more than 40 families and occurs in at least 52 countries (Longcore et al. 1999; Olson et al. 2013).

Batrachochytrium species are members of the chytrids, a group of simple-bodied, microscopic fungi distinguished by the production of motile asexual spores (zoospores). Chytrids occur in open water and moist soils of terrestrial, freshwater, and marine ecosystems (Longcore et al. 1999; Klein 2006). Most chytrids are saprophytes (i.e., derive nutrients from dead or decaying organic matter), such as *Homolaphlyctis polyrhyza*, the closest known relative of *Batrachochytrium* (James et al. 2006). Other chytrids are pathogens of plants, algae, protists, and invertebrates (Powell 1993). The genus *Batrachochytrium* is unique among chytrids in its ability to parasitize vertebrates (Longcore et al. 1999; Martel et al. 2013).

In post-metamorphic amphibians, *Batrachochytrium* invades the superficial epidermis. Invasion begins when a zoospore encysts (i.e., adheres to the skin surface, retracts the flagellum, and forms a cell wall) and produces a germination tube that penetrates several layers of host epidermal cells and channels the contents of the zoospore cyst into a host cell (Greenspan et al. 2012). Over a period of several days, this accumulation of fungal material forms a stationary life stage called a zoosporangium in which a new generation of zoospores is

asexually produced (Berger et al. 2005a). Zoosporangia mature at the same pace as the host molts its epidermal cells and thus reach the outermost skin layer coincident with formation of discharge tubes that release new zoospores onto the host's skin surface and into the environment (Berger et al. 2005a). In early-stage infections, zoosporangia are often clustered in the skin, suggesting fungal population growth by repeated local re-infections (Berger et al. 2005a; Carey et al. 2006; Puschendorf and Bolanos 2006). The infection typically proliferates sub-clinically for weeks to months in susceptible hosts (Woodhams et al. 2003; Berger et al. 2004; Woodhams et al. 2007a). Chytridiomycosis develops when fungal population growth progresses unchecked, eventually reaching a critical density in host skin cells (Carey et al. 2006; Vredenburg et al. 2010). Past this threshold, damage to the skin layers causes loss of water and electrolyte equilibrium and eventual death from cardiac arrest (Voyles et al. 2007; Voyles et al. 2009; Carver et al. 2010; Marcum et al. 2010; Campbell et al. 2012; Wardziak et al. 2013).

The oldest Bd-positive museum specimens predate the recent emergence of chytridiomycosis by more than 100 years, indicating that the pandemic was not the result of a newly evolved relationship between Bd and amphibians (Goka et al. 2009; Rodriguez et al. 2014; Talley et al. 2015). On the contrary, Bd lineages (i.e., groups of isolates that cluster genetically) originating from Africa, Asia, Brazil, and Europe exhibit attenuated virulence and are considered endemic to these regions (Walker et al. 2008; Goka et al. 2009; Farrer et al. 2011; Bai et al. 2012; Schloegel et al. 2012; Dahanukar et al. 2013; Bataille et al. 2013). Genome sequencing suggests that Bd could have been endemic in some parts of the world for millennia (Rosenblum et al. 2008; Joneson et al. 2011; Rosenblum et al. 2013). In contrast, the epicentres of the pandemic (parts of the Americas and Europe, and Australia) may have been previously naïve to Bd, with introductions of the fungus probably attributable to the unregulated global trade of amphibians (Mazzoni et al. 2003; Schloegel et al. 2010; Schloegel et al. 2012). These outbreaks are associated with a specific lineage of Bd, termed the global panzootic lineage (BdGPL; e.g., Piovio-Scott et al. 2014). BdGPL is unique in its high virulence. This lineage has probably replaced many undescribed endemic lineages of Bd in addition to invading Bd-naïve regions across the globe (Schloegel et al. 2012).

1.2 Temperature and Bd

Temperature can strongly affect the population growth of Bd. In pure culture, optimal short-term growth of Bd occurs at 13-25°C (reviewed by Stevenson et al. 2013). Within this range, the fungus can adapt physiologically to optimize growth under predictable daily

temperature fluctuations (Raffel et al. 2013) and exhibits the fastest exponential growth rates when fluctuating temperature regimes reach the warmest optimal temperatures (Stevenson et al. 2014). At below-optimal temperatures, the fungus grows slowly but may still be virulent by trading off slower growth rates for increased fecundity (Woodhams et al. 2008; Stevenson et al. 2013) and zoospore longevity (Voyles et al. 2012). The lethal thermal maximum of Bd in constant-temperature environments is 26–29°C, depending on the isolate (Stevenson et al. 2013). In the field, host populations in warm, dry forests (dry substrate temperatures $\geq 30^\circ\text{C}$ for at least one hour when frogs are active on land; Daskin et al. 2011) can persist even when infection prevalence is high (Puschendorf et al. 2011). In these ‘environmental refuges’, host populations do not appear to possess inherent resistance or tolerance mechanisms but rather to survive with low infection intensities because of environmental checks on pathogen growth (Daskin et al. 2011; Puschendorf et al. 2011). In contrast, the fungus thrives under cool field conditions (15–25°C) and has thus taken a disproportionately high toll on amphibian populations in montane rainforests (Skerratt et al. 2007; Lips 2016). In the Wet Tropics region of Queensland, Australia, Bd has been linked to population declines of at least eight frog species (McDonald and Alford 1999; Alford 2010), including the apparent extinction of *Litoria nyakalensis*. Populations of some species disappeared from upland rainforests (> 400 m) but persisted in lowland rainforests (McDonald and Alford 1999; Alford 2010). In species that have since recovered or recolonized the uplands and are now distributed at a range of elevations, the prevalence of Bd still tends to be highest at high elevations and at cooler times of year (McDonald et al. 2005; Woodhams and Alford 2005; Llewelyn et al. 2010; Sapsford et al. 2013).

Even within montane rainforests, ectothermic host body temperatures may range from below to above the optimum for fungal pathogens within the span of a single day (Roznik 2013) and individual probability of infection decreases with increases in the proportion of sampled individual body temperatures that are above 25°C (Rowley and Alford 2013; Roznik 2013). Frogs may behaviourally raise their body temperatures by selecting warm microhabitats, for instance in response to pathogen recognition (i.e., behavioural fever) or to aid metabolism or reproduction (Richards-Zawacki 2010; Murphy et al. 2011; Rowley and Alford 2013). Alternatively, changes in frog body temperature may occur passively, with fluctuations in the micro-environments of individuals or the macro-environments of populations (Rowley and Alford 2013; Roznik et al. 2015a).

In rainforest ecosystems where environmental conditions are suitable for Bd growth most of the time, processes exposing frogs to warmer microclimates may briefly elevate frog

body temperatures so that they are above the thermal optimum range of the fungus. At our long-term rainforest field sites in the Australian Wet Tropics where Bd is endemic, frog body temperatures commonly, although briefly, reach 26-29°C and can reach up to 36°C (Roznik 2013). This suggests that in the field Bd can tolerate short periods of exposure to temperatures that only marginally exceed its growth optimum (26-29°C), but the effects of these exposures on rates of population growth of Bd in host tissue are unknown. **One of the main foci of my thesis is to investigate the effects of these ‘heat spikes’ on the fitness of Bd and the course of Bd infections.** The importance of studying actual body temperature regimes, rather than constant temperatures, average temperatures of habitats, or even temperature regimes of habitats is becoming clearer as more studies have focused on how temperature regimes affect disease progression. For example, temperature fluctuations can lead to mortality in habitats in which mean temperatures appear ideal (Vickers and Schwarzkopf 2016). Understanding the influence on Bd growth of individual temperature regimes experienced by frogs will clarify how some frog populations persist when mean temperatures in their environments are within the range that is ideal for Bd growth (Bower et al. 2017).

Temperature also strongly influences immune responses in ectotherms (Feder and Burggren 1992). Many immune functions increase at warm temperatures, when metabolic rates are high, and decrease at cold temperatures, when metabolic rates are low, energy is in shorter supply, and many parasites are inactive (Rollins-Smith and Woodhams 2012). Because of the temperature-dependency of immune functions in ectotherms, animals with higher body temperatures may experience less morbidity and mortality from infection than animals with lower body temperatures. For example, mortality rates in Bd-infected mountain yellow-legged frogs were lower at 22°C than at 17°C, even though both temperatures are within the optimal thermal range for growth of Bd (Andre et al. 2008).

One strategy that ectotherms may use to cope with low temperatures is thermal acclimation, the adjustment of cellular and physiological processes in response to environmental conditions (Feder and Burggren 1992). However, thermal acclimation requires time, resulting in sub-optimal levels of immunity following temperature changes, while the immune system undergoes adjustments (Raffel et al. 2006). During periods of suboptimal immunity following temperature changes, animals may be particularly susceptible to disease (Ramsey et al. 2010). Red-spotted newts (Raffel et al. 2015) and Cuban tree frogs (Raffel et al. 2013) had higher Bd infection levels following temperature shifts compared to thermally acclimated individuals. These increases in levels of infection were greater when animals

experienced a temperature decrease (acclimated to 25°C; suddenly exposed to 15°C) than when animals experienced a temperature increase (acclimated to 15°C; suddenly exposed to 25°C; Raffel et al. 2013, 2015). Understanding the possible role of temperature shifts in disease outbreaks is important for species conservation, especially since climate change is expected to cause increases in temperature extremes and variability (Easterling 2000; Yeh et al. 2009). However, the Bd literature lacks comparative reporting on immune indicators, such as host white blood cell (WBC) profiles, before and after temperature shifts, which could lend mechanistic insight to our current understanding of this pathogen and others as they relate to climate variability. **Another focus area of my thesis is to investigate how temperature shifts influence the immune systems of Bd-infected frogs.**

Although thermoregulation producing heat spikes, whether it is a normal part of day-to-day physiology or represents a behavioural fever response, may positively affect the ability of frogs to avoid, tolerate, or clear Bd infections, because Bd alters internal homeostasis and water balance, infections by it may alter frogs' ability to tolerate elevated temperatures. **My project thus set out to examine the effects of Bd infection on the heat sensitivity of frog hosts** and how this may influence selection of warm microhabitats. Changes in heat sensitivity could pose a substantial fitness cost to frogs that use behavior to elevate body temperature, which may intentionally or coincidentally serve to decrease parasite performance or increase immune function and thereby reduce infection risk or the intensity of existing infections. Understanding the ways that parasites could discourage protective thermoregulatory behaviors is particularly important considering that anthropogenic climate change is causing the global climate and the microclimates experienced by animals to become warmer and more extreme.

1.3 Aims of thesis

The aim of my thesis was to examine the effects of host **temperature variation** on interactions between frogs and Bd, with an emphasis on how temperature variability influences host susceptibility and pathogen fitness. Specifically, I:

- Designed customized, fluctuating-temperature incubators for controlled experiments
- Studied the effects of **temperature shifts** on the immune systems of Bd-infected frogs
- Studied the effects of Bd infection on **heat sensitivity** of frog hosts

- Studied the effects of **diurnal body temperature variability** on frog-Bd interactions by measuring:
 - Effects of heat spikes representing **median** conditions experienced by frogs
 - Effects of heat spikes representing **individual** frog temperature regimes

1.4 Structure of thesis

My thesis is presented as a series of five stand-alone, but interrelated, manuscripts (Chapters 2–6) that are either published or will be submitted for publication. This format has resulted in some unavoidable repetition, mainly in the introductions and methods. Because all manuscripts include multiple co-authors, the text in my thesis uses personal pronouns that are plural rather than singular. At the start of each chapter, I have listed all co-authors and their contributions to the manuscript. One additional manuscript is included as an appendix; this study is part of the body of work I completed during my candidature but stands apart from the other studies.

Chapter 2 Low-cost fluctuating-temperature chamber for experimental ecology

Sasha E. Greenspan, Wayne Morris, Russell Warburton, Lexie Edwards, Richard Duffy, David A. Pike, Lin Schwarzkopf, Ross A. Alford

This chapter has been published in *Methods in Ecology and Evolution* and is reproduced here with permission.

Link to article: <http://onlinelibrary.wiley.com/doi/10.1111/2041-210X.12619/full>

Citation: Greenspan SE, Morris W, Warburton R, Edwards L, Duffy R, Pike DA, Schwarzkopf L, Alford RA (2016) Low-cost fluctuating-temperature chamber for experimental ecology. *Methods in Ecology and Evolution* 7:1567–1574.

Contributions: SEG, WM, WR, DAP, LS, and RAA co-developed the study. SEG, WM, RW, LE, and RD carried out the lab work. SEG carried out the statistical analyses, drafted the manuscript, and developed the figures and tables except Figs. 2.1 (WM) and 2.2 (RW). All co-authors provided editorial input.

2.1 Abstract

Commercially available fluctuating temperature chambers are large and costly. This poses a challenge to experimental ecologists endeavouring to recreate natural temperature cycles in the laboratory because the large number of commercial chambers required for replicated study designs is prohibitively expensive to purchase, requires a large amount of space, and consumes a great deal of energy. We developed and validated a design for economical, programmable fluctuating-temperature chambers based on a relatively small (23 litre) commercially manufactured constant-temperature chamber (\$140US) modified with a customized, user-friendly microcontroller (\$15US). Over a 1-week trial, these chambers reliably reproduced a real-world fluctuating (13.1°C to 35.5°C) body temperature regime of an individual frog, with a near-perfect 1:1 fit between target and actual temperatures ($y=1.0036x+0.1366$, $R^2 = 0.9977$, 95% confidence interval for slope = 1.0026, 1.0046). Over 30-day trials, they also reliably produced a simpler daily fluctuating-temperature scheme (sine wave fluctuating between 10-25°C each 24 hours) and a range of constant temperature regimes. The design is inexpensive and simple to assemble in large numbers, enabling genuine replication of even highly complex, many-treatment study designs. For example, it is possible to simultaneously examine in replicate chambers the responses of organisms to constant regimes, regimes that fluctuate following the means experienced by populations, and regimes that exactly mimic fluctuations measured over any length of time for particular individuals that differ in behaviour or microhabitat use. These chambers thus vastly expand the pool of resources available for manipulative experiments in thermal biology and ecology.

2.2 Introduction

Recreating real-world temperature cycles in the laboratory has extensive applications in experimental ecology. Unfortunately, commercial fluctuating-temperature chambers are currently much costlier than their constant-temperature equivalents (minimum prices in the low thousands, e.g., Winter et al. 2008, and power consumption in hundreds of watts/hour). As a consequence, most research facilities contain a limited number of constant or fluctuating-temperature chambers, which restricts the complexity of study designs, and often limits replication (e.g., Stevenson et al. 2014). Hurlbert (1984; 2009) defines a ‘replicate’ as the smallest experimental unit to which a treatment is independently applied. Samples within a single chamber are statistically non-independent because chambers inevitably differ in ways other than programmed thermal regimes. The inherent differences among chambers may lead to differences in sample responses that appear to be caused by treatments, but are caused by other, unknown effects. True replication thus occurs at the level of the chamber, with each chamber representing one experimental unit. In facilities for which the high cost of obtaining or running many fluctuating-temperature chambers is prohibitive, it is common to apply each experimental treatment to only one chamber, so experiments are effectively un-replicated (e.g., Stevenson et al. 2014). One solution to this problem is to use smaller, less expensive chambers (Raffel et al. 2013). Those presently in use, however, lack temperature control features that allow them to reproduce complex, real-world, multi-day temperature regimes.

We developed and validated a method for converting a relatively small (23 litre), low power (60 watts maximum), commercially manufactured constant-temperature chamber (\$140US) to an economical, programmable fluctuating-temperature chamber by adding a customized, user-friendly microcontroller (\$15US). This device can reproduce detailed temperature regimes of any length, including ones that match temperature regimes recorded in the field. These chambers provide a cost-effective and compact alternative to larger, more expensive fluctuating-temperature chambers currently available, enabling facilities with limited research funds to construct and use a replicated experimental infrastructure.

2.3 Methods

Chamber

We modified a commercially available, constant-temperature heating and cooling chamber marketed for reptile egg incubation and designed for use in the home or car (Reptile Egg Incubator; Petsden Australia Pty. Ltd., Kilsyth, Victoria, Australia; \$140US; temperature

sensor accurate to $\pm 2^{\circ}\text{C}$). The unit contains a 60W Peltier heating and cooling device and operates at 12V DC or 220-240V/50HZ AC and draws 55W. The exterior (35 cm x 42.5 cm x 48 cm) includes a removable cover at the back of the unit for easy access to internal components, a transparent plastic door for viewing the interior of the chamber, a digital temperature display, and a carrying handle. The interior (27cm x 23 cm x 37 cm) includes adjustable plastic shelving, LED lighting, a fan, and a water tray to augment humidity in the chamber. Any insulated container could be modified for fluctuating-temperature capabilities by following our procedures with some modification, for example by selecting and separately fitting a Peltier-effect heating and cooling module.

Microcontroller

We used an Arduino microcontroller. Arduino is an open-source electronics prototyping platform based on simple, customizable hardware and software (www.arduino.cc; (Wheat 2011)). Arduino was developed as an easy-to-use tool for people without electronics or programming expertise. An extensive collection of open-source hardware schematics, code, and web tutorials is available to aid beginners (see <http://playground.arduino.cc>). We selected the Arduino UNO R3 microcontroller board fitted with a data-logging shield (i.e., add-on board; V1.0, Deek-Robot, Shenzhen, China). The UNO board has 32 KB of on-board memory, 14 digital input/output pins that operate at 5V, 14 analogue inputs, six 10-bit analogue-to-digital channels, and a USB port. The UNO can be powered via USB connection or with an external power supply of 6-20V. The data-logging shield has a real-time clock and an SD card socket. The data-logging interface is compatible with any SD or MMC flash memory card up to 32G and supports FAT16 and FAT32 card formatting. *Sketches* (i.e., operational code for the microcontroller) were written in a simple, C-based programming language in Arduino Integrated Development Environment (IDE) software (Margolis 2011).

Modifications

We connected the chamber's built-in Peltier device, a digital temperature and humidity sensor (DTH22; accurate to 0.1°C ; precise to 0.5°C), a tri-coloured (blue, green, red) LED module (Keyes), and the chamber's built-in LED lighting (optional) to digital input and output pins on the microcontroller (Fig. 2.1). We added a 10K Ohm pull-up resistor to the temperature and humidity sensor and mounted it inside the chamber. We mounted the tri-coloured LED module on the microcontroller and connected the chamber's 12V DC power supply to the microcontroller. We also connected the chamber's fan to this power supply to

ensure that continuous air circulation prevents the formation of temperature gradients in the chamber. Finally, we fitted an additional relay to the built-in light circuit to make it possible to program light cycles as well as temperature programs. All materials for the microcontroller and hardware modifications were purchased for <\$15US.

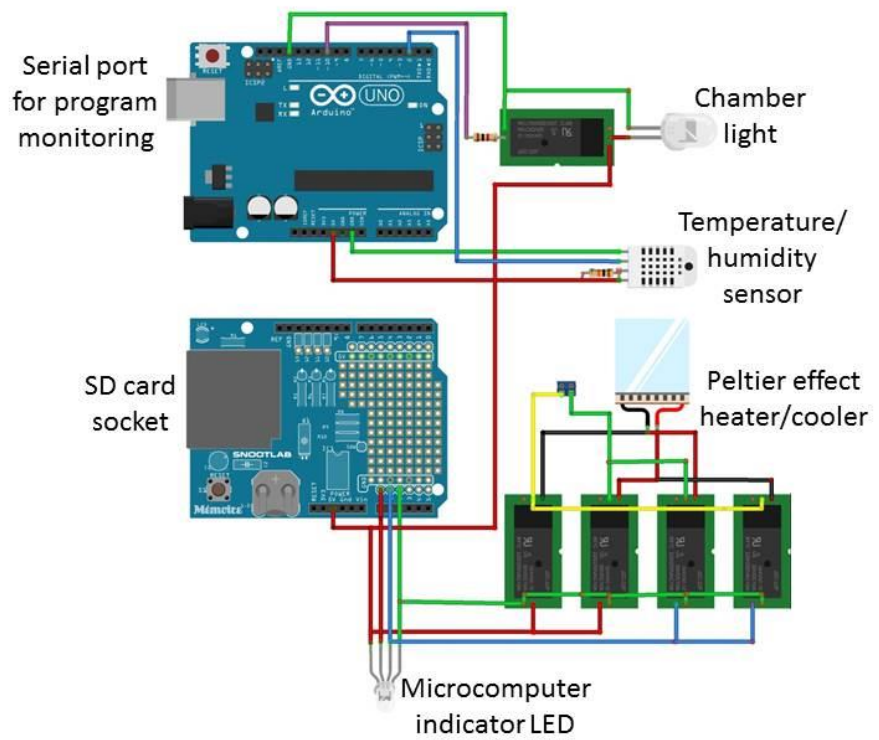


Figure 2.1 Schematic of Arduino UNO microcontroller and electronic components for an economical fluctuating-temperature chamber.

Operation

The operational code is compiled and loaded onto the microcontroller with Arduino IDE software, initiating a sequence of temperature control commands. Arduino allows ample flexibility in this type of task sequence; we outline one such option below and in Figure 2.2. Using our source code (<https://codebender.cc/sketch:345500>), the user first writes a comma-delimited *scheme* text file that includes the day number, time, and target temperature for each temperature step in a fluctuating-temperature regime of any length with time intervals of any length (Table 2.1a). The file is loaded onto an SD card and inserted into the card socket on the data-logging shield. A *schedule* text file (a comma-delimited, real-time version of the scheme) is automatically built on the SD card upon reading a new scheme (Table 2.1b). If the scheme file contains temperature steps $> 0.1^{\circ}\text{C}$ (the accuracy resolution of the temperature sensor), an optional task may be added to the operational code, by which intermediary temperature steps are interpolated and added to the schedule to facilitate smooth temperature transitions.

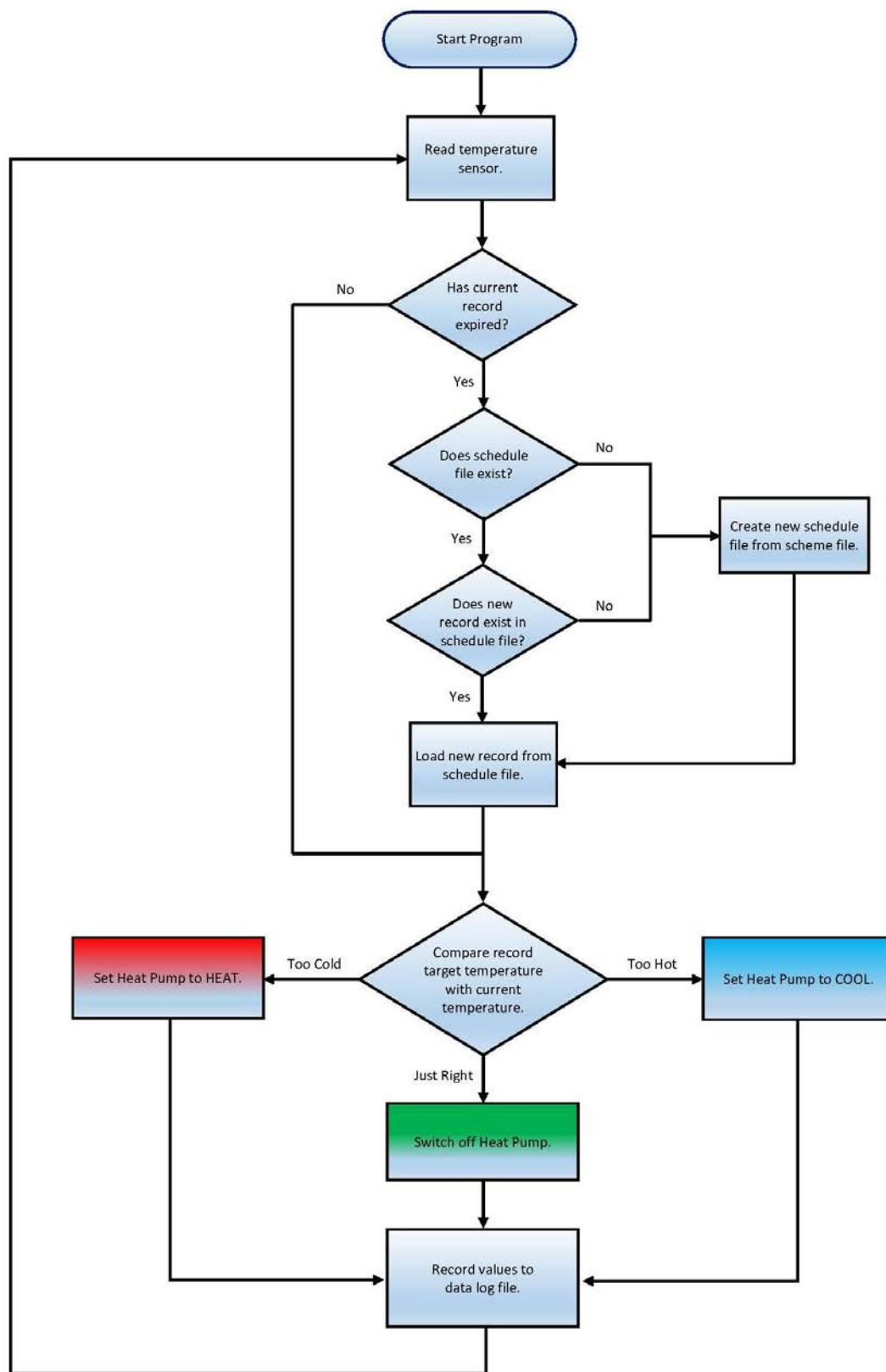


Figure 2.2 Outline of temperature control task sequence for an economical fluctuating-temperature chamber operated with an Arduino UNO microcontroller.

The schedule is scanned for the temperature assigned to the current time. This *target* temperature is then compared to a reading from the temperature sensor (the *actual* temperature). If the actual temperature is greater than the target temperature, a digital output is triggered to switch on the Peltier unit's cooling relay and turn the tri-coloured LED to blue to indicate that the chamber is cooling. If the actual temperature is less than the target temperature, a digital output is triggered to switch on the Peltier unit's heating relay and switch the tri-coloured LED to red to indicate that the chamber is heating. If the actual temperature is equal to the target temperature, a digital output is triggered to turn off the Peltier unit and turn the tri-coloured LED to green to indicate that the chamber is neither heating nor cooling. This cycle of temperature adjustment is repeated at a user-defined frequency (we chose every 1 second), and the actual temperature of the chamber is also logged at a user-defined frequency in an automatically generated, time-stamped, comma-delimited *datalog* text file on the SD card.

The performance of the device can be monitored with the serial monitor feature in the Arduino IDE when the microcomputer is connected to a computer via USB. The serial monitor is a pop-up window that lists user-specified serial data (e.g., date and time, current target temperature, current actual temperature) at a user-defined frequency. We also built an optional device for system monitoring without a standard computer. We fitted an Arduino Mega 2560 board with a 3.5" serial LCD display module, a TFT shield, and a serial plug to match the serial output from the UNO. The user can plug this portable device into the chamber's microcomputer, turn on the LCD display, and read serial data as it is emitted from the microcomputer.

Table 2.1 Example of a fluctuating-temperature scheme (a) and schedule (i.e., real-time version of the scheme; b) used to program an economical, Arduino-based, fluctuating-temperature chamber.

a. Scheme			b. Schedule		
Day	Time (HH:MM:SS)	Temperature (°C)	Date	Time (HH:MM:SS)	Temperature (°C)
1	00:00:00	10.0	1 Jan 2016	00:00:00	10.0
1	00:26:00	10.1	1 Jan 2016	00:26:00	10.1
1	00:45:00	10.2	1 Jan 2016	00:45:00	10.2
1	00:59:00	10.3	1 Jan 2016	00:59:00	10.3
1	01:10:00	10.4	1 Jan 2016	01:10:00	10.4
1	01:19:00	10.5	1 Jan 2016	01:19:00	10.5
1	01:28:00	10.6	1 Jan 2016	01:28:00	10.6
1	01:36:00	10.7	1 Jan 2016	01:36:00	10.7
.
.
.
1	22:16:00	10.7	1 Jan 2016	22:16:00	10.7
1	22:23:00	10.6	1 Jan 2016	22:23:00	10.6
1	22:31:00	10.5	1 Jan 2016	22:31:00	10.5
1	22:40:00	10.4	1 Jan 2016	22:40:00	10.4
1	22:49:00	10.3	1 Jan 2016	22:49:00	10.3
1	23:00:00	10.2	1 Jan 2016	23:00:00	10.2
1	23:14:00	10.1	1 Jan 2016	23:14:00	10.1
1	23:33:00	10	1 Jan 2016	23:33:00	10
1	23:59:59	10	1 Jan 2016	23:59:59	10

Validation

We evaluated several aspects of temperature control for the device. Each of the validation schemes described below was validated with a unique chamber/microcontroller setup in a climate-controlled laboratory (near-constant 23°C). First, we measured maximum rates of heating and cooling between 10-40°C. We used a scheme in which the temperature increased hourly from 10°C and then decreased hourly from 40°C in increments of 5°C (Fig. 2.3a). We logged the actual temperature once per second from the digital temperature sensor that we added to the chamber (DTH22; accurate to 0.1°C; precise to 0.5°C). For each 5°C increase or decrease in temperature, we calculated the rate of change in degrees Celsius per minute.

Second, we measured reliability of temperature control for a fluctuating (13.1°C to 35.5°C) temperature scheme that matched body temperature data recorded in the field for a small ectotherm (Fig. 2.4a). This temperature scheme was determined by recording the body temperatures of an individual tree frog, *Litoria serrata*, in its native habitat (Roznik 2013; Stevenson et al. 2014). A temperature-sensitive radio-transmitter (Model A2414; Advanced Telemetry Systems, Isanti, MN; pulse rate varied with temperature following a calibration curve provided by the manufacturer) was attached to the frog with a thread waistband (Roznik 2013; Stevenson et al. 2014). Transmitter signal pulse rate was recorded every 15 minutes for seven consecutive days with an automated data-logging receiver (Model SRX400A; Lotek Wireless, Newmarket, ON, Canada). We filled in occasional missing temperature values using values calculated by maximum entropy interpolation (Dowse and Ringo 1987; Dowse 2009). For this trial scheme, we logged the actual chamber temperatures once per minute for seven days using the digital temperature sensor that we added to the chamber (DTH22; accurate to 0.1°C; precise to 0.5°C).

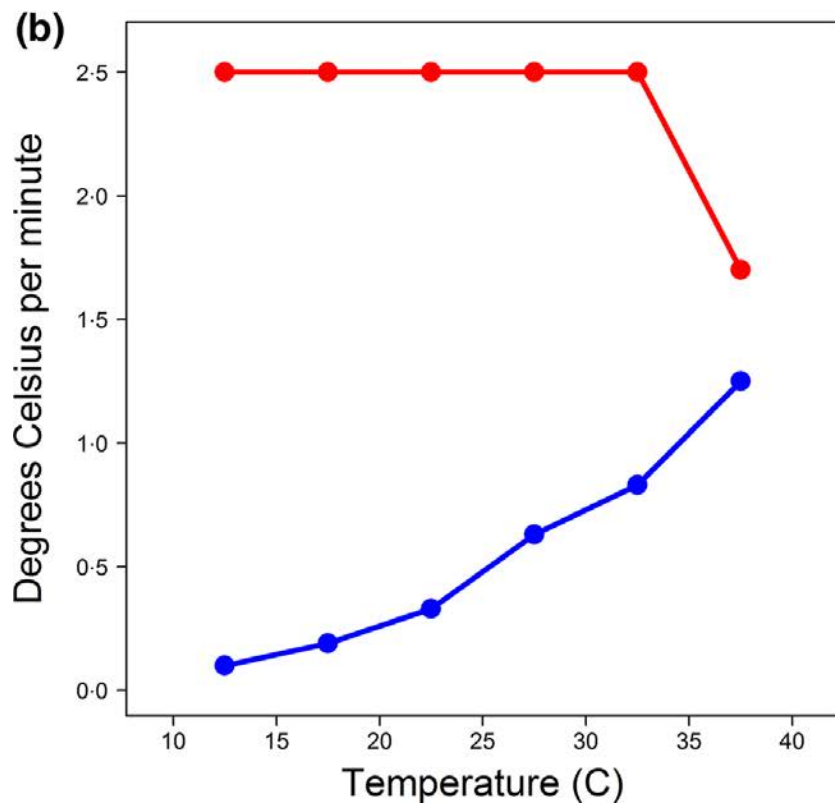
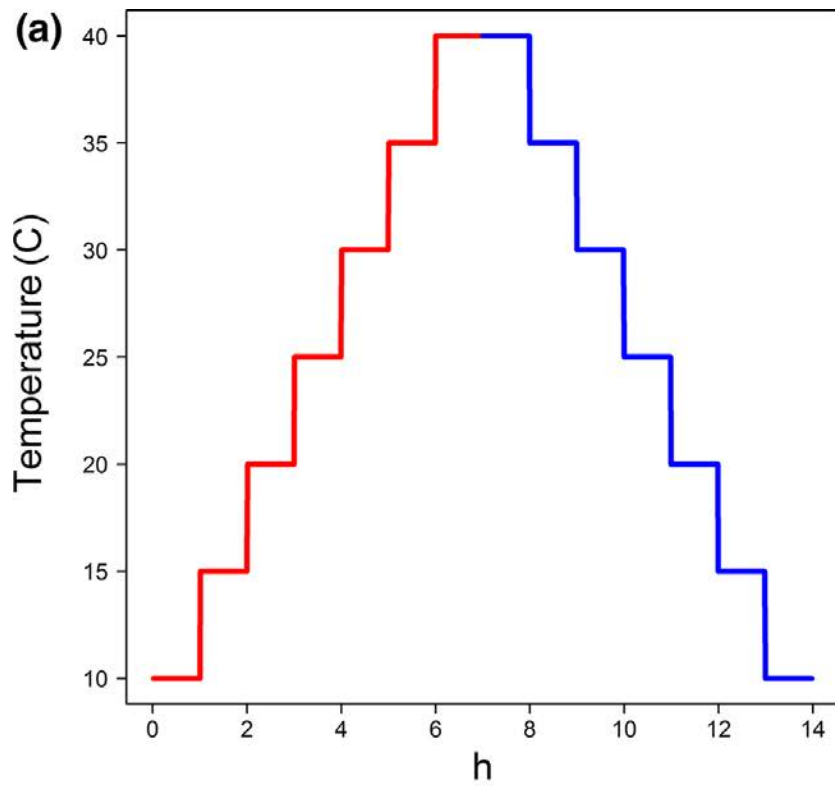


Figure 2.3 For an economical fluctuating-temperature chamber operated with an Arduino UNO microcontroller, (a) the temperature scheme used to measure maximum rates of heating and cooling and (b) maximum rates of heating and cooling over 5°C temperature intervals.

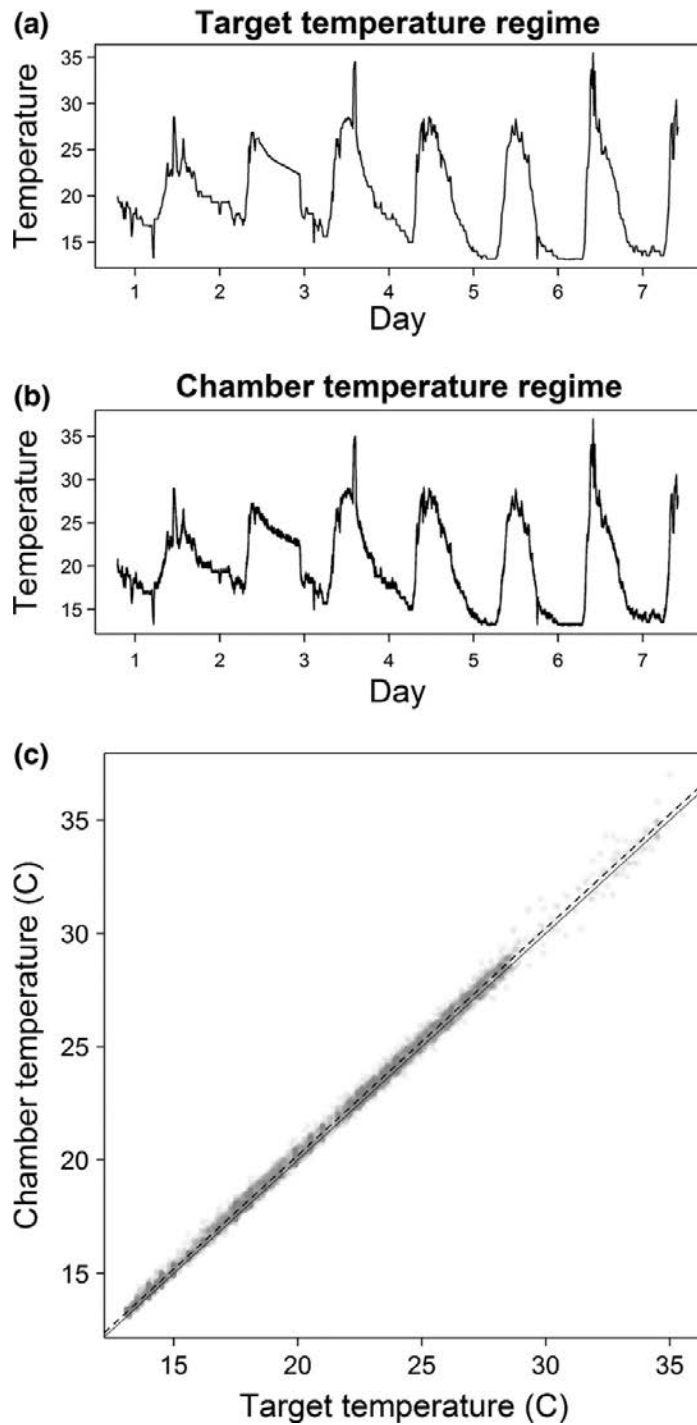


Figure 2.4 For an economical fluctuating-temperature chamber operated with an Arduino UNO microcontroller, (a) a target temperature scheme used to measure reliability of temperature control for exact, real-world temperature regimes recorded in the field, (b) the actual chamber temperatures during the reliability trial, logged once per minute for seven days, and (c) the linear regression comparing actual chamber temperatures to target temperatures during the seven-day reliability trial. Gray dots = actual temperatures. Solid line = slope of 1. Dashed line = regression line.

Third, we measured reliability of temperature control for a repeating daily temperature scheme comprising a sine wave fluctuating between 10-25°C over 24 hours (Fig. 2.5a). Fourth, we measured reliability of temperature control for six constant-temperature schemes covering a range of temperatures in the fluctuating schemes (Fig. 2.6a). The constant temperature schemes were 10°C, 13°C, 16°C, 19°C, 22°C, and 25°C (Fig. 2.6a). For the sine wave and constant temperature trial schemes, we logged the actual chamber temperatures once per minute for 30 days from the digital temperature sensor that we added to the chamber (DTH22; accurate to 0.1°C; precise to 0.5°C). We compared actual and target temperatures for the two fluctuating-temperature trials using linear regression performed in R software (version 3.0.3; R Core Team 2015).

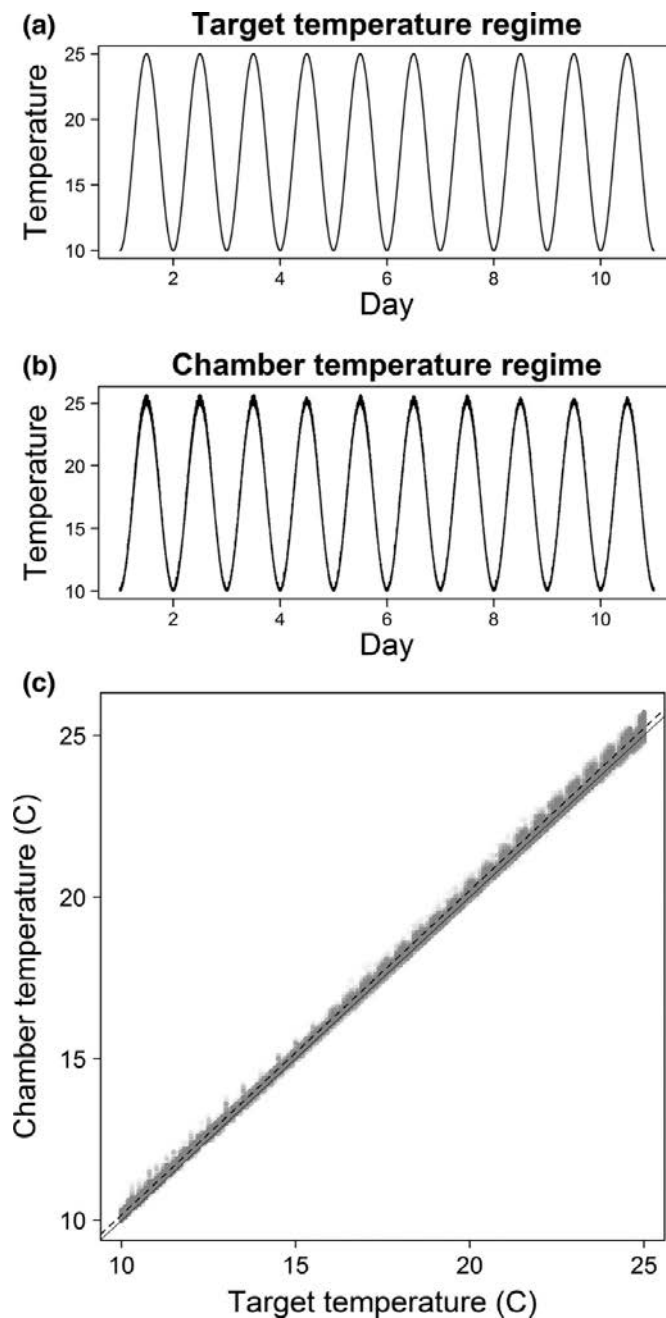


Figure 2.5 For an economical fluctuating-temperature chamber operated with an Arduino UNO microcontroller, (a) a target temperature scheme used to measure reliability of temperature control for arbitrarily fluctuating temperature regimes, in this case a sine wave fluctuating between 10-25°C over 24 hours, (b) the actual chamber temperatures during the reliability trial, logged once per minute for 30 days (only the first ten days are shown), and (c) the linear regression comparing actual chamber temperatures to target temperatures during the 30-day reliability trial. Gray dots = actual temperatures. Solid line = slope of 1. Dashed line = regression line.

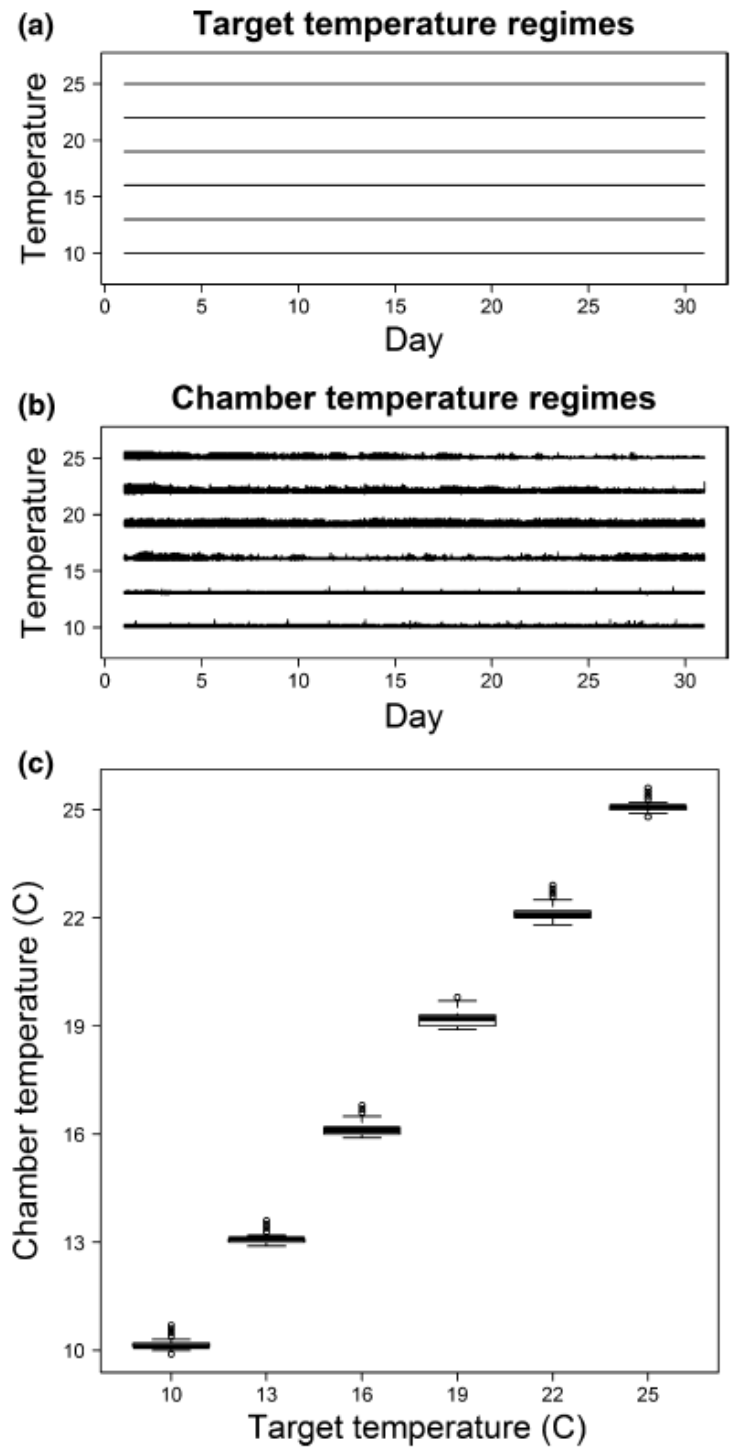


Figure 2.6 For an economical fluctuating-temperature chamber operated with an Arduino UNO microcontroller, (a) the target temperature schemes used to measure reliability of temperature control for constant temperature regimes, (b) the actual chamber temperatures during the reliability trials, logged once per minute for 30 days, and (c) boxplots summarizing actual chamber temperatures during the 30-day reliability trials. We used a unique chamber/microcontroller setup for each constant target temperature trial.

2.4 Results

The chambers heated at a maximum rate of 2.5°C per minute between 10-35°C; this slowed to 1.7°C per minute above 35°C (Fig. 2.3b). The maximum rate of cooling ranged from 1.3°C per minute between 40-35°C to 0.1°C per minute between 15-10°C (Fig. 2.3b). The chambers reliably produced our designated fluctuating-temperature schemes (Figs. 2.4b, 2.5b), with a near-perfect 1:1 fit between target and actual temperatures over the course of each trial period (field-based scheme: $y=1.0036x+0.1366$, $R^2 = 0.9977$, 95% confidence interval for slope = 1.0026, 1.0046, 95% confidence interval for intercept = 0.1167, 0.1564, Fig. 2.4c; sine wave scheme: $y=0.9974x+0.1720$, $R^2 = 0.9993$, 95% confidence interval for slope = 0.9972, 0.9976, 95% confidence interval for intercept = 0.1680, 0.1760, Fig. 2.5c). For the scheme based on actual frog field measurements, the actual temperature remained within 2.0°C of the corresponding target temperature throughout the trial and remained within 1.0°C of the corresponding target temperature for 99.8% of the trial period. The average difference between pairs of target and actual temperatures was $0.21^\circ\text{C} \pm 0.23^\circ\text{C}$ (SD). For the sine wave scheme, the actual temperature remained within 0.9°C of the corresponding target temperature throughout the trial and the average difference between pairs of target and actual temperatures was $0.14^\circ\text{C} \pm 0.13^\circ\text{C}$ (SD). The chambers also reliably maintained constant temperatures (Fig. 2.6b, c). Average temperatures \pm SD for the 10°C, 13°C, 16°C, 19°C, 22°C, and 25°C schemes over the 30-day trial period were $10.13^\circ\text{C} \pm 0.08^\circ\text{C}$, $13.08^\circ\text{C} \pm 0.06^\circ\text{C}$, $16.12^\circ\text{C} \pm 0.12^\circ\text{C}$, $19.17^\circ\text{C} \pm 0.16^\circ\text{C}$, $22.09^\circ\text{C} \pm 0.14^\circ\text{C}$, and $25.10^\circ\text{C} \pm 0.12^\circ\text{C}$, respectively. The small discrepancies between the target and actual temperatures in our validation trials were predictable (actual slightly greater than target), so the chambers could easily be calibrated for even better accuracy.

2.5 Discussion

We developed a microcomputer and operational code that can produce virtually any ecologically-relevant temperature regime in an insulated chamber *via* fine control of a Peltier-effect heating and cooling system. The potential ecological and other applications for these chambers are vast in scope. We demonstrated that they can produce highly consistent constant temperatures, and can produce varying temperatures as simple as a daily sine-wave temperature scheme through to an exact reproduction of the fluctuating body temperature regime of an individual ectotherm over many days. Thus, these chambers can be used for temperature experiments examining both the average temperature regimes of populations or

environments as well as the exact temperature regimes of individuals or microhabitats over any length of time. As a tool, they hold immense promise for addressing questions in fields such as global change biology, eco-physiology, and disease ecology, among the many other subjects that fall within the sphere of thermal biology.

Additionally, these chambers are small and inexpensive enough that many can be easily constructed and run, thus enabling users to achieve genuine statistical replication in thermal biology experiments. Although these chambers are smaller than typical fluctuating temperature growth chambers designed for plants, they are suitable for manipulative experiments utilizing organisms of various sizes and developmental stages, from microbes and invertebrates to small vertebrates, and from embryos to adults. Finally, with additional simple modifications, the same microcontroller and programming features may be used to experimentally manipulate and measure a diverse array of other physical variables – essentially, any variable that can be applied to an insulated container (e.g., humidity, light, UV-radiation) – thus extending the applicability of these chambers to many other disciplines within ecology, in addition to those within thermal biology.

We caution that care must be taken in study design to ensure experimental independence, even when multiple chambers are employed (Fig. 2.7). For example, to avoid physically interdependent replication, chambers assigned to the same treatment should not all share one DC power supply and chambers assigned to the same treatment should always be interspersed with chambers allocated to other treatments. Our laboratory with 48 individual chambers has a maximum of six chambers that share a common DC power supply (Figure 2.7). In this case, chambers in each group of six should be assigned to different temperature treatments to maintain independence. In addition, the minimum and maximum temperatures attainable using Peltier-effect devices depend on ambient temperature. If chambers are to be used under ambient conditions that differ by more than a few degrees from the 23°C under which we conducted our trials, or that fluctuate over a wide range, we advise users to test the suitability of a prototype in their operating environment prior to constructing an array of chambers and undertaking experiments.

The main limiting factor in our microcontroller design was low on-board memory, which restricted programming options; we encourage users to consider a 256 KB mega-board as an alternative to the UNO. Although our microcontroller worked reliably, we would also recommend using either a manufactured chamber with improved internal components or a custom-built chamber. After frequent use, some built-in heat pumps failed, which we attribute

to the rough workmanship of the built-in heat sinks and resulting poor contact between heat sinks and heat pumps. We repaired this problem by filing the contact area of the heat sink to create a smooth surface and firmly restoring the contact between the heat sink and heat pump; however, this type of manipulation was difficult given the rigid internal structure of the chamber. See <http://www.warburtech.com> for our latest developments in product design, which include expanded on-board microcontroller memory and a chamber comprised of a simple insulated box.



Figure 2.7 Laboratory setup with 48 economical, fluctuating-temperature chambers, each operated by an Arduino UNO microcontroller.

2.6 Highlights

- We designed a customized, fluctuating-temperature chamber for controlled thermal biology experiments.
- In validation trials, replicate chambers accurately produced constant temperatures, a sine wave temperature regime, and the temperature regime of a wild frog.
- These chambers expand the pool of resources available for manipulative experiments in thermal biology and ecology.

Chapter 3 White blood cell profiles in amphibians help to explain disease susceptibility following temperature shifts

Sasha E. Greenspan, Deborah S. Bower, Rebecca J. Webb, Lee Berger, Donna Rudd, Lin Schwarzkopf, Ross A. Alford

This chapter has been published in *Developmental and Comparative Immunology* and is reproduced here under the terms of the Elsevier author publishing agreement.

Link to article: <http://www.sciencedirect.com/science/article/pii/S0145305X17304263>

Citation for article: Greenspan SE, Bower DS, Webb RJ, Berger L, Rudd D, Schwarzkopf L, Alford RA (2017) White blood cell profiles help to explain disease susceptibility of ectotherms following temperature shifts. *Developmental and Comparative Immunology* 77:280–286.

Citation for data in Tropical Data Hub: Greenspan, S. (2017). Infection load data for Chapter 3 of PhD thesis: Thermal thresholds in the amphibian disease chytridiomycosis. James Cook University. [Data Files] <http://dx.doi.org/10.4225/28/5a0fccef41d3>
DOI: [10.4225/28/5a0fccef41d3](https://doi.org/10.4225/28/5a0fccef41d3)

Contributions: All authors co-developed the study. SEG, DSB, and RJW carried out the lab work. SEG carried out the statistical analyses with assistance from LS and RAA. SEG drafted the manuscript and developed the figures and tables. All authors provided editorial input.

3.1 Abstract

Temperature variability, and in particular temperature decreases, can increase susceptibility of amphibians to infections by the fungus *Batrachochytrium dendrobatidis* (Bd). However, the effects of temperature shifts on the immune systems of Bd-infected amphibians are unresolved. We acclimated frogs to 16°C and 26°C (baseline), simultaneously transferred them to an intermediate temperature (21°C) and inoculated them with Bd (treatment), and tracked their infection levels and white blood cell profiles over six weeks. Average weekly infection loads were consistently higher in 26°C-history frogs, a group that experienced a 5°C temperature decrease, than in 16°C-history frogs, a group that experienced a 5°C temperature increase, but this pattern only approached statistical significance. The 16°C-acclimated frogs had high neutrophil:lymphocyte (N:L) ratios (suggestive of a hematopoietic stress response) at baseline, which were conserved post-treatment. In contrast, the 26°C-acclimated frogs had low N:L ratios at baseline which reversed to high N:L ratios post-treatment (suggestive of immune system activation). Our results suggest that infections were less physiologically taxing for the 16°C-history frogs than the 26°C-history frogs because they had already adjusted immune parameters in response to challenging conditions (cold). Our findings provide a possible mechanistic explanation for observations that amphibians are more susceptible to Bd infection following temperature decreases compared to increases and underscore the consensus that increased temperature variability associated with climate change may increase the impact of infectious diseases.

3.2 Introduction

Temperature strongly influences immune responses in ectotherms (Feder and Burggren 1992). Many immune functions increase at warm temperatures, when metabolic rates are high, and decrease at cold temperatures, when metabolic rates are low, energy is in shorter supply, and many parasites are inactive (Rollins-Smith and Woodhams 2012). For instance, numbers of circulating lymphocytes, the most abundant white blood cell in amphibians, reptiles, and fish, are often high at warm temperatures and low at cold temperatures (Wright and Cooper 1981; Cooper et al. 1992; Zapata et al. 1992; Rollins-Smith and Woodhams 2012). As a result of the temperature-dependency of immune functions in ectotherms, animals with higher body temperatures may experience less morbidity and mortality from infection than animals with lower body temperatures. For example, mortality rates in mountain yellow-legged frogs (*Rana muscosa*) infected with the widespread fungal parasite *Batrachochytrium dendrobatidis* (Bd) were lower at 22°C than at 17°C, even though both temperatures are within the optimal thermal range for growth of Bd (Andre et al. 2008). Similarly, western clawed frogs (*Silurana tropicalis*) cleared Bd infections significantly faster at 26°C compared to 18°C, independent of the temperature-dependent growth rates of the parasite (Ribas et al. 2009).

One strategy that ectotherms may use to cope with low temperatures is thermal acclimation, the adjustment of cellular and physiological processes in response to environmental conditions (Feder and Burggren 1992). For example, circulating neutrophils (phagocytic white blood cells) increased in northern leopard frogs (*Rana pipiens*) after prolonged cold (5°C for 5 mo), an adaptation that may decrease disease susceptibility at low temperatures, when other defenses are less active (Maniero and Carey 1997). Similarly, phagocytic activity of white blood cells increased in cold-acclimated common toads (*Bufo bufo*) and fire salamanders (*Salamandra salamandra*), an adaptation that may have evolved to prepare animals in winter dormancy for increases in injury and infection risk in spring (Pxytycz and Jozkowicz 1994). However, thermal acclimation requires time, resulting in sub-optimal levels of immunity following temperature changes, while the immune system undergoes adjustments (Raffel et al. 2006). Cold acclimation may require months of adjustment time; in wild red-spotted newts (*Notophthalmus viridescens*) monitored in autumn, neutrophil levels were lower than expected even after two months of average temperature decreases (Raffel et al. 2006). In contrast, lymphocytes returned to expected levels after only 14 days in spring,

since the lag effect for temperature increases is limited only to the 7-11 days required for development of stem cells into mature white blood cells (Raffel et al. 2006).

During periods of suboptimal immunity following temperature changes, animals may be particularly susceptible to disease (Ramsey et al. 2010). Red-spotted newts (Raffel et al. 2015) and Cuban tree frogs (*Osteopilus septentrionalis*; Raffel et al. 2013) had higher Bd infection levels following temperature shifts compared to thermally acclimated individuals. These increases in levels of infection were greater when animals experienced a temperature decrease (acclimated to 25°C; suddenly exposed to 15°C) than when animals experienced a temperature increase (acclimated to 15°C; suddenly exposed to 25°C; Raffel et al. 2013, 2015). Similarly, average monthly decreases in temperature predicted Bd-related declines of *Atelopus* spp. better than average monthly increases in temperature (Raffel et al. 2013). Understanding the possible role of temperature shifts in disease outbreaks is important for species conservation, especially since climate change is expected to cause increases in temperature extremes and variability (Easterling 2000; Yeh et al. 2009)). Although amphibian populations in the most consistently thermally variable habitats may be protected from ill effects of Bd, probably due to heat intolerance of the fungus (Murray et al. 2011; Liu et al. 2013; Olson et al. 2013; Sapsford et al. 2015), increases in the frequency or intensity of heat waves in habitats usually characterized by more moderate temperature ranges will, by definition, be followed by increases in the frequency or intensity of temperature drops (back to 'normal' temperatures) which are associated with impaired immunity (Raffel et al. 2013). However, the Bd literature lacks comparative reporting on immune indicators, such as host white blood cell (WBC) profiles, before and after temperature shifts, which could lend mechanistic insight to our current understanding of this pathogen and others as they relate to climate variability.

The mechanisms of protective immunity against Bd have not been fully elucidated, but innate resistance has been associated with cutaneous antimicrobial peptides (Woodhams et al. 2007a; Woodhams et al. 2007b; Van Rooij et al. 2015) and specific MHC (Major Histocompatibility Complex) type II alleles, which suggests there is an immune cell component (Bataille et al. 2015). Amphibians have the same types of WBC as mammals (lymphocytes, neutrophils, monocytes, basophils, and eosinophils), with similar appearances and functions (Hadji-Azimi et al. 1987). The WBC profile, meaning the relative proportions of each WBC type in the blood stream, can be used to assess hematopoietic productivity and the level of immune system activation (Davis et al. 2008). Lymphocytes and neutrophils usually make up the majority of WBCs (Davis and Durso 2009) and the ratio of these cells is often used on its own

as a reliable indicator of the status of the immune system (Davis et al. 2008). High relative proportions of circulating neutrophils and low relative proportions of circulating lymphocytes (high N:L ratio) are characteristic of a hematopoietic stress response or an activated immune system in amphibians (Bennett and Daigle 1983; Cooper et al. 1992; Maniero and Carey 1997; Davis and Maerz 2008) and other vertebrates (Davis et al. 2008). The functional explanation for high N:L ratios is that they may enhance immune preparedness under stressful conditions, when animals are likely to encounter immune challenge (Dhabhar et al. 1994; Dhabhar et al. 1995). Recruiting neutrophils into circulation may enhance the inflammatory reaction, while trafficking lymphocytes out of circulation and into tissues may enhance immune surveillance or protect these cells from inhibitory effects of stress hormones (Dhabhar et al. 1994; Dhabhar et al. 1995).

Our aim was to track WBC profiles alongside Bd infection levels in frogs experiencing either a temperature increase or decrease. We acclimated Australian green tree frogs (*Litoria caerulea*) to 16°C or 26°C, measured their WBC profiles when thermally acclimated, and then simultaneously inoculated a treatment group with Bd and transferred all frogs to an intermediate temperature (21°C). We then monitored WBC profiles and infection levels over six weeks and compared immune parameters among temperature and infection treatments.

3.3 Methods

Study animals

Our experiment was carried out under James Cook University Animal Ethics permit A1991. Study animals were captive-bred juveniles (16°C-acclimated: 45–57 mm; 26°C-acclimated: 43–53 mm) from two clutches of *L. caerulea* (sourced from Narre Aquarium and Reptile Centre, Narre Warren, Victoria, Australia). *Litoria caerulea* are widely distributed across the northern half of Australia, hence can tolerate a range of climates including thermally fluctuating arid regions and rainforests. Use of captive-reared frogs ensured no previous exposure to Bd, which can influence the progression of subsequent infections (McMahon et al. 2014). For a separate initial study, forty-six individuals were raised in temperature-controlled rooms for 24 months and maintained on a natural photoperiod in individual enclosures. Twenty-six individuals were housed in a 16°C room; twenty individuals were housed in a 26°C room. All frogs were maintained under the same husbandry protocols and skin swabs were occasionally collected from each individual as part of the initial study.

Bd cultures and inoculations

We used the Bd isolate Paluma-Lseratta-2012-RW-1. This isolate is maintained at the College of Public Health, Medical, and Veterinary Sciences, James Cook University. It originated from an adult *Litoria serrata* that was collected from a rainforest in the Australian Wet Tropics and died in captivity. The isolate had been cryo-archived after two passages in nutrient broth. We revived aliquots of this isolate and cultured it in tryptone/gelatin hydrolysate/lactose (TGhL) broth in 25-cm³ tissue culture flasks, passaging it five times before the experiment and maintaining cultures at 22°C.

To obtain zoospores for each trial, we added cultured broth to Petri dishes containing TGhL broth in 1% agar. Plates were partially dried in a laminar flow cabinet, incubated at 21°C for four days, and then maintained alternately at 4°C and 21°C to sustain growth and zoospore production. We then added up to 5 ml of deionized (DI) water to the dishes to form a zoospore suspension. We combined the liquid contents of each dish and calculated the concentration of zoospores with a hemocytometer (Neubauer Improved Bright-line). We prepared a sham (control) inoculant by following the same protocol but with Petri dishes containing only nutrient agar.

For the study, we removed frogs from the temperature-controlled rooms and immediately divided them into 26 temperature-controlled chambers (day 0; see below). Inoculations were then administered in the chambers. To ensure infection, we inoculated frogs on two consecutive days (days 0 and 1). On each day, we added DI water to the zoospore suspension to produce a final concentration of 6×10^5 zoospores per ml. To inoculate, we placed each frog into an individual 250-ml plastic container and added 5 ml (enough to cover the bottom of the container) of zoospore inoculant (n = 16 16°C-acclimated frogs; n = 10 26°C-acclimated frogs) or sham inoculant (n = 10 * 16°C-acclimated frogs; n = 10 * 26°C-acclimated frogs) to each container. All Bd inoculations were performed in chambers set to 21°C. We left frogs in inoculant baths for 12 hours per day. After each inoculation period, we returned frogs with their inoculant to individual permanent enclosures comprising 70 x 120 x 170 mm plastic containers lined with tap water-saturated paper towels.

Experimental treatments

All Bd-inoculated frogs (n = 16 * 16°C-acclimated frogs; n = 10 * 26°C-acclimated frogs) were inoculated and housed at 21°C, a temperature intermediate between the 16°C and 26°C acclimation temperatures. Because we used only one test temperature (21°C), the intrinsic growth rate of the pathogen was held constant. To account for immunologic effects of

temperature changes independent of infection, some sham-inoculated frogs (n = 5 from each acclimation temperature) were also housed at 21°C. To account for confounding immunologic variables (e.g., stress from handling, blood sampling, changes in housing), some sham-inoculated frogs (n = 5 from each acclimation temperature) were housed at their acclimation temperatures (16°C or 26°C). Experimental Bd inoculations often yield infection rates < 100% and infection levels are commonly variable over time. We therefore used a lower number of sham-inoculated control animals (n = 5 per treatment) than Bd-inoculated treatment animals (n = 10–16 per treatment) to maximize our samples of infected individuals and capture natural variability in infection levels.

Replicate temperature-controlled chambers (Greenspan et al. 2016) were programmed to perform each treatment temperature (16 chambers at 21°C, five chambers at 16°C, and five chambers at 26°C) and frogs were housed individually in permanent enclosures within the chambers. The chambers were arranged in eight spatial blocks (Fig. 3.1), each of which contained two 21°C chambers and five of which also contained one 16°C chamber and one 26°C chamber. The location of each chamber within each block was determined randomly. Frogs from each temperature (16°C, 21°C, or 26°C) x infection (Bd-inoculated or sham-inoculated) treatment were assigned to chambers with the goal of maximizing the statistical independence of our samples (Fig. 3.1). Each chamber could accommodate four frog enclosures. When uneven sample sizes precluded the placement of four frogs in a chamber, we added unoccupied enclosures containing moist paper towel to minimize differences in chamber conditions (Fig. 3.1). We systematically rotated the placement of the frog enclosures within each chamber (coinciding with frog feeding) to ensure that they were evenly exposed to any small differences in local temperatures that might exist within the chamber.

The actual temperature of each chamber (measured with a digital temperature sensor [DTH22; accurate to $\pm 0.1^\circ\text{C}$] mounted inside each chamber) was recorded every minute and confirmed with Thermochron iButton temperature loggers (Maxim Integrated Products, Sunnyvale, California, USA; accurate to $\pm 0.5^\circ\text{C}$) that recorded chamber temperatures every 15 minutes. Actual chamber temperatures remained within 0.5°C of target temperatures during the experiment.

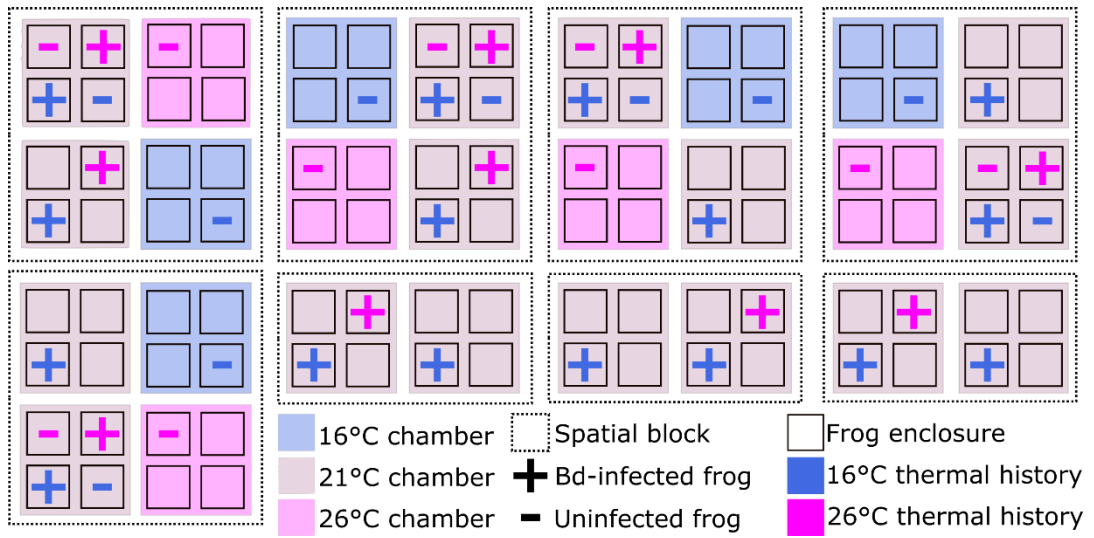


Figure 3.1 Configuration of temperature-controlled chambers.

Frog husbandry and infection monitoring

Temperature-controlled chambers were programmed to maintain a 12 hr: 12 hr photoperiod. Three times per week, we replaced moistened paper towels and fed frogs crickets *ad libitum*. We checked frogs daily for signs of chytridiomycosis (e.g., lethargy, reddening of feet, excessive skin shedding).

To monitor Bd infection status and intensity over the course of the experiment, we swabbed frogs one week before removal from the temperature-controlled rooms (all tested Bd-negative) and 6 d, 14 d, 21 d, 29 d, 36 d, and 41 d post-inoculation, following a standard protocol (Stockwell et al. 2015). We determined the number of Bd zoospore genome equivalents per swab with a real-time quantitative PCR protocol modified from Boyle et al. (Boyle et al. 2004). After the experiment, we treated frogs for Bd infections with the antifungal Itraconazole (Brannelly et al. 2012).

Blood collection

Blood samples (0.1 ml) were collected by cardiac puncture with 26-ga needles one week before removing frogs from temperature-controlled rooms (baseline) and on days 6, 21, and 33 (Heatley and Johnson 2009; Forzán et al. 2017). For ethical reasons, we made a maximum of three attempts to extract blood and were unable to obtain samples from all animals on every sampling day. Blood smears were air-dried, stained with Wright's stain, and observed by light microscopy at 100x. To perform a differential WBC count, we located the section of the blood smear with an even monolayer of cells (red blood cells as close together as possible without overlapping). We then counted and identified 200 WBCs per slide with a modified battlement technique (MacGregor et al. 1940). We identified WBCs as lymphocytes, neutrophils, monocytes, basophils, and eosinophils (Hadji-Azimi et al. 1987; Claver and Quaglia 2009; Arikan and Cicek 2014; Fig. 3.2). We calculated WBC profiles for each frog by dividing the number of each cell type by the total number of cells counted. For sampling days 21 and 33, we also counted the number of microscope fields examined to reach 200 WBCs and used this number as an estimate of the relative concentration of WBCs in the blood (Heatley and Johnson 2009). We did not calculate relative WBC concentration for sampling day 6 because we used heparinized needles, the syringes of which contained residual liquid, which diluted those samples.

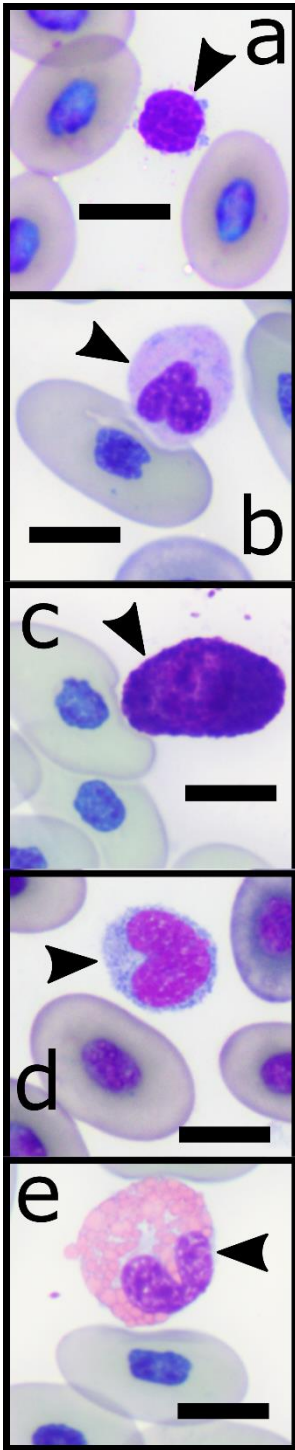


Figure 3.2 Representative micrographs of each WBC type (marked with arrowheads).
Lymphocyte (a), neutrophil (b), basophil (c), monocyte (d), eosinophil (e). Bar = 10 μ m.

Statistical analysis

We analyzed our data using Program R software (R Core Team, 2015). To test for effects of temperature shifts on frog infection levels, we used a linear mixed effects model (lmer function in lme4 package; Bates et al. 2015) with log-transformed infection loads as the response variable, acclimation temperature (16°C or 26°C), sampling day (day 6, 14, 29, 36, 41) and their interaction as fixed effects, and frog individual as a random effect. Problems with swab storage or extraction made it likely that the infection loads were underestimated on day 21, so we excluded the infection load data for that sampling day from the analysis.

With our dataset of *Litoria caerulea* WBC profiles, we first compared bootstrapped 2.5th, 25th (first quartile), 50th (median), 75th (third quartile), and 97.5th quantiles for baseline proportions of each WBC type to those of 161 free-ranging *L. caerulea* (Young et al. 2012). Prior to further statistical analyses, we arcsine square root-transformed the proportions of each WBC type to approximate normal distributions. To compare the WBC profiles of frogs on each blood sampling day, we performed permutation multivariate analyses of variance (MANOVAs; adonis function in vegan package; method = Euclidean; 5,000 permutations; Oksanen et al. 2016), with proportions of each WBC type as the response variables and acclimation temperature (16°C or 26°C) as the predictor variable. For sampling days after the temperature shift (days 6, 21, 33), we only included frogs shifted to the intermediate temperature (21°C) and we included infection status (infected or uninfected) as an additional predictor. To test for confounding immunologic factors, we performed permutation MANOVAs with WBC profiles of sham-inoculated frogs (separately for those with uninterrupted exposure to 16°C and uninterrupted exposure to 26°C) as the response variable and blood sampling event (baseline, day 6, day 21, day 33) as the predictor variable. When permutation MANOVAs indicated significant differences between groups, we visualized differences in WBC profiles with plots generated from canonical discriminant analyses.

To test for effects of experimental treatments on relative WBC concentrations, we fit a generalized linear model (glm function in stats package; R Core Team, 2015) with the number of microscope fields as the response variable, acclimation temperature and infection status as interactive predictor variables, and a Poisson error distribution.

3.4 Results

Hereafter, the terms '16°C-history' and '26°C-history' refer to frogs that were inoculated and housed at 21°C, but with 16°C and 26°C temperature histories, respectively. All

Bd-inoculated frogs had detectable Bd infections by day 6 except for three 16°C-history individuals that developed detectable infections by day 14. Our linear mixed-effect model indicated a highly significant effect of day ($\text{chisq} = 37.561$; $\text{df} = 1$; $p < 0.001$); infection loads generally increased over time (Fig. 3.3). On day 33, we observed excessive skin shedding (a clinical sign of chytridiomycosis) in three 16°C-history frogs and one 26°C-history frog. One 16°C-history frog died on day 41, at which point we terminated the experiment and treated all frogs with Itraconazole. Infection loads, although quite variable within groups, consistently averaged higher among the 26°C-history frogs than among the 16°C-history frogs (Fig. 3.3). The results of our linear mixed-effect analysis indicated that this effect was close to statistical significance ($\text{chisq} = 3.632$; $\text{df} = 1$; $p = 0.057$). By the time of the last two sampling events on days 36 and 41, the average infection loads of 26°C-history frogs were 84,175 and 94,718 zoospore equivalents higher than those of 16°C-history frogs, respectively (Fig. 3.3).

Baseline WBC proportions fell within the range (or, in the case of monocytes, slightly below the range) of previously published values for 161 free-ranging *Litoria caerulea* (Young et al. 2012), but were less variable than in the free-ranging individuals, often with medians and quartiles not aligned with those for free-ranging individuals (Fig. 3.4). Baseline WBC profiles differed between the two acclimation temperatures (permutation MANOVA for baseline data; $p = 0.002$). Profiles of 16°C-acclimated frogs were relatively neutrophil-rich and lymphocyte-poor (open blue circles in fig. 3.5a, b), whereas profiles of 26°C-acclimated frogs were relatively neutrophil-poor and lymphocyte-rich (open pink circles in fig. 3.5a, b). Lymphocytes were the most abundant WBC type (averaging 66% among 16°C-acclimated frogs and 80% among 26°C-acclimated frogs at baseline), followed by neutrophils (16°C: 28%; 26°C: 15%), basophils (16°C: 2%; 26°C: 3%), monocytes (16°C: 2%; 26°C: 1%) and eosinophils (16°C: 1%; 26°C: 1%; Fig. 3.4). Monocytes and eosinophils were infrequently encountered throughout the experiment and their relative percentages contributed little to differences among the WBC profiles of experimental groups. We therefore focus on lymphocytes, neutrophils, and basophils for the remainder of the paper.

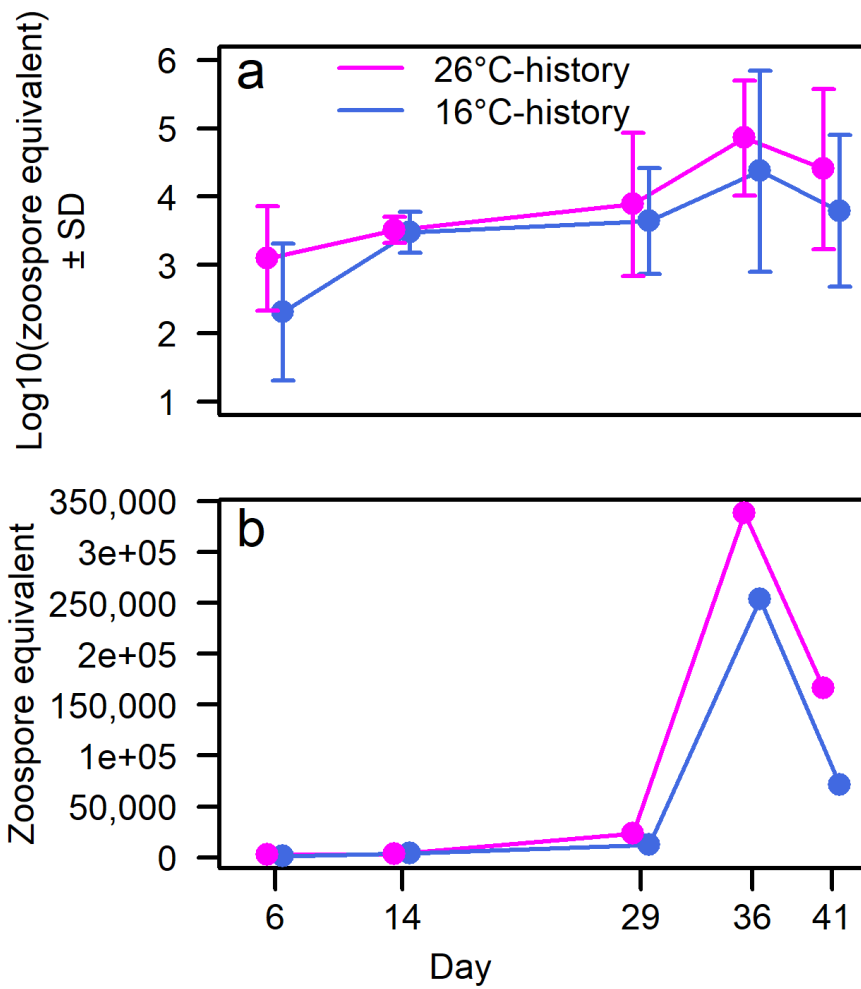


Figure 3.3 (a) Average of logged Bd zoospore equivalents (\pm SD) in *Litoria caerulea* housed at 21°C but acclimated to 26°C (pink) or 16°C (blue) prior to inoculation. (b) Actual zoospore equivalents for reference.

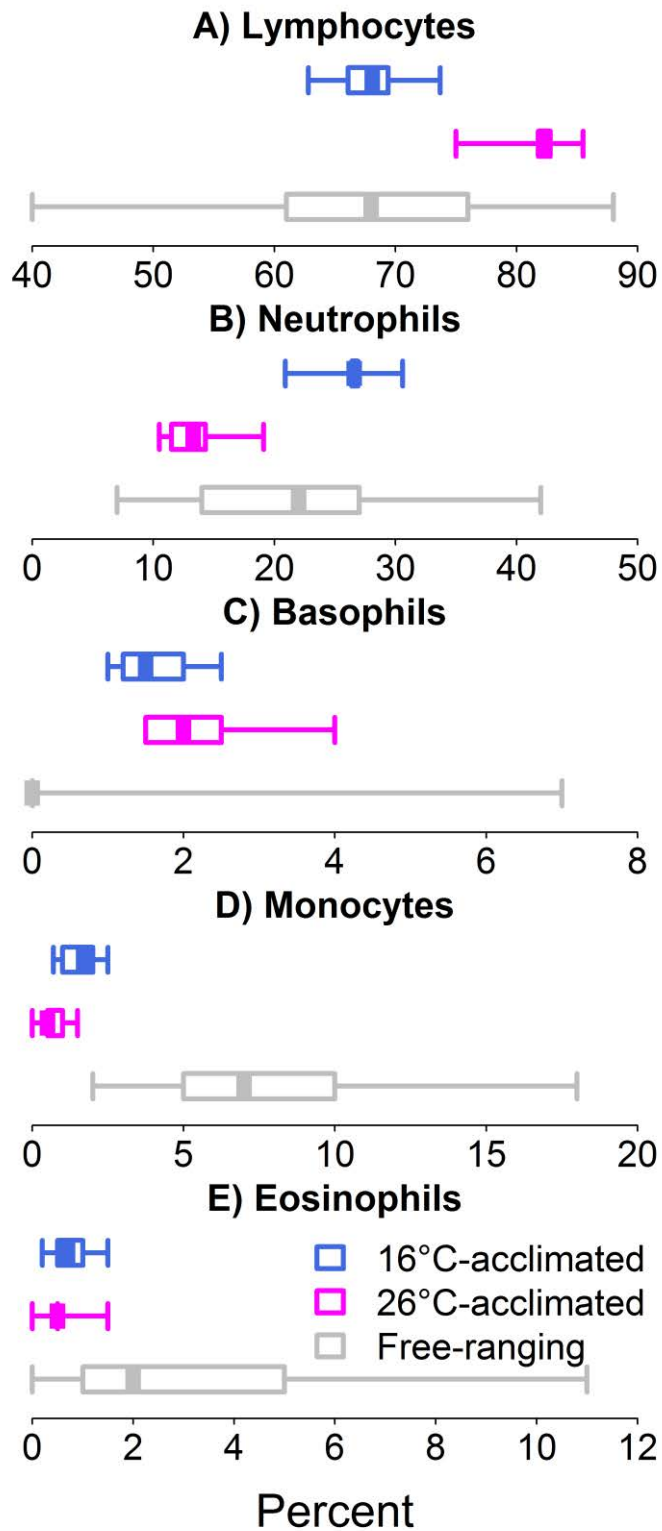


Figure 3.4 Bootstrapped descriptive statistics for the white blood cell profiles of 16°C-acclimated, 26°C-acclimated, and free-ranging (Young et al. 2012) *Litoria caerulea*.

After inoculation with Bd and the shift to 21°C, we failed to detect differences in WBC profiles between the two acclimation temperatures (permutation MANOVAs; day 6: $p = 0.157$; day 21: $p = 0.178$; day 33: $p = 0.088$). The WBC profiles of Bd-infected, 16°C-history frogs generally remained as relatively neutrophil-rich and lymphocyte-poor as at baseline (blue lines are relatively flat in fig. 3.5a, b). Average percentages of lymphocytes in infected, 16°C-history frogs were 58% (day 6), 65% (day 21), and 58% (day 33), which were similar to an average of 66% at baseline (blue line in fig. 3.5a). Likewise, average percentages of neutrophils in infected, 16°C-history frogs were 30% (day 6), 23% (day 21), and 27% (day 33), which were similar to an average of 28% at baseline (blue line in fig. 3.5b). In contrast, the WBC profiles of infected, 26°C-history frogs shifted from relatively lymphocyte-rich and neutrophil-poor at baseline to neutrophil-rich and lymphocyte-poor after the temperature shift (sharp decline in pink line after baseline in fig. 3.5a; sharp incline in pink line after baseline in fig. 3.5b). Average percentages of lymphocytes in infected, 26°C-history frogs were 42% (day 6), 59% (day 21), and 50% (day 33), compared to a higher average of 80% at baseline (pink line in fig. 3.5a). Average percentages of neutrophils in infected, 26°C-history frogs were 37% (day 6), 27% (day 21), and 34% (day 33), compared to a lower average of 15% at baseline (pink line in fig. 3.5b). The infected, 26°C-history frogs also differed from the other experimental groups in their markedly high proportions of basophils on all three sampling days (closed pink circles in fig. 3.5c).

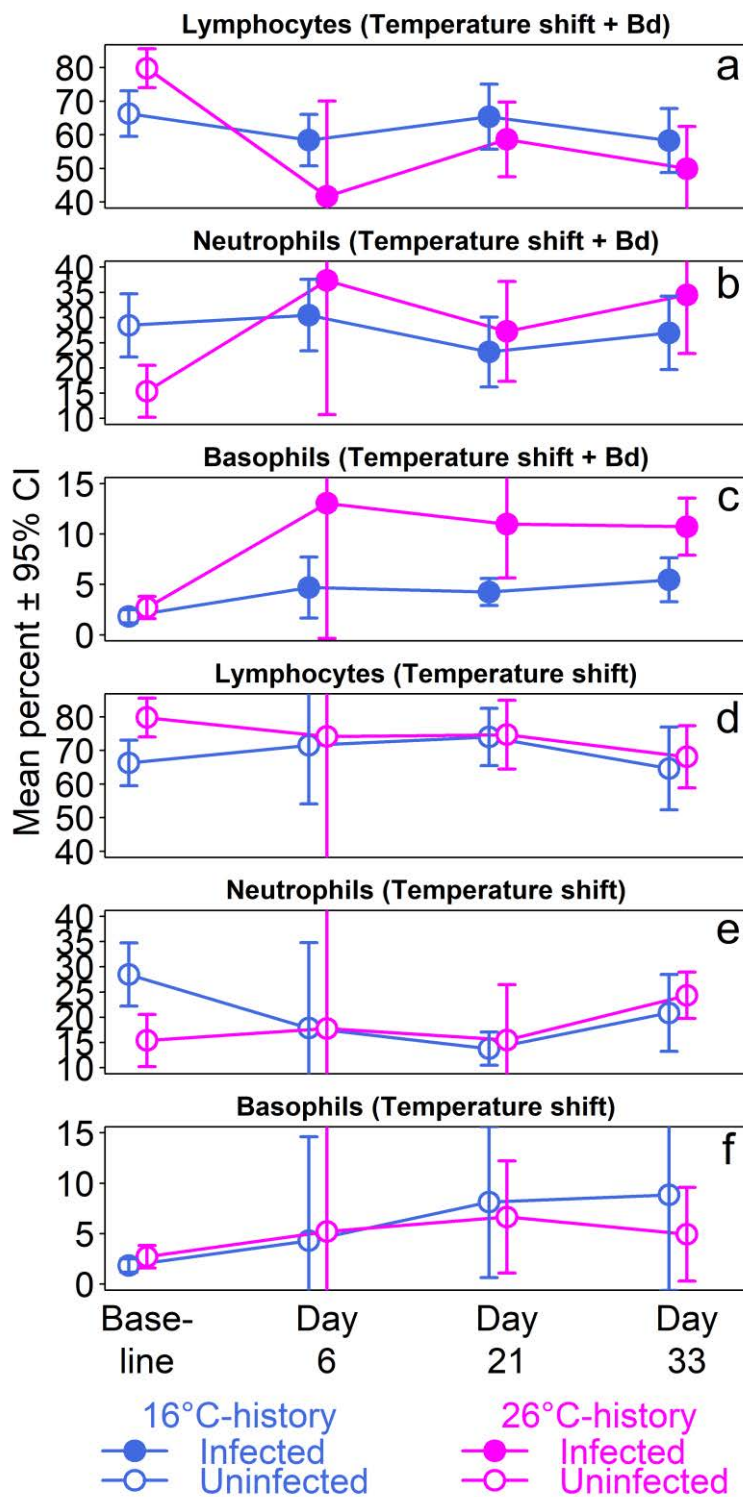


Figure 3.5 Relative percentages of circulating lymphocytes, neutrophils, and basophils for *Litoria serrata* at baseline (housed at 16°C or 26°C) and at three time intervals post-treatment (shifted to 21°C). A treatment group was inoculated + with *Batrachochytrium dendrobatidis* after baseline white blood cell profiles were recorded (a-c). A control group was sham-inoculated and remained uninfected (d-f).

We detected a statistically significant effect of infection status on WBC profiles for day 6 and day 21 but not for day 33 (permutation MANOVAs; day 6: $p = 0.008$; day 21: $p = 0.019$; day 33: $p = 0.084$). In contrast to the infected frogs, which either maintained or acquired relatively high N:L ratios following inoculation and exposure to 21°C, the uninfected frogs generally maintained or acquired relatively low N:L ratios (Fig. 3.5d, e). Compared to baseline, N:L ratios generally remained static in 26°C-history frogs (pink lines between baseline and day 21 are relatively flat in fig. 3.5d, e) and decreased in 16°C-history frogs (incline in blue line after baseline in fig. 3.5d; decline in blue line after baseline in fig. 3.5e). Among control frogs that remained exposed to their acclimation temperatures during the experiment, the relative numbers of WBCs did not differ by day (0 d, 6 d, 21 d, 33 d; cold: $p = 0.522$; hot: $p = 0.444$), suggesting that immunologic factors were not confounded by experimental handling and blood collection.

Our generalized linear models revealed statistically significant interactive effects of acclimation temperature and infection status on the number of microscope fields examined for day 21 ($z = 6.595$; $p < 0.001$) and day 33 ($z = 4.571$; $p < 0.001$). Among 16°C-history frogs, numbers of microscope fields examined were similar between infected and uninfected frogs (Fig. 3.6). Among 26°C-history frogs, numbers of microscope fields were markedly higher for infected frogs than for uninfected frogs, indicating lower relative concentrations of circulating WBCs in infected frogs (Fig. 3.6).

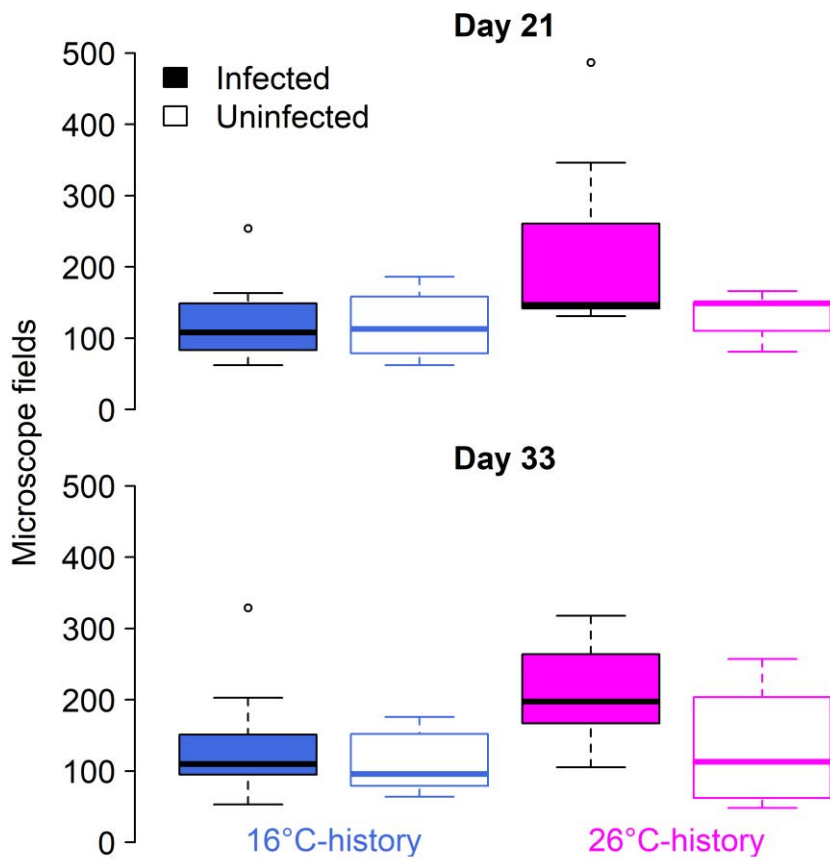


Figure 3.6 Number of microscope fields examined to identify 200 white blood cells (WBC) in blood smears from *Litoria serrata* housed at 21°C from four infection status (*Batrachochytrium dendrobatidis* [Bd]-infected vs. uninfected) X thermal history (16°C vs. 26°C) treatments at two time intervals post-inoculation. We used this metric as an estimate of the relative concentration of WBCs in the blood; the higher the number of microscope fields, the lower the concentration of WBCs.

3.5 Discussion

In our study, average infection loads of frogs housed at 21°C were higher in frogs previously acclimated to 26°C, a group that experienced a 5°C temperature decrease, than in frogs previously acclimated to 16°C, a group that experienced a 5°C temperature increase. This result is consistent with the findings that increases in Bd loads associated with temperature shifts were greater following temperature decreases than following temperature increases in red-spotted newts (Raffel et al. 2015) and Cuban tree frogs (Raffel et al. 2013) and could help to explain mass die-offs of wild green tree frogs in and around Brisbane, Australia, shortly after temperature drops (Berger et al. 2004). Although this pattern only approached statistical significance, our results are convincing considering that Bd infection loads are commonly quite variable within experimental groups (e.g., Voyles et al. 2009) and that we observed this pattern over five separate sampling days, whereas previous studies measured infection loads on only a single sampling day (Raffel et al. 2013, 2015). By the end of our experiment, the average infection load of 26°C-history frogs was nearly 100,000 zoospore equivalents higher than those of 16°C-history frogs, a difference that could drastically lower chances of survival in this disease system (Briggs et al. 2010; Vredenburg et al. 2010; Kinney et al. 2011).

By quantifying WBC profiles before and after a temperature shift, we identified a possible mechanism for the observation that taxonomically and ecologically diverse amphibian species are more susceptible to Bd infection following temperature decreases compared to temperature increases. Both 16°C- and 26°C-history frogs exhibited the signature WBC profile of an activated immune system following inoculation with Bd. This outcome is consistent with the previous findings that Bd-infected *Litoria caerulea* (our study species; Peterson et al. 2013; Young et al. 2014), *Lithobates catesbeianus* (Davis et al. 2009), *Pseudacris regilla*, and *Rana cascadae* (Gervasi et al. 2014) had elevated numbers of neutrophils, lower numbers of lymphocytes than healthy individuals, or both. Our study is distinct from most others in capturing these changes on multiple sampling days and beginning early in the progression of infection (day 6). However, the 16°C- and 26°C-history frogs in our study differed in that 16°C-history frogs had high N:L ratios at baseline, indicating thermal effects on haematopoiesis, which were conserved post-treatment (inoculation with Bd + temperature shift). High N:L ratios in cold-acclimated frogs may indicate an evolutionary adaptation to seasonality, in which the cellular immune system is primed for future vulnerability, such as the transition from inactive (cool or cold) to active (warm or hot) periods when the animal is likely to encounter increased immune challenge (Cooper et al. 1992). For example, northern leopard frogs (*Rana*

pipens) in hibernation for 5 mo had elevated proportions of circulating neutrophils (Maniero and Carey 1997) and cold-acclimated fire salamanders (*Salmandra salamandra*) and common toads (*Bufo bufo*) had elevated levels of phagocytic activity of white blood cells (Pxytycz and Jozkowicz 1994), adaptations that could protect animals when other immune defenses are less active, or prepare the animal for increased risk of encountering immune challenges in spring (Pxytycz and Jozkowicz 1994). Thus, infection with Bd may have caused fewer changes to the immune system in the 16°C-history frogs, because they had already adjusted immune parameters in response to stressful climatic conditions (cold).

In contrast, the 26°C-acclimated frogs had low N:L ratios at baseline, which reversed as early as 6 d post-treatment. In addition, the 26°C-history frogs had higher proportions of circulating basophils and lower relative WBC concentrations. Previous observations on the links between proportions of basophils and Bd infection were inconclusive (Woodhams et al. 2007a; Raffel et al. 2010) but basophils are considered to play a major role in responses to parasitic infections and basophilia has also been linked to high levels of stress in reptiles (Frye 1991; Karasuyama and Yamanishi 2014). Since hematocrits were not measured, variation in relative WBC concentrations could have been confounded by differences in hydration status between groups. However, this is unlikely because all groups in this analysis were housed at 21°C and chytridiomycosis did not result in altered hematocrits in previous laboratory infections (Voyles et al. 2009). Alternatively, low relative WBC concentrations may indicate slowed production due to exhaustion after extended immune stimulation, stress, or immunosuppression (Gervasi and Foufopoulos 2008), which could be an effect of high Bd burdens (Young et al. 2014; Brannelly et al. 2016). Thus, infection with Bd may have been relatively more physiologically taxing for the 26°C-history frogs because they had not previously acclimated to challenging conditions.

Although the frogs in our study responded to Bd with signs of activated cellular immune functions, they still developed infection intensities that were potentially lethal (Briggs et al. 2010; Vredenburg et al. 2010; Kinney et al. 2011). Migration of WBCs to sites of infection (inflammation) is rarely observed in animals with severe Bd infections (Berger et al. 1998; Pessier et al. 1999; Berger et al. 2005b), at least in part because Bd has the ability to release immune-inhibiting molecules from its cell wall (Rollins-Smith et al. 2015). Instead, researchers have proposed that the redistribution of WBCs in Bd-infected animals may be more strongly stimulated by increases in epidermal damage, secondary bacterial infections, or general infection-induced stress (Berger et al. 2005a; Davis et al. 2009). In the only study, to our

knowledge, to conflict with our results pertaining to WBC profiles of Bd-infected animals, Bd-infected *L. chloris*, a species that is less susceptible to Bd infection than *L. caerulea*, had fewer circulating neutrophils than uninfected frogs (Woodhams et al. 2007a). The authors suggested that in contrast to more susceptible species in which neutrophils are rarely seen on skin histology, the relative resistance of this species to Bd infection could be linked to an ability to somehow bypass the immune-inhibiting products of Bd and mount an effective inflammatory response in which neutrophils migrated out of circulation and into sites of infection (Woodhams et al. 2007a).

Although it is generally accepted that cold temperatures are immunosuppressive to amphibians, our study demonstrates that this may be an oversimplification of the interactions between temperature and immunity in ectotherms. We demonstrate that making physiological adjustments to cope with cold temperatures (acclimating) may actually prime the cellular immune system for some of the challenges of Bd infection. A caveat to our study, however, is that the WBC profiles of wild *L. caerulea* (Young et al. 2012) were much more variable than those of frogs from our constant-temperature acclimation treatments, potentially because wild frogs experience diurnal and seasonal fluctuations in body temperature. Thus, differences between the WBC profiles of frogs from different habitats may not always be as clear-cut as in a controlled laboratory setting. Even so, our data suggest that frogs facing increases in temperature may be better poised to confront infections than those facing decreases in temperature. These findings underscore the concern raised by Raffel et al. (2012) that increases in the frequency of heat waves predicted under climate change will by definition be followed by increases in the frequency of temperature drops (back to 'normal' temperatures) which are associated with impaired immunity. However, this may be limited to habitats in which temperature ranges are generally small to intermediate, because frogs living in locations with extreme temperatures may not have Bd (Olson et al. 2013). A useful avenue for future study will be more in-depth immune profiling at fluctuating frog body temperatures, particularly when more is known about the components of the immune system that are protective against Bd.

3.6 Highlights

- We assessed frog immunity after infection and a temperature increase or decrease.
- Cold-acclimated frogs had active immune systems before and after the treatment (infection and temperature increase).
- Hot-acclimated frogs had active immune systems only after the treatment (infection and temperature decrease) and had higher Bd burdens than the cold-acclimated frogs.
- Cold acclimation may prime the immune system for some challenges of infection.
- This helps explain high levels of disease susceptibility after temperature decreases.

Chapter 4 Infection increases vulnerability to climate change via effects on host thermal tolerance

Sasha E. Greenspan, Deborah S. Bower, Elizabeth A. Roznik, David A. Pike, Gerry Marantelli, Ross A. Alford, Lin Schwarzkopf, Brett R. Scheffers

This chapter has been published in Scientific Reports by Nature Publishing Group as an open access article under the terms of the Creative Commons Attribution License and is reproduced here with no changes.

Link to article: <https://www.nature.com/articles/s41598-017-09950-3>

Link to license: <https://creativecommons.org/licenses/by/4.0/>

Citation for article: Greenspan SE, Bower DS, Roznik EA, Pike DA, Alford RA, Schwarzkopf L, Scheffers BR (2017). Infection increases vulnerability to climate change via effects on host thermal tolerance. Scientific Reports 7:9349.

Citation for data in Tropical Data Hub: Greenspan, S. (2017). *Batrachochytrium dendrobatidis* infection data for Chapter 4 of PhD thesis: Thermal thresholds in the amphibian disease chytridiomycosis. James Cook University. [Data Files]

<http://dx.doi.org/10.4225/28/5a0d1c14511d8>

DOI: [10.4225/28/5a0d1c14511d8](https://doi.org/10.4225/28/5a0d1c14511d8)

Contributions: SEG and BRS co-developed the study. SEG, DSB, and BRS carried out the lab work. SEG carried out the statistical analyses with assistance from RAA and BRS. SEG drafted the manuscript and developed the figures and tables except Fig. 5.4 (BRS). All authors provided editorial input.

4.1 Abstract

Unprecedented global climate change and increasing rates of infectious disease emergence are occurring simultaneously. Infection with emerging pathogens may alter the thermal thresholds of hosts. However, the effects of fungal infection on host thermal limits have not been examined. Moreover, the influence of infections on the heat tolerance of hosts has rarely been investigated within the context of realistic thermal acclimation regimes and potential anthropogenic climate change. We tested for effects of fungal infection on host thermal tolerance in a model system: frogs infected with the chytrid *Batrachochytrium dendrobatidis*. Infection reduced the critical thermal maxima (CT_{max}) of hosts by up to $\sim 4^{\circ}\text{C}$. Acclimation to realistic daily heat pulses enhanced thermal tolerance among infected individuals, but the magnitude of the parasitism effect usually exceeded the magnitude of the acclimation effect. In ectotherms, behaviors that elevate body temperature may decrease parasite performance or increase immune function, thereby reducing infection risk or the intensity of existing infections. However, increased heat sensitivity from infections may discourage these protective behaviors, even at temperatures below critical maxima, tipping the balance in favor of the parasite. We conclude that infectious disease could lead to increased uncertainty in estimates of species' vulnerability to climate change.

4.2 Introduction

Projections of the future global climate indicate that temperature means, variances, and extremes will change (Easterling 2000; Räisänen 2002; Meehl 2004; Schar et al. 2004; Yeh et al. 2009; Stocker et al. 2013). These changes may be hazardous for some animals by shifting daily, seasonal, or intermittent temperature cycles away from optimal conditions or closer to lethal extremes (Bernardo and Spotila 2006). Risks to populations due to climate change can be estimated using warming tolerance, which is the difference between the species' maximum heat tolerance (critical thermal maximum [CT_{max}]) and maximum environmental temperature (Lutterschmidt and Hutchison 1997; Somero 2005; Deutsch et al. 2008; Duarte et al. 2012). When this value is large, individuals theoretically have a high thermal safety margin in the context of rising environmental temperatures (Duarte et al. 2012). In contrast, when this value is small, risk is high because even slight increases in environmental temperatures may cause the body temperatures of individuals to reach lethal limits (Welbergen et al. 2008). This is further compounded when temperatures approaching critical thermal maxima lead to behaviors or ecological interactions that reduce fitness. For example, heat stress may cause individuals to seek refuge at the expense of activities that promote fitness (e.g., foraging or reproduction) (Sinervo et al. 2010). Similarly, altered temperature patterns may lead to changes in phenology, resource availability, or predator interactions that threaten individual and population survival (Ockendon et al. 2014).

Thermal stress and fitness costs associated with global climate change are likely to occur in combination with other natural and anthropogenic stressors such as land use change, environmental contaminants, and disease (Brook et al. 2008; Carilli et al. 2010; Nowakowski et al. 2017). Fungal diseases are currently emerging at record rates, posing a direct threat to global biodiversity in the face of climate change (Fisher et al. 2012). Reduced maximum thermal tolerance can be a major side effect of infections in amphibians (Sherman 2008), fish (Vaughan and Coble 1975; Lutterschmidt et al. 2007), and mollusks (Vernberg and Vernberg 1963; McDaniel 1969; Lee and Cheng 1971; Tallmark and Norrgren 1976; Lauckner 1980; Lauckner 1983; Bates et al. 2011). For example, ill newts *Notophthalmus viridescens* infected with a mesomycetozoon parasite had lower CT_{max} than uninfected newts (by 0.6–1.7°C; Sherman 2008). Similarly, resistance to high temperature (hours at 25°C until 50% mortality) was lower in brook trout *Salvelinus fontinalis* infested with gill lice *Salmincola edwardsii*, and was inversely correlated with extent of secondary bacterial infection, a measure of fish health (Vaughan and Coble 1975). Thus, infections have the potential to synergistically interact with

ectotherm physiology to reduce warming tolerance, which could render individuals and populations more vulnerable to rising temperatures from climate change or habitat modification. However, the effect of fungal infection on host thermal limits has not been tested and the influence of infections on host thermal limits has rarely been investigated in the context of realistic, fluctuating thermal acclimation regimes.

Here we investigate interactions between fungal disease and upper thermal tolerance in a model host-pathogen system: frogs infected with the chytrid *Batrachochytrium dendrobatidis* (Bd; Longcore et al. 1999). We experimentally infected frogs with Bd and acclimated them to constant cool temperatures or daily heat pulses mimicking the body temperature regimes of frogs in nature. We then examined the effects of Bd infection status, infection intensity and acclimation on their critical thermal maxima and considered the implications of our findings in light of current and projected global change.

4.3 Methods

Acclimation temperature treatments

To generate realistic acclimation temperature treatments, we used body temperature data from *Litoria serrata*, a stream-associated frog of the Australian Wet Tropics (Roznik 2013). We used temperature-sensitive radio-transmitters (Model A2414; Advanced Telemetry Systems, Isanti, MN) to record the body temperatures of 54 male frogs in rainforests during the dry season (when Bd is typically most prevalent in this region; Roznik 2013). The radio-transmitters recorded frog body temperatures every 15 min for 5–11 d. We created simplified, rectangular-wave acclimation temperature treatments to approximate the patterns we found in the field data. We derived the trough temperatures of the rectangular wave treatments from the overall medians of individual median body temperatures at the two high elevation sites (750-800 m elevation; 15°C) and two low elevation sites (20-100 m elevation; 18°C) where tracking occurred (Roznik 2013). We derived the crest temperatures of the rectangular wave treatments from the median of individual maximum body temperatures > 25°C at the same sites (high elevation: 26°C; low elevation: 29°C; Roznik 2013). We derived the crest length of the rectangular waves from the median of the individual maximum lengths of time that frogs spent with body temperatures >25°C for all sites combined (4 h; Roznik 2013).

Thus, our two high elevation treatments were (1) a daily rectangular wave with trough at 15°C for 20 h per day and crest at 26°C for four hours per day (hereafter high elevation heat pulse; inoculated: n = 11; control: n = 5) and (2) a constant 15°C control treatment (hereafter

high elevation constant; inoculated: n = 11; control: n = 5; Figure 4.1). Our two low elevation treatments were (1) a daily rectangular wave with trough at 18°C for 20 hours per day and crest at 29°C for four hours per day (hereafter low elevation heat pulse; inoculated: n = 17; control: n = 5) and (2) a constant 18°C control treatment (hereafter low elevation constant; inoculated: n = 10; control: n = 5; Figure 4.1). The constant temperature control treatments (15°C and 18°C) served as a standard against which to observe effects of acclimation to realistic heat pulses on host thermal tolerance. Our temperature treatments are also pertinent to *Bd* physiology as this fungus shows optimal short-term growth at 15–25°C, and ceases growth and reproduction at 26–29°C (Longcore et al. 1999; Piotrowski et al. 2004; Stevenson et al. 2013).

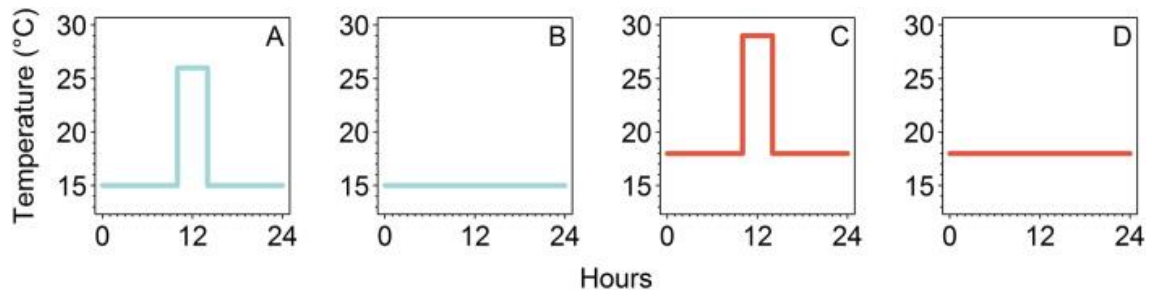


Figure 4.1 Daily acclimation temperature regimes for experiment investigating the effects of *Batrachochytrium dendrobatidis* infection status, infection intensity, and thermal acclimation on the upper thermal tolerance of the model amphibian host *Litoria spenceri*. (A) daily rectangular wave with trough at 15°C and crest at 26°C for four hours, (B) constant 15°C, (C) daily rectangular wave with trough at 18°C and crest at 29°C for four hours, (D) constant 18°C.

Bd cultures and inoculations

We used the *Bd* isolate Paluma-Lseratta-2012-RW-1. This isolate is part of the collection maintained at the College of Public Health, Medical, and Veterinary Sciences, James Cook University. This isolate originated from an adult *L. serrata* that was collected from Birthday Creek, a site in the Wet Tropics region of Queensland, Australia (18°58'54" S, 146°10'02" E), and died in captivity. The isolate had been cryo-archived after two passages in nutrient broth. We revived an aliquot of the isolate and cultured it in tryptone/gelatin hydrolysate/lactose (TGhL) broth in 25-cm³ tissue culture flasks, passaging it twice before the experiment and maintaining cultures at 22°C.

To obtain zoospores for inoculations, we inoculated Petri dishes containing TGhL broth in 1% agar with ~1/3 ml of cultured broth. Plates were partially dried in a laminar flow cabinet, incubated at 21°C for four days, and then maintained alternately at 4°C and 21°C to sustain growth and zoospore production. For each inoculation, we added up to 4 ml of deionized (DI) water to the dishes to form a zoospore suspension. We then combined the liquid contents of each dish, calculated the concentration of zoospores with a hemocytometer (Neubauer Improved Bright-line), and added DI water to produce a final concentration of 1×10^6 zoospores per ml. We prepared a sham (control) inoculant by following the same protocol but with Petri dishes containing only nutrient agar.

All experimental protocols were approved by the James Cook University Animal Ethics Committee in accordance with permit A2234. We experimentally infected captive-reared (sourced from a captive breeding facility at the Amphibian Research Centre, Victoria, Australia), juvenile *Litoria spenceri*. Use of captive-reared frogs ensured no previous exposure to *Bd*, which can influence the progression of subsequent infections (McMahon et al. 2014); captive-reared *L. serrata* were unavailable. Our host species basks on streamside rocks and thus could experience similar patterns of temperature variation in its native habitat (Gillespie and Hollis 1996). Experimental *Bd* inoculations often yield infection rates < 100% and infection levels are commonly quite variable over time. We therefore used a lower number of sham-inoculated control animals (n = 5 per treatment) than *Bd*-inoculated treatment animals (n = 10–17 per treatment) to maximize our samples of infected individuals and capture natural variability in infection levels.

We inoculated frogs on three consecutive days. To inoculate, we placed each frog into an individual 70-ml plastic container and added 3 ml of zoospore inoculant or sham inoculant (enough to cover the bottom of the container) to each container using a syringe. We left frogs

in inoculant baths for eight hours per day. To ensure regular contact of frogs with the inoculant, we monitored frogs every 15 minutes during each inoculation period. If a frog had climbed out of the inoculant onto the wall of the container, we gently tilted the container to bathe the frog in the inoculant. After each inoculation period, we returned frogs with their inoculant to individual permanent enclosures comprising 70 x 120 x 170 mm plastic containers lined with tap water-saturated paper towel.

We allocated frogs in their individual enclosures to 24 temperature-controlled chambers (Greenspan et al. 2016) on the day after the last inoculation. Six replicate chambers were programmed to execute each of the four acclimation temperature treatments. The chambers were arranged in a blocked design, such that there were six spatial blocks, each containing one chamber following each of the four temperature treatments. The location of each temperature treatment within each block was determined randomly. We distributed inoculated and control frogs into the chambers as evenly as possible and reduced effects of frog history and body size by assigning frogs to temperature treatments proportionally by clutch of origin (reported by captive breeding facility) and snout-urostyle length (measured prior to inoculation). We systematically rotated the placement of the frog enclosures within each chamber every other day to ensure that they were evenly exposed to any local differences in temperature that might exist within the chamber.

Frog disease monitoring and husbandry

To monitor Bd infection status and intensity, we swabbed frogs upon delivery from the captive breeding facility (all frogs tested negative for Bd before the experiment) and every eight days thereafter following a standard protocol (Stockwell et al. 2015). We determined the number of Bd zoospore genome equivalents (ZGE) per swab with a real-time quantitative PCR protocol modified from Boyle et al. (2004).

The temperature-controlled chambers were programmed to maintain a 12 hr: 12 hr light: dark cycle. Every other day, we moistened the paper towels in frog containers with tap water as needed to maintain a consistent moisture level (paper towels were saturated but there was no standing water) and fed frogs pinhead crickets *ad libitum*. We changed paper towels at every other feeding and measured CT_{max} on days on which feeding did not occur.

CT_{max} measurement and statistical analysis

Our goal was to measure CT_{max} when frogs had well-developed infections but before they displayed clinical signs of infection. By day 36, infection loads in most inoculated frogs

were relatively high; in an effort to avoid morbidity and mortality from infection, we measured CT_{max} for a subset of inoculated frogs ($n = 6$ of the most heavily infected frogs in each acclimation temperature treatment) as well as for all control frogs ($n = 5$ per temperature treatment) on day 36. We then determined relative risk of morbidity and mortality using a receiver operating characteristic (ROC) analysis for a concurrent experiment with the same cohort of *L. spenceri* (Stockwell et al. 2016). This analysis indicated that frogs with infection loads $>13,700$ ZGE had a 63% chance of dying or showing signs of chytridiomycosis. Subsequently, we measured CT_{max} for the remaining inoculated frogs gradually over time, as swab results indicated that frogs were approaching or had exceeded the threshold infection intensity of 13,700 ZGE. We measured CT_{max} within 48 hours of swabbing. All frogs were processed by day 56 except for 10 frogs from the low elevation heat pulse treatment that were excluded from analyses because they never reached the threshold infection intensity and eventually cleared their infections, possibly due to their temperature treatments. All inoculated frogs had sub-clinical Bd infections when we measured CT_{max} .

To measure CT_{max} , we placed individual frogs into a perforated container containing a suspended thermocouple. Each frog was brought to room temperature in its permanent enclosure and then transferred to the perforated container and placed in a temperature-controlled chamber (Greenspan et al. 2016) programmed to increase from room temperature at a rate of $\sim 1^{\circ}\text{C}$ per minute. This rate of temperature increase allows the body temperature of small ectotherms to follow ambient temperature without an appreciable time lag, and is routinely used for measuring CT_{max} (Scheffers et al. 2013; Kolbe et al. 2014).

We used two measures of CT_{max} (Lowe and Vance 1955): onset of spasms (Kowalski et al. 1978) and loss of righting ability (Lee and Rinne 1980). Onset of spasms, when frogs began displaying erratic movements such as increased jumping and leg twitches, was the first sign of thermal discomfort. We considered this metric to be a conservative estimate of the temperature at which a frog will seek refuge from high temperatures in the wild. After onset of spasms, at each 1°C increase in chamber temperature, we quickly opened the chamber, gently moved the container until the frog jumped, and closed the chamber. Loss of righting ability, an animal's upper heat threshold, was determined when animals were unable to right themselves for three seconds after this manipulation. To minimize stress to the frogs, we elected to record the ambient (i.e., thermocouple) temperature at each behavioral indicator of CT_{max} for each frog. Frogs were then immediately placed in room-temperature water to recuperate (all frogs

survived). After a recovery period following CT_{max} measurement, we treated Bd infections with Itraconazole (Brannelly et al. 2012).

To determine frog body temperatures at CT_{max} , we later exposed four haphazardly selected *L. spenceri* of average sizes to the same program of gradually increasing temperature in the same chamber, following Itraconazole treatment. For each frog, we recorded body temperature at 25°C, 30°C, 35°C, and 40°C ambient temperature. We measured body temperature with a non-contact infrared thermometer (OS425-LS, Omega Engineering Ltd, Irlam, Manchester, UK; emissivity 0.95) (Rowley and Alford 2007). We then modeled the relationship between ambient and body temperatures using linear regression and used this analysis to convert ambient CT_{max} temperatures to body temperatures for all experimental frogs ($y = 0.7985x + 4.0675$; $R^2 = 0.9886$; 95% confidence interval for slope = 0.751, 0.846; 95% confidence interval for intercept = 2.503, 5.632).

We used R software for all statistical analyses (R Core Team 2015). We used analyses of covariance (ANCOVAs; Anova function in car package; Fox and Weisberg 2011) to test for effects of Bd infection status (infected or uninfected), elevation (high [15°C] vs. low [18°C] acclimation treatments), heat exposure (pulse [26°C or 29°C] vs. constant acclimation treatments) and interactions between infection status and acclimation on our metrics of CT_{max} , with snout-urostyle length as a covariate ($n = 69$; $\alpha = 0.05$). To determine whether infection intensity might affect thermal tolerance, we performed separate ANCOVAs using data for infected frogs only, with log-transformed ZGE values as the infection variable ($n = 39$; $\alpha = 0.05$).

4.4 Results

The critical thermal maxima of our model frog species *Litoria spenceri*, measured as temperature at onset of spasms and temperature at loss of righting ability, were significantly lower for Bd-infected frogs than for uninfected frogs (spasms: $p < 0.001$; righting: $p = 0.009$; Table 4.1; Figure 4.2), after controlling for a positive relationship between frog snout-urostyle length and critical thermal maxima (Table 4.1). Across acclimation temperature treatments, mean temperature at onset of spasms (\pm SD) ranged from 34.2°C \pm 2.1°C to 35.6°C \pm 3.1°C in infected frogs and 36.2°C \pm 1.4°C to 38.5°C \pm 1.2°C in uninfected frogs (Table 4.2). Likewise, mean temperature at loss of righting ability ranged from 37.4°C \pm 2.2°C to 39.9°C \pm 1.3°C in infected frogs and 39.6°C \pm 0.5°C to 40.5°C \pm 1.0°C in uninfected frogs (Table 4.2; Figure 4.2).

Table 4.1 Summary of analyses of covariance on the effects of *Batrachochytrium dendrobatidis* infection status, infection intensity, elevation, (high [15°C] vs. low [18°C] acclimation treatments), heat exposure (pulse [26°C or 29°C for four hours per day] vs. constant acclimation treatments) and the interactions between infection and acclimation on two metrics of the critical thermal maximum (temperature at onset of spasms and temperature at loss of righting response) for the model amphibian host *Litoria spenceri*, with frog snout-urostyle length as a covariate.

Response	Predictor	Infection status				Infection intensity			
		Sum of Squares	DF	F-value	P-value	Sum of Squares	DF	F-value	P-value
Onset of spasms	Snout-urostyle length	20.59	1	4.382	0.041	8.523	1	1.309	0.261
	Infection	70.08	1	14.912	< 0.001	0.349	1	0.0536	0.818
	Elevation	1.08	1	0.2291	0.634	0.042	1	0.0065	0.936
	Heat	3.05	1	0.6482	0.424	8.649	1	1.3286	0.258
	Infection x elevation	1.88	1	0.4000	0.530	0.077	1	0.0119	0.914
	Infection x heat	16.27	1	3.461	0.068	7.074	1	1.0866	0.305
	Residuals	244.38	52			208.312	32		
Loss of righting	Snout-urostyle length	6.46	1	3.689	0.060	6.874	1	3.2534	0.081
	Infection	12.75	1	7.2832	0.009	1.089	1	0.5153	0.478
	Elevation	0.02	1	0.0118	0.914	3.257	1	1.5415	0.223
	Heat	4.25	1	2.4268	0.125	1.227	1	0.5807	0.452
	Infection x elevation	4.51	1	2.5762	0.115	4.754	1	2.2500	0.143
	Infection x heat	11.29	1	6.446	0.014	3.173	1	1.5015	0.229
	Residuals	91.06	52			67.614	32		

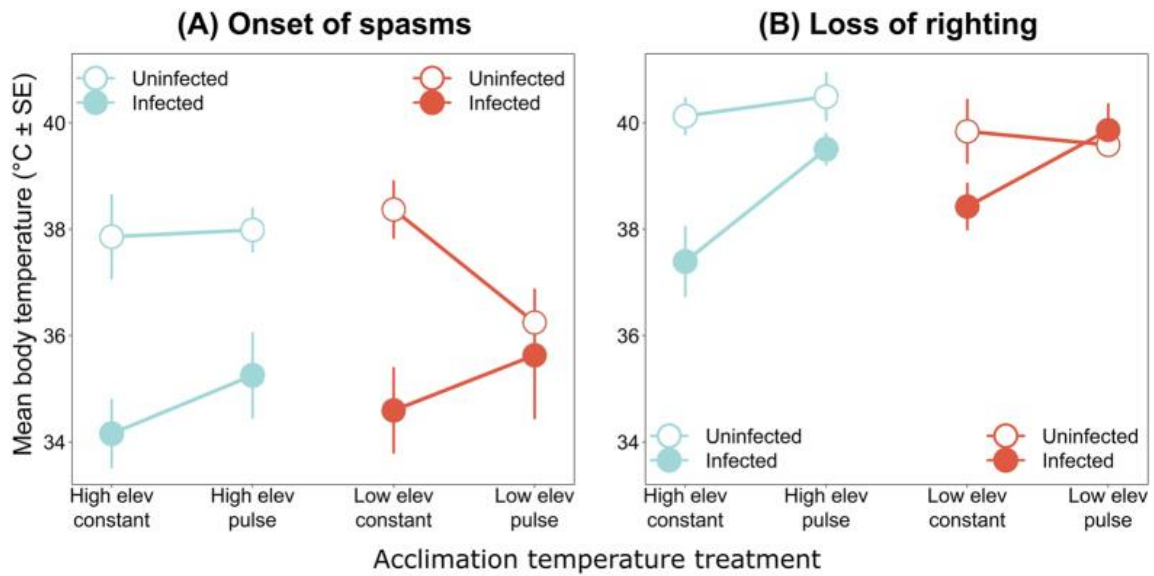


Figure 4.2 Average critical thermal maxima (\pm SE) for the model amphibian host *Litoria spenceri* acclimated to four temperature treatments, with and without infections by the fungus *Batrachochytrium dendrobatidis*. Metrics of the critical thermal maximum were (A) body temperature at onset of spasms and (B) body temperature at loss of righting ability.

Table 4.2 Average critical thermal maxima for the model amphibian host *Litoria spenceri* with and without infections by the fungus *Batrachochytrium dendrobatidis* and average infection intensities of the infected individuals.

Elevation	Temperature regime	Infection intensity (zoospore genome equivalents)		Temperature at onset of spasms (°C)		Temperature at loss of righting (°C)	
		Mean ± SD for day 36 (sample size)	Mean ± SD for all frogs (sample size)	Mean ± SD in infected (sample size)	Mean ± SD in control (sample size)	Mean ± SD in infected (sample size)	Mean ± SD in control (sample size)
High (15°C)	Constant	101,267 ± 161,587 (6)	67,402 ± 133,720 (11)	34.2 ± 2.1 (11)	37.9 ± 1.7 (5)	37.4 ± 2.2 (11)	40.1 ± 0.8 (5)
	Pulse (26°C)	18,113 ± 11,568 (6)	28,486 ± 34,567 (11)	35.3 ± 2.6 (11)	38.0 ± 0.9 (5)	39.5 ± 0.9 (11)	40.5 ± 1.0 (5)
Low (18°C)	Constant	187,267 ± 307,555 (6)	123,031 ± 244,297 (10)	34.6 ± 2.5 (10)	38.5 ± 1.2 (5)	38.4 ± 1.4 (10)	39.8 ± 1.3 (5)
	Pulse (29°C)	8,853 ± 13,121 (6)	9,121 ± 11,999 (7)	35.6 ± 3.1 (7)	36.2 ± 1.4 (5)	39.9 ± 1.3 (7)	39.6 ± 0.5 (5)

The magnitude of the effect of infection status on temperature at loss of righting ability depended on acclimation to heat pulses ($p = 0.014$; Table 4.1); compared to uninfected individuals, the temperature at loss of righting for infected individuals under constant acclimation regimes was reduced by an average of up to 2.7°C , whereas the temperature at loss of righting for infected individuals under pulsed acclimation regimes was only reduced by an average of up to 1°C (Table 4.2; Figure 4.2). A similar pattern emerged for the magnitude of the effect of infection status on temperature at onset of spasms, although this was not statistically significant. Specifically, the temperature at onset of spasms for infected individuals under constant acclimation regimes was reduced by an average of up to 3.9°C , whereas the temperature at onset of spasms for infected individuals under pulsed acclimation regimes was only reduced by an average of up to 2.7°C (Table 4.2; Figure 4.2).

Infection intensity at the time of CT_{max} measurement varied widely among temperature treatments (Figure 4.3). By day 36, the day that we measured CT_{max} in six of the most highly infected frogs from each temperature treatment, the mean infection load exceeded our established threshold for disease development (13,700 ZGE) in all treatments except the low elevation heat pulse treatment (Table 4.2). After day 36, all frogs from both high elevation treatments and the low elevation constant treatment eventually exceeded the threshold infection intensity. In contrast, only one frog from the low elevation heat pulse treatment exceeded the threshold infection intensity after day 36; the other 10 of 17 frogs in this treatment (59%) maintained low infection loads, eventually cleared their infections, and were therefore excluded from the study. Although infection status had a significant effect on CT_{max} , we were unable to detect a statistically significant effect of infection intensity on CT_{max} (Table 4.1). However, low elevation heat pulse was the only treatment in which (1) the negative effect of infection on CT_{max} was greatly reduced (standard errors of mean CT_{max} temperatures for infected and uninfected frogs overlap; Figure 4.2) and (2) the average infection loads on day 36 and for the entire duration of the experiment did not exceed the threshold level of 13,700 ZGE (Table 4.2; Figure 4.3).

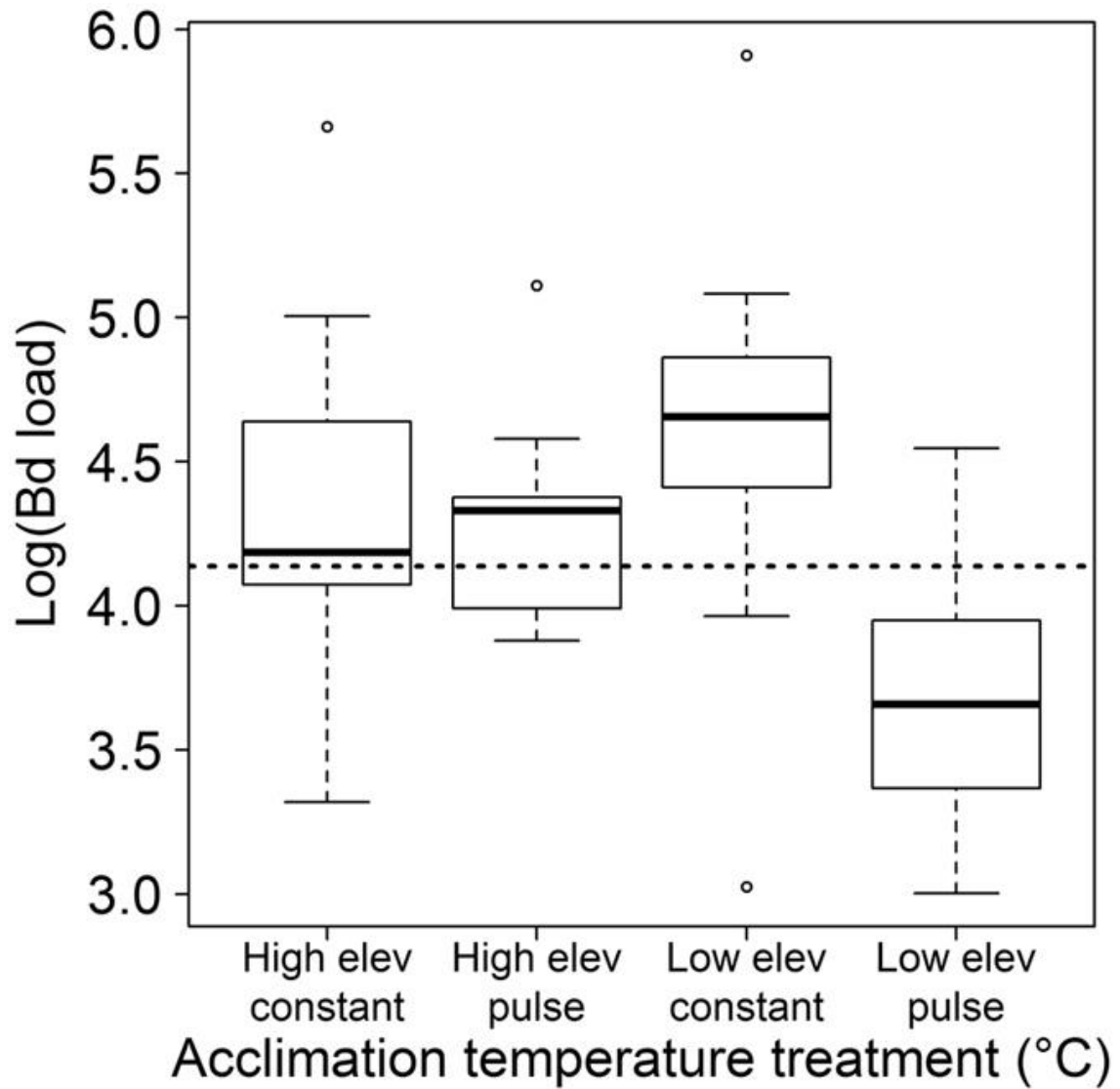


Figure 4.3 *Batrachochytrium dendrobatidis* infection intensities at the time of measuring the critical thermal maxima of infected *Litoria spenceri* acclimated to four temperature treatments. Dashed line indicates an infection intensity threshold above which frogs were estimated to be at high risk for morbidity and/or mortality from infection.

4.5 Discussion

The global climate and the microclimates experienced by animals are becoming warmer and more extreme (Easterling 2000; Meehl 2004; Rahmstorf and Coumou 2011; Rummukainen 2012), increasing risk of population losses and even species extinctions by decreasing the margin of safety between the maximum heat thresholds of organisms and the maximum ambient temperatures they encounter. For example, recent extirpations of *Sceloporus* lizards were linked to elevated maximum temperatures during the breeding season, which restricted individuals to cool refuges at the expense of foraging and reproduction and in turn caused declining population growth rates since the 1970s (Sinervo et al. 2010). On a shorter-term timescale, record high temperatures on a single day in 2002 were associated with deaths of thousands of flying foxes (*Pteropus* spp.) in eastern Australia (Welbergen et al. 2008). Three years later, and in a neighboring Australian state, another heat wave nearly drove the upland endemic white lemuroid possum (*Hemibelideus lemuroides*) to extinction (Laurance 2011).

The thermal safety margins of organisms may be compressed not only by rises in environmental temperatures but also reductions in maximum heat tolerance. In our study, heavy fungal infections lowered the critical thermal maxima of juvenile frogs by up to ~4°C. The maximum heat tolerance of organisms can be determined by temperature effects on the molecules, cells, and biochemical reactions of organ systems, including the circulatory, respiratory, and nervous systems (Portner 2002; Clark et al. 2013; Ern et al. 2015). The temperature resistance of these systems could plausibly decrease if already weakened by Bd infection or stress, especially since Bd causes tissue damage (Berger et al. 2005b) and blocks oxygen, water, and electrolyte balance through the skin (Voyles et al. 2009). Alternatively, lowered thermal tolerance could indicate manipulation of host physiology by the fungus to promote movement of the host to microhabitats that favor the fungus, which has a low tolerance for elevated temperatures. Further studies are needed to determine the physiological and evolutionary causes of reduced thermal tolerance from infection and the synergistic effects of infection and temperature on fitness at non-critical temperatures.

Ours is the first study to directly test for the effects of a fungal parasite on the upper thermal tolerance of its hosts. Existing literature on the interactions between infection and the upper thermal tolerance of animals is limited to six marine mollusk host species, one freshwater mollusk host species, eight freshwater fish host species, and one amphibian host species (a newt), with trematodes as the dominant parasite (Table 4.3). Whereas upper

thermal tolerance of hosts was enhanced in only 10.5% (2/19) of these host-parasite systems and did not change in 31.5% (6/19) of these systems, our finding that *Bd* infections lowered host thermal tolerance is consistent with 58% (11/19) of host thermal responses to parasites (Table 4.3), including the only previous study of thermal thresholds in parasitized amphibians (Sherman 2008) and similar studies of parasitized fish (Vaughan and Coble 1975; Lutterschmidt et al. 2007) and mollusks (Vernberg and Vernberg 1963; McDaniel 1969; Lee and Cheng 1971; Tallmark and Norrgren 1976; Lauckner 1980; Lauckner 1983; Bates et al. 2011). What does this mean for the present and coming decades, during which animals will face unprecedented changes in the global climate and in rates of infectious disease emergence? Our results suggest that infections by parasites and pathogens may profoundly alter the thermal physiology of hosts, often eliciting significantly reduced heat tolerance. We argue that a diminished upper temperature threshold may not only increase risk of population losses in accordance with the warming tolerance hypothesis (Lutterschmidt and Hutchison 1997; Somero 2005; Deutsch et al. 2008; Duarte et al. 2012), but also to perpetuate infections by altering host thermoregulatory behavior, with added implications for host survival.

Table 4.3 Review of studies on the effects of infections on upper thermal tolerance in animal hosts.

Agent phylum	Agent species	Host taxon	Host species	Effect on thermal tolerance	Reference
Arthropoda	<i>Lernaea cyprinaceae</i>	freshwater fish	<i>Pimephales promelas</i>	no effect	Vaughan and Coble 1975
Arthropoda	<i>Salmincola edwardsii</i>	freshwater fish	<i>Salvelinus fontinalis</i>	decreased	Vaughan and Coble 1975
Choanozoa	<i>Ichthyophonous</i> -like sp.	newt	<i>Notophthalmus viridescens</i>	decreased	Sherman 2008
Chytridiomycota	<i>Batrachochytrium dendrobatidis</i>	frog	<i>Litoria spenceri</i>	decreased	Greenspan <i>et al.</i> this study
Platyhelminthes	<i>Crassiphiala bulboglossa</i>	freshwater fish	<i>Perca flavescens</i>	no effect	Vaughan and Coble 1975
Platyhelminthes	<i>Cryptocotyle lingua</i>	marine snail	<i>Littorina littorea</i>	decreased	McDaniel 1969
Platyhelminthes	<i>Himasthla elongata</i> , <i>Renicola roscovita</i>	marine clam	<i>Cardium edule</i>	decreased	Lauckner 1983
Platyhelminthes	<i>Lepocreadium ovalis</i> , <i>Zoogonus rubellus</i>	marine snail	<i>Nassarius obsoletus</i>	decreased	Vernberg and Vernberg 1963
Platyhelminthes	<i>Maritrema</i> sp.	marine snail	<i>Zeacumantus subcarinatus</i>	increased	Bates <i>et al.</i> 2011
Platyhelminthes	<i>Philophthalmus</i> sp.	marine snail	<i>Zeacumantus subcarinatus</i>	decreased	Bates <i>et al.</i> 2011
Platyhelminthes	<i>Schistosoma mansoni</i>	freshwater snail	<i>Biomphalaria glabrata</i>	decreased	Lee and Cheng 1971
Platyhelminthes	<i>Uvulifer ambloplitis</i>	freshwater fish	<i>Notropis chrysocephalus</i>	no effect	Hocket and Mundahl 1989
Platyhelminthes	<i>Uvulifer ambloplitis</i>	freshwater fish	<i>Notropis spilopterus</i>	no effect	Hocket and Mundahl 1989
Platyhelminthes	<i>Uvulifer ambloplitis</i>	freshwater fish	<i>Pimephales notatus</i>	no effect	Hocket and Mundahl 1989
Platyhelminthes	10 species*	marine snail	<i>Cerithidea californica</i>	no effect	Sousa and Gleason 1989
Platyhelminthes	3 species**	marine snail	<i>Nassarius obsoletus</i>	increased	Riel 1975
Platyhelminthes (dominant), Acanthocephala, Nematoda	6 species***	freshwater fish	<i>Lepomis macrochirus</i>	decreased	Lutterschmidt <i>et al.</i> 2007
Platyhelminthes (dominant), Acanthocephala, Nematoda	7 species****	freshwater fish	<i>Lepomis megalotis</i>	decreased	Lutterschmidt <i>et al.</i> 2007
Platyhelminthes	unknown	marine snail	<i>Littorina littorea</i>	decreased	Lauckner 1980
Platyhelminthes	unknown	marine snail	<i>Nassarius reticulatus</i>	decreased	Tallmark and Norrgren 1976

**Acanthoparyphium spinulosum*, *Austrobilharzia* sp., *Catatropis johnstoni*, *Echinoparyphium* sp., *Euhaplorchis californiensis*, *Himasthla rhigedana*, *Parorchis acanthus*, unidentified cyathocotylid, unidentified microphallid, unidentified renicolid

***Zoogonus lasius*, *Himasthla quissetensis*, *Lepocreadium setiferoides*

*** Platyhelminthes: *Neascus* sp., *Proteocephalus* sp.; Nematoda: *Spinitectus carolini*, *Camallanus oxycephalus*, unidentified larvae; Acanthocephala: *Neoechinorhyncus cylindratus*

**** Platyhelminthes: *Crepidostomum cornutum*, *Neascus* sp., *Proteocephalus* sp.; Nematoda: *Spinitectus carolini*, *Camallanus oxycephalus*, unidentified larvae; Acanthocephala: *Neoechinorhyncus cylindratus*

In ectothermic hosts, including frogs, behaviors that elevate body temperature may decrease heat-intolerant parasite performance or increase immune function, thereby reducing infection risk or the intensity of existing infections (Richards-Zawacki 2010; Rowley and Alford 2013; Roznik et al. 2015a). Our study demonstrates the infection-limiting benefits of thermoregulation – for most frogs, four hours of daily exposure to 29°C (in our low elevation heat pulse treatment) was sufficient to prevent infection levels from exceeding the threshold marking increased risk for morbidity and/or mortality from infection. A recently proposed conceptual model that expands on the relationship between CT_{max} and infection risk predicts that infection risk will increase as the difference between the CT_{max} of the host and parasite decreases (tolerance mismatch hypothesis; Figure 4.4; Nowakowski et al. 2016) because infection risk is higher when the host occupies microenvironments that are also favorable for the parasite. Species' CT_{max} are highly variable even within genera and can be overestimated using laboratory techniques (Chown et al. 2009; Rezende et al. 2011). While our model host species performed at the high end of the CT_{max} spectrum (Catenazzi et al. 2014), our study suggests that in ecological systems in which tolerance mismatch is precariously small, high parasite burdens can shrink the gap between host and pathogen thermal tolerances even further (Figure 4.4), potentially discouraging protective thermoregulatory behaviors, even at temperatures below upper maxima, and tipping the balance in favor of the parasite.

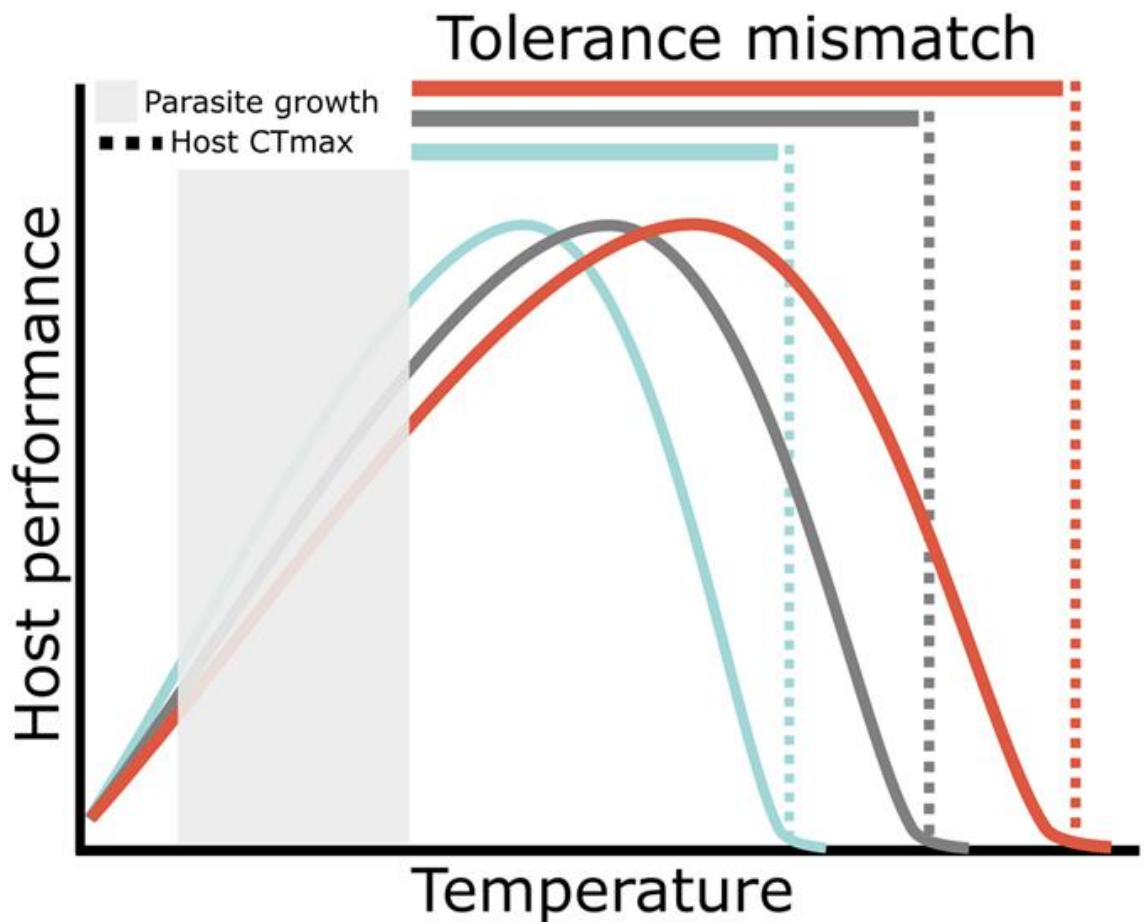


Figure 4.4 The tolerance mismatch hypothesis predicts that infection risk will decrease as the difference in the thermal tolerance of the host and pathogen (tolerance mismatch) increases. This schematic illustrates the potential effects of parasitic infection on tolerance mismatch for disease systems in which the thermal tolerance of hosts exceeds that of the parasite. Consider a host with a thermal tolerance represented by the gray dotted line. If it becomes infected, its upper thermal tolerance may be reduced (blue dotted line), decreasing tolerance mismatch (blue bar). The host is now more likely to occupy microhabitats (blue performance curve) that are favorable for the parasite, at the expense of protective thermoregulatory behaviors. In rare cases, infections might increase (red dotted line) or have no effect (gray dotted line) on thermal tolerance, thus expanding (red bar) or maintaining (gray bar) the magnitude of thermal mismatch.

In contrast to heavy infections, mild infections may not significantly lower host thermal tolerance. The low elevation heat pulse treatment was the only group in which (1) most individuals had infection loads below the threshold for disease development, and (2) the CT_{max} of infected and uninfected individuals was similar, suggesting that any effects of light infection levels on the thermal tolerance of frogs were minimal. However, this warrants further study, especially because we did not detect a statistically significant effect of infection intensity on CT_{max} (Table 4.1).

We observed higher upper thermal tolerances in infected frogs that were acclimated to realistic daily heat pulses than in infected frogs that were acclimated to constant cool temperatures. These results highlight the importance of incorporating biologically meaningful acclimation temperature regimes into the design of experiments and support the recent finding that small-bodied hosts may be more capable of temperature acclimation than previously thought (Rohr et al., in review). Whereas Rohr et al. (in review) found that the magnitude of acclimation plasticity may be underestimated in laboratory experiments due to its dependence on acclimation duration and body mass, our use of an atypically long acclimation duration (≥ 36 days) and small-bodied hosts suggests that our study is robust to these common experimental artifacts. Importantly, however, under most of our acclimation treatments, the magnitude of the parasitism effect exceeded the magnitude of the acclimation effect. This suggests that for populations of some species, even as thermal tolerances are adjusted to long-term increases in temperature from climate change, any benefit this provides to warming tolerance may not be sufficient to protect animals from the thermal consequences of parasitism.

In contrast to infected frogs, which exhibited enhanced thermal tolerances when acclimated to daily heat pulses, we did not detect this acclimation effect in uninfected frogs (i.e., uninfected frogs exhibited similar [or lower, in the case of onset of spasms in the low elevation heat pulse treatment] thermal tolerances when exposed to daily heat pulses compared to constant cool temperatures). It is unclear why the temperature at onset of spasms was reduced in uninfected frogs from the low elevation heat pulse treatment. Lack of an acclimation effect in the other paired constant temperature vs. heat pulse treatments could be attributed to inherent physiological limits (i.e., a ceiling effect) on thermal tolerance or tradeoffs between thermal tolerance and acclimation plasticity (Stillman 2003). A related avenue for future research is the capacity for heat hardening and resistance adaptation in common parasites.

While gradual increases in average temperatures could favor the hosts of some parasites, such as cool-loving fungi, our study illustrates that we may currently be unable to predict the combined effects of infections and climate change on host populations. Of particular concern are unpredictable heat waves that are long enough to impose thermal stress on hosts but are too short to be therapeutic, for example by ridding hosts of heat-intolerant parasites, or to allow for thermal acclimation. We conclude that infectious disease could lead to increased uncertainty in estimates of species' vulnerability to climate change.

4.6 Highlights

- We assessed the effects of Bd on the upper thermal tolerance of frogs
- Bd infection reduced the critical thermal maxima of frogs by up to ~4°C.
- Acclimation to daily heat pulses enhanced thermal tolerance among infected individuals but usually not by enough to make up for the effect of infection.
- Our results suggest that increased heat sensitivity from infections may discourage thermoregulatory behaviors that decrease parasite performance or increase immune function, even at temperatures below critical maxima.

Chapter 5 Realistic heat pulses protect frogs from disease under simulated rainforest frog thermal regimes

Sasha E. Greenspan, Deborah S. Bower, Rebecca J. Webb, Elizabeth A. Roznik, Lisa A. Stevenson, Lee Berger, Gerry Marantelli, David A. Pike, Lin Schwarzkopf, Ross A. Alford

This chapter has been published in *Functional Ecology* and is reproduced here with permission.

Link to article: <http://onlinelibrary.wiley.com/doi/10.1111/1365-2435.12944/full>

Citation: Greenspan SE, Bower DS, Webb RJ, Roznik EA, Stevenson LA, Berger L, Marantelli G, Pike DA, Schwarzkopf L, Alford RA. 2017. Realistic heat pulses protect frogs from disease under simulated rainforest frog thermal regimes. *Functional Ecology* 31:2274–2286.

Link to data in Dryad: <http://datadryad.org/resource/doi:10.5061/dryad.989r4>

Contributions: All authors co-developed the study. SEG, DSB, and RJW carried out the lab work. SEG carried out the statistical analyses with assistance from RAA. SEG drafted the manuscript and developed the figures and tables. All authors provided editorial input.

5.1 Abstract

Recent emergences of fungal diseases have caused catastrophic global losses of biodiversity. Temperature is one of the most important factors influencing host-fungus associations but the effects of temperature variability on disease development are rarely examined. The chytrid pathogen *Batrachochytrium dendrobatidis* (Bd) has had severe effects on populations of hundreds of rainforest-endemic amphibian species but we know little about the effects of rainforest-specific host body temperature cycles on infection patterns. To address this challenge, we used body temperature regimes experienced in nature by tropical Australian frogs to guide a controlled experiment investigating the effects of body temperature fluctuations on infection patterns in a model host (*Litoria spenceri*), with emphasis on exposing frogs to realistic 'heat pulses' that only marginally exceed the thermal optimum of the fungus. We then exposed cultured Bd to an expanded array of heat pulse treatments and measured parameters of population growth to help resolve the role of host immunity in our *in vivo* results. Infections developed more slowly in frogs exposed to daily 4-h heat pulses of 26°C or 29°C than in frogs in constant temperature treatments without heat pulses (control). Frogs that experienced heat pulses were also less likely to exceed infection intensities at which morbidity and mortality become likely. Ten of 11 (91%) frogs from the daily 29°C heat pulse treatment even cleared their infections after approximately nine weeks. Cultured Bd grew more slowly when exposed to heat pulses than in constant-temperature control treatments, suggesting that mild heat pulses have direct negative effects on Bd growth in nature, but precluding us from determining whether there was a concurrent benefit of heat pulses to host immunity. Our results suggest that even in habitats where *average* temperatures may be suitable for fungal growth and reproduction, infection risk or the outcome of existing infections may be heavily influenced by short but frequent exposures to temperatures that only slightly exceed the optimum for the fungus. Our findings provide support for management interventions that promote warm microenvironments for hosts, such as small-scale removal of branches overhanging critical habitat or provision of artificial heat sources.

5.2 Introduction

Disease-induced extinctions and population collapses of wildlife have driven concerns about emerging fungal pathogens to the forefront of conservation science worldwide (Fisher et al. 2012; Bellard et al. 2016; Fisher et al. 2016). Temperature is one of the most important factors influencing the geographic distribution of fungal pathogens and host-pathogen interactions (Burdon 1987). In nature, ectothermic host body temperatures may range from below to above the optimum for fungal pathogens within the span of a single day (Roznik 2013). This complicates efforts to predict and test the effects of temperature on the host-pathogen relationship in nature. As a result, current information on the temperature-dependent population growth of fungal pathogens on hosts under field conditions is limited to only a few studies. For instance, the virulence of the insect-pathogenic fungus *Beauveria bassiana* decreased under field conditions (Howard et al. 2011), a response attributed to occasional environmental temperature spikes outside the fungus' optimal growth range (Kutywayo et al. 2006; Howard et al. 2011; Santos et al. 2011). This suggests that the physiological processes of fungal pathogens may be highly responsive to temperature fluctuations, especially when peak temperatures exceed optimal conditions, but this has rarely been explicitly tested.

The effects of fluctuating temperature cycles on host immune systems are also poorly known (Martin 2009). Northern bobwhites (*Colinus virginianus*) that experienced daily cold stress (6 h per day at -20°C for 4 d) were more resistant to infection with the bacteria *Pasteurella multocida* than those that experienced daily heat stress (4 h per day at 39°C for 4 d), a response attributed to a cold stress induced increase in phagocytic white blood cell activity (Dabbert et al. 1997). In contrast, the T-lymphocyte mediated immune response of tree swallows (*Tachycineta bicolor*) was suppressed on or immediately following cool days, when insect abundance tended to be low, leading to reduced food intake and subsequent declines in body condition (Lifjeld et al. 2002). Although cool temperature spikes produced opposite changes in immune responses in these studies, they both indicate that there may be little lag time between temperature-influenced changes in the physiological condition of individuals and immune performance. Temperature fluctuations may be a particularly important determinant of the strength of the immune response in ectotherms, in which physiological rates are highly correlated with temperature (Feder and Burggren 1992).

Batrachochytrium dendrobatidis (Bd) is one of the most pervasive wildlife pathogens and has caused declines or extinctions of nearly 400 amphibian species since the 1970s (Lips

2016). In post-metamorphic amphibians, *Bd* infects the superficial epidermis. In early-stage infections, zoosporangia (i.e., intracellular stage) are often clustered in the skin, suggesting fungal population growth by repeated local re-infections (Carey et al. 2006). Chytridiomycosis develops when fungal population growth progresses unchecked, eventually reaching a critical density in host epidermis (Carey et al. 2006). Past this virulence threshold, damage to the skin layers causes loss of water and electrolyte equilibrium and eventual death from cardiac arrest (Voyles et al. 2009).

Like many other biologically and economically important fungi, the performance of *Bd* under constant temperatures has been well described. In pure culture, optimal short-term growth of *Bd* occurs at 15-25°C (Longcore et al. 1999; Berger et al. 2004; Piotrowski et al. 2004; Woodhams et al. 2008; Stevenson et al. 2013). Between 4-15°C, the fungus grows slowly but may still possess high virulence potential by trading off slower growth rates for increased fecundity (Woodhams et al. 2008; Stevenson et al. 2013) and zoospore longevity (Voyles et al. 2012). Growth and reproduction cease at isolate-specific thresholds between 26 and 28°C (Longcore et al. 1999; Berger et al. 2004; Piotrowski et al. 2004; Woodhams et al. 2008; Stevenson et al. 2013). The fungus may resume growth when transferred from 26-28°C to lower temperatures, but will generally die or fail to resume growth after extended (\geq one week) exposure to 29°C (Longcore et al. 1999; Piotrowski et al. 2004; Stevenson et al. 2013), moderate (4 d) exposure to 32°C, or brief (4 h) exposure to 37°C (Johnson et al. 2003). The results of these studies of *Bd* in pure culture align with the results of several experiments in which captive amphibians were exposed to *Bd*. For example, post-metamorphic amphibians cleared infections after exposure to 30°C for 10 d (Chatfield and Richards-Zawacki 2011), 32°C for 5 d (Retallick and Miera 2007) or 37°C for \sim 16 h (Woodhams et al. 2003) and larval amphibians cleared infections after exposure to \geq 26°C for 5 d (Geiger et al. 2011).

A more recent line of research suggests that *Bd* is also affected by temperature fluctuations. In the laboratory, the fungus can adapt physiologically to optimize growth under predictable daily temperature fluctuations within a suitable temperature range for *Bd* (25°C during the day and 15°C during the night; Raffel et al. 2013). However, this may not translate into an appreciable advantage for *Bd* if the host can simultaneously adapt to optimize immunity (Raffel et al. 2013). In the field, host populations in warmer, drier habitats (dry substrate temperatures \geq 30°C for at least one hour when frogs are active on land; (Daskin et al. 2011)) can persist even when infection prevalence is high (Puschendorf et al. 2011). In these 'environmental refuges', host populations do not appear to possess inherent resistance or

tolerance mechanisms but rather survive with low infection intensities as a result of environmental checks on pathogen growth (Daskin et al. 2011; Puschendorf et al. 2011). In contrast, the fungus thrives under cool field conditions (15-25°C) and has thus taken a disproportionately high toll on amphibian populations in montane rainforests (Skerratt et al. 2007; Lips 2016).

Even within montane rainforests, probability of infection decreases with increasing frequencies of frog body temperatures above 25°C (Roznik 2013; Rowley and Alford 2013). Frogs may behaviourally raise their body temperatures by selecting warm microhabitats, for instance in response to pathogen recognition (i.e., behavioural fever) or to aid metabolism or reproduction (Richards-Zawacki 2010; Murphy et al. 2011; Rowley and Alford 2013). Alternatively, changes in frog body temperature may occur passively or by chance, with natural or anthropogenic fluctuations in the micro-environments of individuals or the macro-environments of populations (Rowley and Alford 2013; Roznik et al. 2015a). In rainforest ecosystems where environmental conditions are suitable for Bd growth most of the time, these processes may briefly elevate frog body temperatures so that they exceed the thermal optimum of the fungus. At our long-term rainforest field sites in the Australian Wet Tropics where Bd is endemic, frog body temperatures commonly, although briefly, reach 26-29°C and can reach up to 36°C (Roznik 2013). This suggests that in the field Bd can tolerate short periods of exposure to temperatures that only marginally exceed its growth optimum (26-29°C), but the effects of these exposures on rates of population growth of Bd in host tissue are unknown. We used body temperature data collected in nature from frogs in the Australian Wet Tropics to guide a controlled experiment investigating the effects of diurnal heat pulses on Bd infection patterns in a model amphibian host. We then exposed cultured Bd to an expanded array of diurnal heat pulse treatments and measured parameters of population growth to help resolve the role of host immunity in our *in vivo* results.

5.3 Methods

Temperature treatments

We generated eight temperature treatments with body temperature data from *Litoria serrata* (Fig. 5.1; Roznik 2013). *Litoria serrata* is a stream-associated frog of the Australian Wet Tropics that experienced declines from chytridiomycosis and now persists in endemic association with Bd (McDonald and Alford 1999; Woodhams and Alford 2005). We recorded the body temperatures of 54 male frogs during winter (the cool/dry season when Bd is most

prevalent) at two low- and two high-elevation study sites (Roznik 2013) where Bd occurs. The low-elevation sites were Kirrama Creek #1 in Girramay National Park (4–18 July 2011; 18.203°S, 145.886°E, 100 m; N = 11) and Stoney Creek in Djiru National Park (12–25 August 2011; 17.920°S, 146.069°E, 20 m; N = 14). The high elevation sites were Birthday Creek in Paluma Range National Park (19 July–1 August 2011; 18.980°S, 146.168°E, 800 m; N = 15) and Windin Creek in Wooroonooran National Park (26 August–8 September 2011; 17.365°S, 145.717°E, 750 m; N = 14). We attached a temperature-sensitive radio-transmitter (Model A2414; Advanced Telemetry Systems, Isanti, MN) to each frog with a waistband made of silicone tubing and cotton thread. The pulse rate of the signal emitted by each transmitter varied according to temperature. We recorded the pulse rate of each transmitter every 15 minutes for five to 11 consecutive days with an automated data-logging receiver (Model SRX400A; Lotek Wireless, Newmarket, ON, Canada; Roznik 2013). We later converted the pulse rates to temperatures with calibration curves provided for each transmitter by the manufacturer.

For each elevation (high and low), we constructed a series of square wave temperature treatments representing simplified frog thermal regimes. We derived the trough temperatures for the square waves from the overall median of individual median body temperatures (high elevation: 15°C; low elevation: 18°C). We derived the crest (i.e., heat pulse) temperatures for the square waves from the median of individual maximum body temperatures > 25°C (high elevation: 26°C; low elevation: 29°C). We derived the crest lengths for the square waves (heat pulse durations) from the overall maximum length of time that frogs spent with body temperatures >25°C (7 h) and the median of the individual maximum lengths of time that frogs spent with body temperatures >25°C (4 h).

Thus, the four high elevation temperature treatments were: a daily rectangular wave with trough at 15°C and crest at 26°C for (1) 7 h, (2) 4 h, and (3) 1 h (to determine effects of very brief daily heat pulses), as well as (4) a constant 15°C control treatment (Fig. 5.1). The four low elevation temperature treatments were: a daily rectangular wave with trough at 18°C and crest at 29°C for (1) 7 h, (2) 4 h, and (3) 1 h (to determine effects of very brief daily heat pulses), as well as (4) a constant 18°C control treatment (Fig. 5.1). The constant temperature control treatments (15°C and 18°C) were suitable for short-term Bd growth (Longcore et al. 1999; Berger et al. 2004; Piotrowski et al. 2004; Woodhams et al. 2008; Stevenson et al. 2013) and thus served as a standard against which to observe effects of heat pulses on fungal growth.

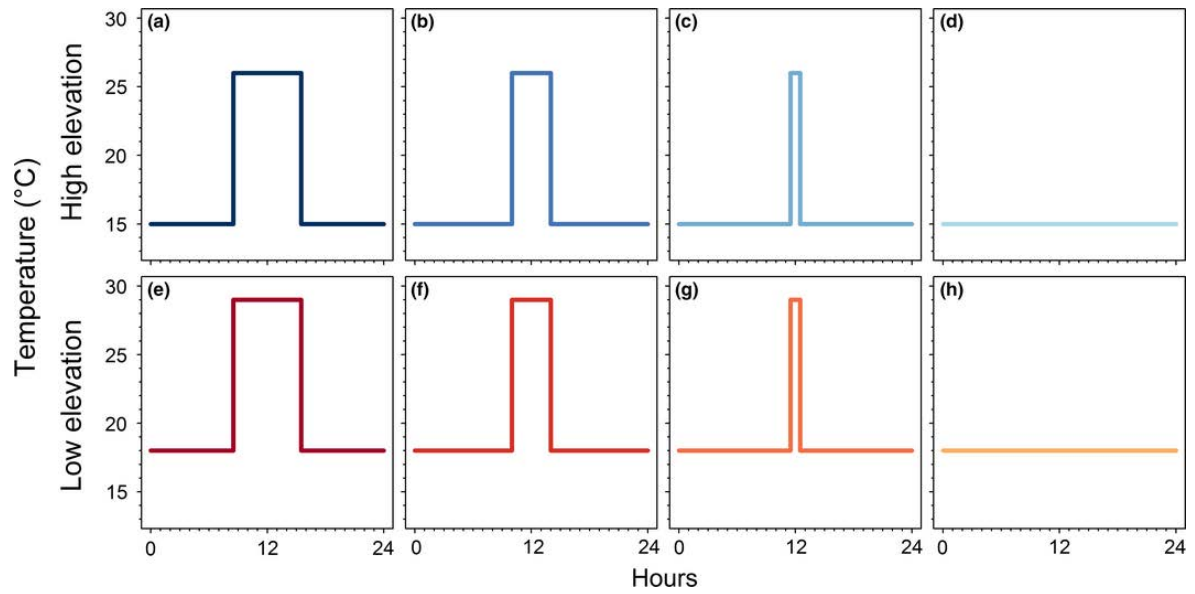


Figure 5.1 Daily temperature treatments for experiment investigating effects of daily heat pulses on in vitro growth of *Batrachochytrium dendrobatidis* (Bd; a–h) and on in vivo Bd infection dynamics in a model amphibian host (b, d, f, h). We generated temperature treatments with body temperature data from *Litoria serrata* in high-elevation (blue gradient; a–d) and low-elevation (red-orange gradient; e–h) rainforests of the Australian Wet Tropics.

Bd cultures

We used the *Bd* isolate Paluma-Lseratta-2012-RW-1. This isolate is maintained at the College of Public Health, Medical, and Veterinary Sciences, James Cook University. It originated from an adult *L. serrata* that was collected from Birthday Creek (one of our frog tracking sites) and died in captivity. The isolate was cryo-archived after two passages in nutrient broth. We revived aliquots of this isolate and cultured it in tryptone/gelatin hydrolysate/lactose (TGhL) broth in 25-cm³ tissue culture flasks, passaging it twice before each trial and maintaining cultures at 22°C.

To obtain zoospores for each trial, we added cultured broth to Petri dishes containing TGhL broth in 1% agar. Plates were partially dried in a laminar flow cabinet, incubated at 21°C for four days, and then maintained alternately at 4°C and 21°C to sustain growth and zoospore production. We then added up to 5 ml of deionized (DI) water to the dishes to form a zoospore suspension. We combined the liquid contents of each dish and calculated the concentration of zoospores with a hemocytometer (Neubauer Improved Bright-line). We prepared a sham (control) inoculant by following the same protocol but with Petri dishes containing only nutrient agar.

In vivo experimental infection trial

For the *in vivo* trial, we experimentally infected captive-reared juveniles of the model species *Litoria spenceri*, the spotted tree frog (sourced from a captive breeding facility at the Amphibian Research Centre, Victoria, Australia). Use of captive-reared frogs ensured no previous exposure to *Bd*, which can influence the progression of subsequent infections (McMahon et al. 2014); captive-reared *L. serrata* were unavailable. *Litoria serrata* and *L. spenceri* are both found on vegetation and rocks along forested streams at a range of elevations in eastern Australia (Gillespie and Hollis 1996; Williams 2006). *Litoria spenceri* is susceptible to *Bd* in the wild and its tendency to bask on exposed rock stream banks suggests that it could experience large temperature fluctuations in its native habitat (Gillespie and Hollis 1996; Gillespie and Hines 1999).

To ensure infection, we inoculated frogs on three consecutive days. On each day, we added DI water to the zoospore suspension to produce a final concentration of 1×10^6 zoospores per ml. To inoculate, we placed each frog into an individual 70-ml plastic container and added 3 ml (enough to cover the bottom of the container) of zoospore inoculant ($n = 72$ frogs) or sham inoculant ($n = 24$ frogs) to each container. We left frogs in inoculant baths for 8 h per day. To ensure regular contact of frogs with the inoculant, we monitored frogs every 15

minutes during each inoculation period. If a frog had climbed out of the inoculant onto the wall of the container, we gently tilted the container to bathe the frog in the inoculant. After each inoculation period, we returned frogs with their inoculant to individual permanent enclosures comprising 70 x 120 x 170 mm plastic containers lined with tap water-saturated paper towels.

Sixteen to 18 inoculated frogs (four frogs died during the inoculation for unknown reasons) and six uninfected control frogs were assigned to each of four temperature treatments (both 4-h heat pulse treatments [Fig. 5.1b, f] and both constant-temperature control treatments [Fig. 5.1d, h]). Six replicate temperature-controlled chambers (Greenspan et al. 2016) were programmed to perform each treatment, for a total of 24 chambers, each containing two or three inoculated frogs and one sham-inoculated control frog in separate enclosures. The chambers were arranged in a blocked design, such that there were six spatial blocks, each containing one chamber following each of the four temperature treatments. The location of each temperature treatment within each block was determined randomly. The actual temperature of each chamber (measured with a digital temperature sensor [DTH22; accurate to $\pm 0.1^\circ\text{C}$] mounted inside each chamber) was recorded every minute and confirmed with Thermochron iButton temperature loggers (Maxim Integrated Products, Sunnyvale, California, USA; accurate to $\pm 0.5^\circ\text{C}$) that recorded chamber temperatures every 15 minutes. Actual chamber temperatures remained within 0.5°C of target temperatures during the experiment. We reduced effects of frog history and body size on disease development by assigning frogs to experimental treatments proportionally by clutch (reported by the captive breeding facility) and snout-urostyle length (measured prior to inoculation). We divided frogs into the 24 chambers on the day after the last inoculation. We systematically rotated the placement of the three or four frog enclosures within each chamber every other day to ensure that they were evenly exposed to any small differences in local temperatures that might exist within the chamber. Temperature-controlled chambers were programmed to maintain a 12 hr: 12 hr photoperiod. Every other day, we moistened paper towels with tap water to maintain a consistent moisture level (paper towel saturated but no standing water) and fed frogs pinhead crickets *ad libitum*. We changed paper towels at every other feeding. We refrained from performing husbandry duties at times of day coinciding with heat pulses.

To monitor Bd infection status and intensity over the course of the experiment, we swabbed frogs upon arrival from the captive breeding facility (all tested Bd-negative) and every eight days thereafter, following a standard protocol (Stockwell et al. 2015). We

determined the number of Bd zoospore genome equivalents per swab using a real-time quantitative PCR protocol modified from Boyle et al. (2004) with standards prepared from the Bd isolate CW34. We checked frogs daily for signs of chytridiomycosis (e.g., lethargy, reddening of feet) and first observed these signs on day 36; frogs exhibiting signs of disease were immediately removed from the experiment. A receiver operating characteristic (ROC) analysis (Stockwell et al. 2016) for the first 43 days of the experiment (1 frog died and 14 frogs had shown signs of chytridiomycosis by this time) indicated that frogs with infection loads >13,700 zoospore genome equivalents (ZGE) had a 63% chance of dying or showing signs of chytridiomycosis. Therefore, to prevent subsequent morbidity and mortality, we removed sub-clinically infected frogs from temperature treatments gradually, as swabs from frogs exceeded the threshold infection intensity of 13,700 ZGE. We treated frogs for chytridiomycosis with the antifungal Itraconazole following removal from the experiment (Brannelly et al. 2012). Our experiment was carried out under James Cook University Animal Ethics permit A2234.

In vitro Bd population growth trial

We conducted the *in vitro* trial in tissue culture-treated 96-well plates comprising 12 columns of eight wells. We added TGhL broth to the zoospore suspension to produce a final zoospore concentration of 5×10^5 zoospores per ml. We pipetted 100 μ l of the zoospore suspension into even-numbered columns and 100 μ l of TGhL broth into odd-numbered columns in each plate. We excluded 36 peripheral wells from analyses to avoid well position effects, leaving 30 wells containing the zoospore suspension and 30 wells containing TGhL broth that were included in analyses.

Three replicate temperature-controlled chambers (Greenspan et al. 2016) were programmed to perform each of the eight temperature treatments, for a total of 24 chambers, each containing one inoculated 96-well plate. Actual chamber temperatures were recorded and verified in the same way as for the *in vivo* trial and remained within 0.5°C of target chamber temperatures during the experiment. We rotated plates 180° daily to account for any small temperature gradients in the chambers. We quantified Bd growth by measuring the optical density of each well daily for 7 d (1–2 Bd generations) with a Multiskan Ascent 96/384 plate reader (MTX Lab Systems Inc., Vienna, Virginia, USA) at an absorbance of 492 nm. We then used the daily measurements of optical density to construct population growth curves for each well. We calculated daily optical density values by subtracting the average optical density of the wells containing only TGhL broth in the corresponding plate from the optical density of

each well containing Bd. For each growth curve, we used the grofit package in Program R to fit the curve to a set of conventional, parametric growth functions (logistic, Gompertz, modified Gompertz, and Richards) and a model free spline function, select the best-fitting function according to Akaike's information criterion, and estimate parameters of the best-fitting growth curve (Kahm et al. 2010; R Core Team 2015). The parameters were lag duration (time preceding the exponential growth phase), maximum slope of the curve (representative of the maximum rate of exponential growth), and two measures of total growth: maximum height of the curve and area under the curve (Kahm et al. 2010).

Predicting Bd growth potential

We used published population growth curves for three Bd isolates from Australia (Stevenson et al. 2013) to predict patterns of Bd growth under our temperature treatments. The isolates were collected from infected frogs in Queensland (QLD, northeastern Australia, isolate Paluma-Lgenimaculata #2 [tadpole]-2010-CO), New South Wales (NSW, east-central Australia, isolate AbercrombieR-Lbooroolongensis-09-LB1), and Tasmania (TAS, southeastern Australia, isolate MtWellington- Lewingii [tadpole]-2012-RW1), and thus represent a wide range of temperature conditions to which Bd may be adapted. For each isolate, Stevenson et al. (2013) documented population growth at constant 13°C, 15°C, 17°C, 19°C, 21°C, 23°C, 25°C, 26°C, 27°C, and 28°C.

We constructed thermal performance curves for each isolate by plotting the maximum slope of each constant-temperature growth curve (see grofit methods above) and smoothing the curve with the loess function in Program R (Cleveland et al. 1992; Fig. 5.2a). We used maximum slope as the growth curve parameter with which to construct thermal performance curves because this parameter represents *exponential* Bd growth potential, an important determinant of disease outcome (Briggs et al. 2010).

We then predicted exponential growth potential over 7 d (the length of our *in vitro* experiment) based on the hourly temperatures of our treatments, by plotting cumulative thermal performance for each hourly temperature (solid lines in Fig. 5.2b–g). We also predicted exponential growth potential over 7 d for hypothetical constant-temperature treatments representing the average daily temperature of each heat pulse treatment (dashed lines in Fig. 5.2b–g).

In general, as the duration of heat pulses increased, growth potential for the heat pulse treatments decreased but growth potential for the hypothetical average-temperature

treatments increased. The magnitude of these relationships was greater for the low elevation treatments (red-orange gradient) compared to the high elevation treatments (blue gradient). An exception to this pattern was the unusually high growth potential of the Tasmanian isolate under the high-elevation heat pulse treatments (Fig. 5.2b). This isolate initially grew well at 26°C but stopped growing after the first generation (Stevenson et al. 2013), indicating that our prediction may have overestimated the fitness of this isolate at 26°C.

Based on these predictions, if exposure to 26°C and 29°C disrupt Bd growth on the scale of 1–7 h at a time, we would expect decreases in Bd growth in our experiment as the duration of heat pulses increases. Alternatively, if 26°C and 29°C are too close to optimal temperatures to appreciably disrupt Bd growth on the scale of 1–7 h at a time, and growth is instead more heavily influenced by average daily temperatures, we would expect increases in Bd growth in our experiment as the duration of heat pulses increases.

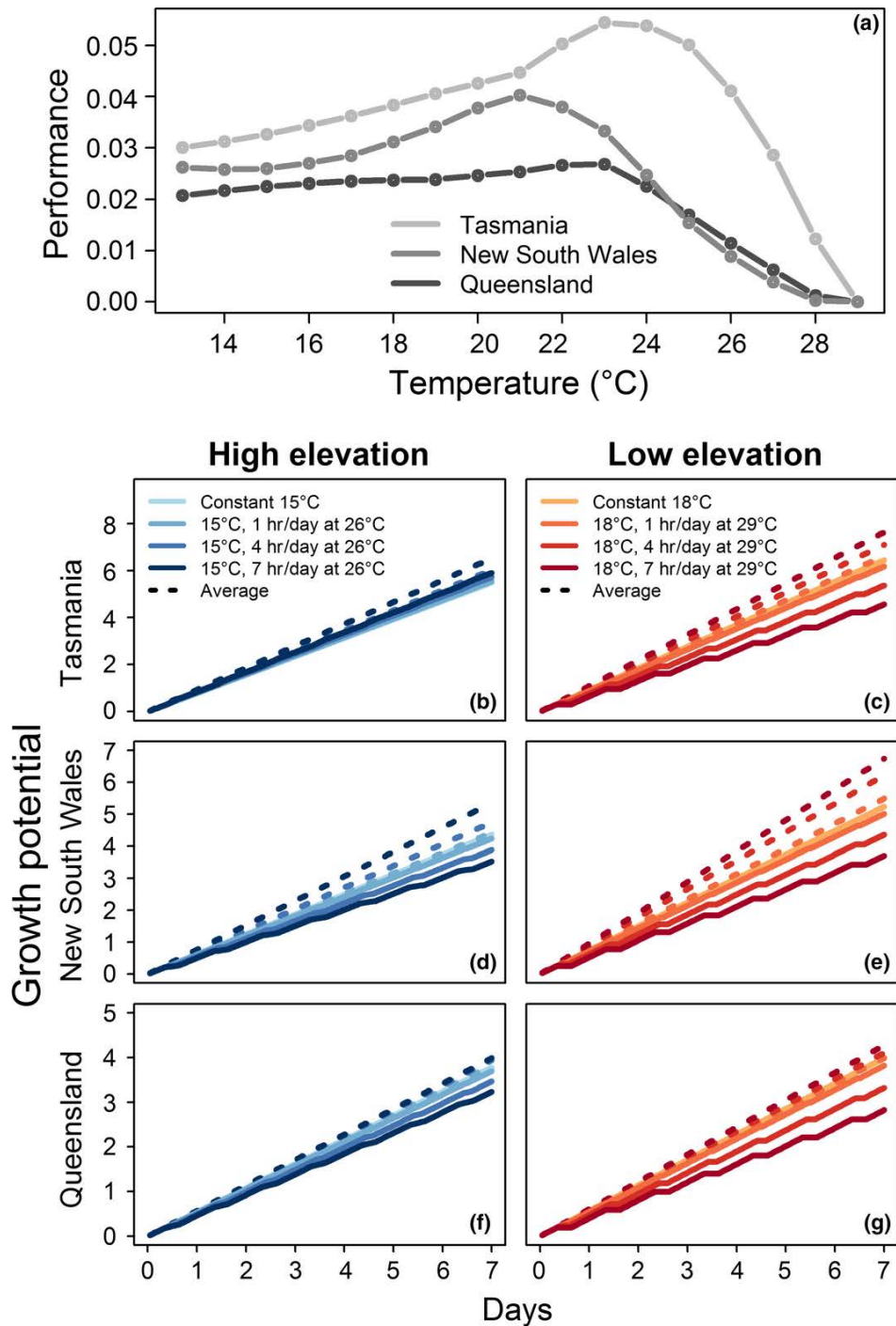


Figure 5.2 *In vitro* population growth potential for *Batrachochytrium dendrobatidis* (Bd) under experimental temperature treatments. We generated thermal performance curves for three Bd isolates (a) based on published constant-temperature population growth curves (Stevenson et al. 2013). Solid lines (b–g) indicate growth potential based on the hourly temperatures of our treatments (cumulative thermal performance for each hourly temperature). Dashed lines (B–G) indicate growth potential for hypothetical constant-temperature treatments representing the average daily temperature of each heat pulse treatment.

Statistical analysis

We performed all statistical analyses with Program R software (R core Team 2015). We estimated differences in survival probabilities between groups of frogs with Cox Proportional Hazards survival analysis (Cox 1972). In this analysis, time until death is the typical response. Instead, we used number of days until frogs reached the threshold infection intensity (13,700 ZGE) as a proxy for death, as this level of infection was linked to death in our ROC analysis and has been linked to development of lethal chytridiomycosis in other species (Briggs et al. 2010; Vredenburg et al. 2010; Kinney et al. 2011). This analysis also accommodates ‘censored’ individuals (i.e., those with incomplete survival records), allowing for inclusion of 10 frogs that never reached the threshold infection intensity and 24 frogs that were removed on day 36 for a concurrent study (six of the most heavily but sub-clinically infected frogs from each of the four temperature treatments).

We then analyzed our data using linear mixed effects models (lmer function in lme4 package; Bates et al. 2015). First, we tested for effects of elevation (high or low), heat exposure (daily 4-h heat pulses or constant cool temperature), and their interactions on log-transformed *in vivo* infection loads for the first 36 days of the experiment (before any frogs were removed from the experiment). We included day of swabbing event (4 d, 12 d, 20 d, 28 d, 36 d) as an additional interactive fixed effect and replicate (1–6) as well as frog (1–3) within chamber (1–4) as random effects.

Second, we tested for effects of elevation (high or low), heat pulse duration (0 h, 1 h, 4 h, 7 h), and their interactions on each of the four *in vitro* population growth parameters, including replicate (1–3) as a random effect. For each combination of elevation and heat exposure/duration in each model, we calculated the least square mean of the response variable (population growth parameter) and performed pairwise comparisons of least square means with general linear hypothesis tests (glht function).

5.4 Results

In our *in vivo* experiment, all inoculated frogs became infected with Bd. Our analysis of infection levels during the first five weeks of the eleven-week study (before any frogs were removed from the experiment) revealed that frog infection intensities increased more slowly and peaked at a lower level in the heat pulse treatments than in the constant temperature treatments ($P < 0.001$), especially under the hotter pulses of the low elevation heat pulse treatment ($P = 0.005$; Figure 5.3; Table 5.1). Among the low elevation treatments, frogs that

experienced heat pulses had markedly lower infection intensities than frogs in the constant 18°C treatment starting at the very first infection monitoring event on day 4 and on each subsequent monitoring event (Fig. 5.3). Among the high elevation treatments, infection levels were similar in the first two weeks of the experiment but began to diverge by day 20, with lower levels in the heat pulse treatment than in the constant temperature treatment (Fig. 5.3). In both the low and high elevation heat pulse treatments, the median infection level did not reach our estimated chytridiomycosis threshold by day 36 (Fig. 5.3). In contrast, in both the low and high elevation constant temperature treatments, infection levels began to exceed our estimated chytridiomycosis threshold on day 20 and median infection levels reached (low elevation) or exceeded (high elevation) the threshold on day 28 (Fig. 5.3). By day 36, 50% of frogs in the low elevation constant temperature treatment had exceeded the threshold infection level and the average infection intensity was 69,091 ZGE greater than in the low elevation heat pulse treatment, in which only 6% of frogs had exceeded the threshold infection intensity (Table 5.2; Fig. 5.3). Similarly, 50% of frogs from the high elevation constant temperature treatment had exceeded the threshold infection level by day 36 and the average infection intensity was 72,519 ZGE greater than in the high elevation heat pulse treatment, in which only 41% of frogs had exceeded the threshold infection intensity (Table 5.2; Fig. 5.3).

Table 5.1 Summary of the results of linear mixed effects models. We modelled the effects of elevation (high [15°C] vs. low [18°C] elevation treatments), heat exposure (heat pulse temperature treatments [26°C or 29°C for four hours per day] vs. constant cool temperature treatments [15°C or 18°C]), and their interactions on log-transformed *Batrachochytrium dendrobatidis* infection loads (number of zoospore genome equivalents detected on swabs) in the model host *Litoria spenceri*. We included day of swabbing event (4 d, 12 d, 20 d, 28 d, 36 d) as an additional interactive fixed effect and replicate (1–6) as well as frog (1–3) within temperature-controlled chamber (1–4) as random effects. We also modelled the effects of elevation, duration of daily heat exposure (0 h, 1 h, 4 h, 7 h), and their interactions on four in vitro population growth parameters for *Batrachochytrium dendrobatidis*, including replicate (1–3) as a random effect. The four population growth parameters were lag duration (time preceding the exponential growth phase), maximum slope of the exponential growth phase, maximum height of the growth curve, and area under the curve.

Experiment	Response	Predictor	Chi Square	DF	P-value
<i>In vivo</i>	Bd infection load	Elevation	7.141	1	0.008
		Heat	61.123	1	<0.001
		Day	92.439	4	<0.001
		Elevation x heat	7.731	1	0.005
		Elevation x day	3.528	4	0.474
		Heat x day	15.171	4	0.004
		Elevation x heat x day	2.307	4	0.679
<i>In vitro</i>	Lag duration	Elevation	8.5823	1	0.003
		Heat pulse duration	54.6165	3	<0.001
		Elevation x heat pulse duration	14.2298	3	0.003
	Max. slope	Elevation	209.70	1	<0.001
		Heat pulse duration	202.19	3	<0.001
		Elevation x heat pulse duration	124.30	3	<0.001
	Max. height	Elevation	0.6705	1	0.413
		Heat pulse duration	394.3840	3	<0.001
		Elevation x heat pulse duration	44.9060	3	<0.001
	Area under curve	Elevation	66.552	1	<0.001
Heat pulse duration		213.985	3	<0.001	
Elevation x heat pulse duration		146.934	3	<0.001	

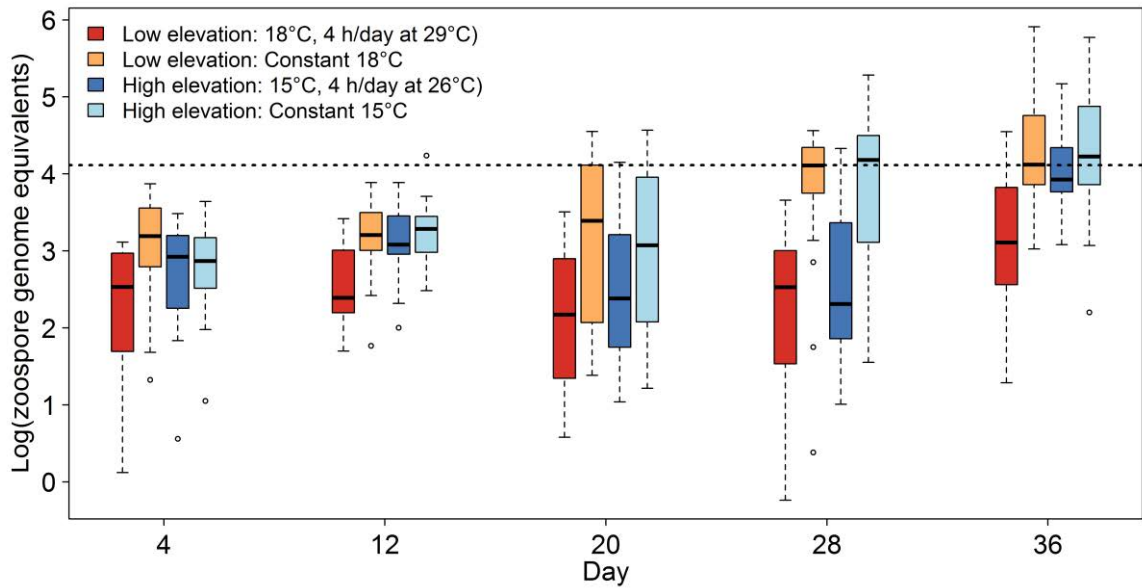


Figure 5.3 *Batrachochytrium dendrobatidis* infection loads (log-transformed zoospore genome equivalents detected on swabs) on the model host *Litoria spenceri* over 36 d of exposure to four temperature treatments. Heavy lines in each box indicate the median value, boxes indicate the 1st and 3rd quartiles, and whiskers indicate the range of the data. The dashed line marks an infection level at which odds predicted morbidity or mortality from chytridiomycosis. Note that over time most frogs gradually exceeded the threshold for morbidity or mortality except those from the low elevation heat pulse treatment, and both low and high elevation heat pulse treatments took longer to approach or exceed this threshold.

Table 5.2 Mean (\pm SD) and maximum *Batrachochytrium dendrobatidis* infection loads (zoospore genome equivalents detected on swabs) on individuals of the model host *Litoria spenceri* after 36 days of exposure to four temperature treatments: low elevation constant (18°C), low elevation heat pulse (18°C with daily 4-h heat pulses of 29°C), high elevation constant (15°C), and high elevation heat pulse (15°C with daily 4-h heat pulses of 26°C).

Elevation	Heat exposure	Mean	SD	Max
Low	Constant	73,740	186,941	811,333
	Heat pulse	4,649	8,585	35,233
High	Constant	99,415	176,727	590,667
	Heat pulse	26,896	43,223	148,333

Our survival analysis corroborated these patterns. The pooled risk of exceeding the threshold infection intensity was lower in both heat pulse treatments than in either of the constant-temperature treatments ($P = 0.02$), with the strength of this relationship significantly greater under hotter pulses ($P = 0.01$; Fig. 5.4). All inoculated frogs from the constant temperature treatments that were followed for the duration of the study had exceeded the threshold infection intensity by day 44, followed by all frogs from the high elevation heat pulse treatment by day 52. Ten of 11 (91%) inoculated frogs from the low elevation heat pulse treatment that were followed for the duration of the study maintained infection loads $< 13,700$ ZGE for the first nine weeks of the study and eventually cleared their infections, as indicated by consecutive swabs that tested negative for Bd on days 68 and 76.

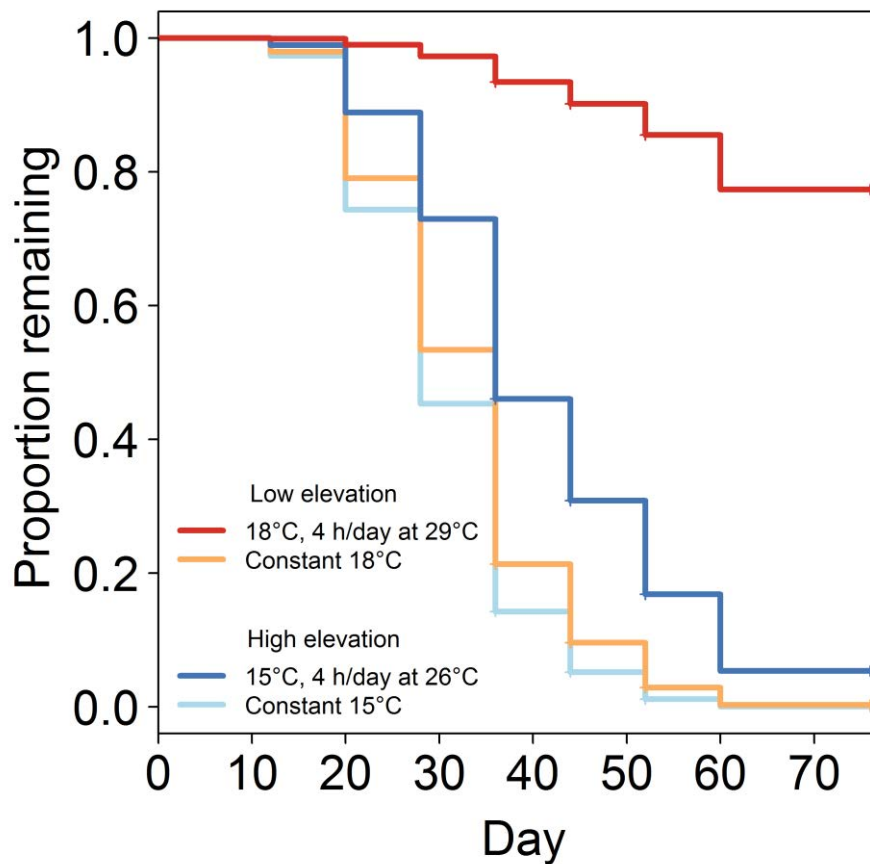


Figure 5.4 Survival probabilities of groups of *Batrachochytrium dendrobatidis*-infected *Litoria spenceri* exposed to four temperature treatments, estimated with a Cox Proportional Hazards analysis. In this analysis, time until death is the typical response. Instead, we used number of days until frogs reached a threshold infection intensity of 13,700 ZGE as a proxy for death. A receiver operating characteristic (ROC) analysis (Stockwell et al. 2016) for the first 43 days of the experiment (1 frog died and 14 frogs had shown signs of chytridiomycosis by this time) indicated that frogs with infection loads >13,700 zoospore genome equivalents (ZGE) had a 63% chance of dying or showing signs of chytridiomycosis. This level of infection has also been linked to development of lethal chytridiomycosis in other species (Briggs et al. 2010; Vredenburg et al. 2010; Kinney et al. 2011).

In our *in vitro* experiment, *Bd* growth generally decreased as the duration of heat pulses increased (Fig. 5.5), corresponding with our estimates of growth potential based on the hourly temperatures of our treatments (solid lines in Fig. 5.2b–g) and contrasting with our estimates of growth potential based on the average daily temperatures of our treatments (dashed lines in Fig. 5.2b–g). Specifically, the lag period increased ($P < 0.001$) and the maximum slope ($P < 0.001$), maximum height ($P < 0.001$), and area under the growth curves ($P < 0.001$) decreased with increasing heat pulse duration (Fig. 5.6; Table 5.1). The negative effect of heat on fungal growth parameters was greatest under the hotter, low-elevation (29°C) pulses (lag: $P = 0.003$; slope: $P < 0.001$; height: $P < 0.001$; area: $P < 0.001$; Table 5.1) – the magnitude of differences in measures of growth among low elevation treatments (red-orange gradients in Fig. 5.6) was greater than that among high elevation treatments (blue gradients in Fig. 5.6). However, for the low elevation treatments, a minimum of 4 h of heat daily was required to detect a statistically significant reduction in maximum slope, maximum height, and area under the curve, and 7 h of heat daily was required to detect a statistically significant increase in lag time (Fig. 5.6). In contrast, for the high elevation treatments, we detected statistically significant reductions in growth parameters after only 1 h of heat exposure (Fig. 5.6).

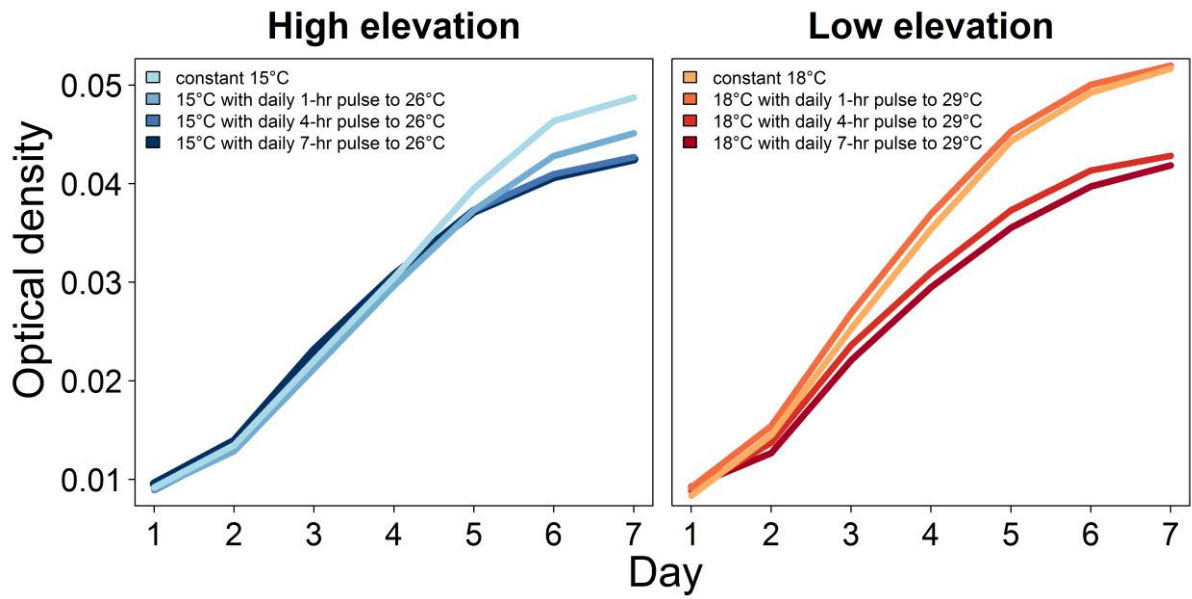


Figure 5.5 Average population growth over 7 d for *Batrachochytrium dendrobatidis* exposed to experimental temperature treatments. Treatments represent body temperature regimes of *Litoria serrata* in high-elevation rainforests (blue gradient) and low-elevation rainforests (red-orange gradient) of the Australian Wet Tropics.

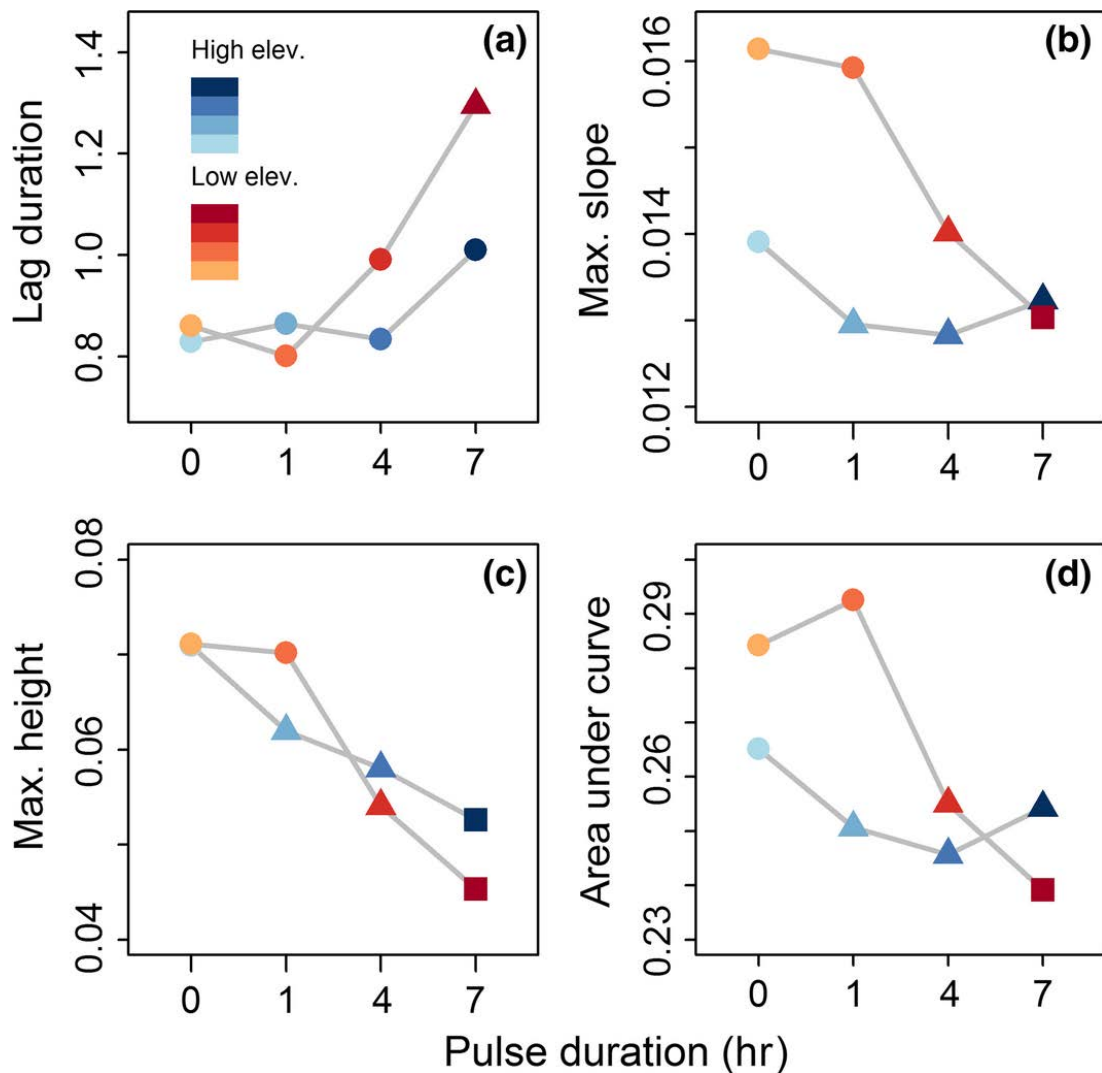


Figure 5.6 Characteristics of population growth curves for *Batrachochytrium dendrobatidis* exposed to experimental temperature treatments. Treatments represent body temperature regimes of *Litoria serrata* in high-elevation rainforests (blue gradient) and low-elevation rainforests (red-orange gradient) of the Australian Wet Tropics and differ in the duration of heat pulses (0 h, 1 h, 4 h, 7 h; darker colours correspond to longer heat pulses). The growth curve parameters were lag duration (time preceding the exponential growth phase), maximum slope of curve, maximum height of curve, and area under curve. Each symbol represents the least square mean of the population growth parameter calculated with linear mixed effects models. Different symbols indicate statistically significant pairwise differences determined with general linear hypothesis tests (glht function in Program R).

5.5 Discussion

In our study, experimentally inoculated frogs remained infected with Bd for at least several weeks, even when they experienced daily 26°C or 29°C heat spikes, temperatures that induce dormancy or mortality in the fungus after longer-term exposure (Piotrowski et al. 2004; Stevenson et al. 2013). This finding indicates that Bd can persist in hosts despite short exposures to temperatures above its thermal optimum, and helps explain the previous observation that warm, dry, 'marginal' habitats support frog communities with high pathogen prevalences (up to 100%; Puschendorf and Hodgson 2013). However, infection loads were markedly lower under daily 4-h temperature spikes of 29°C, representing conditions at our low elevation rainforest sites, compared to the corresponding low elevation constant temperature treatment that lacked heat pulses. After five weeks, the mean infection load in frogs in the low elevation heat pulse treatment was more than 9,000 ZGE below a critical threshold at which odds predicted morbidity or mortality from chytridiomycosis, whereas the mean infection load in the low elevation constant temperature treatment was 60,000 ZGE above the threshold. Ten of 11 (91%) frogs from the low elevation heat pulse treatment whose infections were tracked for the duration of the 11-week study even cleared their infections, although complete infection clearance took at least nine weeks. In contrast, 4-h temperature spikes of 26°C, which are representative of conditions at our high elevation rainforest sites, failed to promote infection clearance by hosts in our study, consistent with previous findings that Bd-related declines are more severe in upland amphibian populations in comparison to lowland populations (Richards et al. 1993; Lips 1999; Stuart et al. 2004). However, the high elevation heat pulse treatment was effective in reducing the rate at which infections exceeded the threshold for morbidity/mortality. Although we did not allow infections to progress to clinical levels, our modified Cox Proportional Hazards analysis suggests a clear survival benefit of these heat pulse treatments, especially the warmer pulses. These results offer new insight into disease responses in our model species *L. spenceri*, an endangered species, but may also be generalized to other species with similar behaviours and habitat preferences.

There are several plausible mechanisms that could explain the differences in infection patterns that we observed between paired constant temperature and heat pulse treatments. First, heat pulses could have had direct negative effects on the growth rate of Bd in host tissue, in accordance with the previous finding that 33°C heat spikes lowered exponential growth of Bd *in vitro* either by reducing rates of zoospore survival or encystment or by reducing production of zoospores within zoosporangia (Daskin et al. 2011). The results of our *in vitro*

study (Fig. 5) were consistent with the prediction that mild heat pulses directly interfere with Bd proliferation on the scale of hours (solid lines in Fig. 5.2b–g) and were opposite to the prediction that Bd growth is more heavily influenced by average daily temperatures (dashed lines in Fig. 5.2b–g). Four-hour heat spikes to 26°C and 29°C substantially delayed the exponential growth phase (lag duration), slowed the apparent rate of exponential growth (max. slope) and reduced overall population growth of Bd (max. height and area under curve) and these effects were most extreme under hotter pulses. That heat pulses had a considerable moderating effect on Bd growth *in vitro* after only 7 d (1–2 Bd generations) suggests that heat pulses could dramatically influence the trajectory of infections over the course of weeks or months in nature. Our work could thus help to explain the previous findings that infection risk among wild frogs decreased with increasing frequency of body temperatures above 25°C (Rowley and Alford 2013; Roznik 2013) and that frog populations in dry forest survived a chytridiomycosis outbreak by perching on sun-warmed rocks upon nightly emergence from streams while neighbouring rainforest populations succumbed to the disease (Puschendorf et al. 2011). Caveats to our study, however, are that we tested only a single Bd isolate and the full heat tolerance spectrum of all known Bd strains has not been established.

A second, non-mutually-exclusive mechanism that could explain the effects of our temperature treatments on infection levels is that heat pulses could have promoted host immunity, either directly because of temperature-dependent rates of physiological processes in ectotherms (Feder and Burggren 1992; Carey et al. 1999; Berger et al. 2004), or indirectly by preventing infections from reaching intensities that otherwise would have overwhelmed the host immune system. However, because we observed direct effects of heat on Bd performance *in vitro*, we could not determine whether there might have been a concurrent effect of heat pulses on host immune function in the *in vivo* trial. The hypothesis that heat pulses simultaneously hindered Bd population growth while facilitating host immunity would help explain our finding that most frogs from the low elevation heat pulse treatment eventually cleared infections despite the relatively rapid generation time of the pathogen. The direct and indirect effects of heat pulses on amphibian immunity would be a useful avenue for future study since temperature strongly influences immune responses in ectotherms (Feder 1992; Berger et al. 2004; Carey et al. 1999), yet previous research has rarely addressed the effects of realistic diurnal temperature patterns on immune parameters.

In our infection experiment, the low elevation heat pulse treatment apparently exceeded a threshold at which the rate of Bd growth was either insufficient to maintain fungal

populations within hosts, the host immune system outpaced the population growth of the fungus, resulting in eventual elimination of infections, or both. The high elevation heat pulse treatment failed to exceed this threshold but strongly reduced infection load, which is an important determinant of disease outcome (i.e., whether an individual develops chytridiomycosis) in this system (Briggs et al. 2010). Together, our results highlight the importance of incorporating realistic, fluctuating temperatures into experiments investigating host-pathogen interactions. Specifically, our results indicate that even in habitats in which *average* environmental temperatures may be suitable for pathogen growth and reproduction, infection risk or the outcome of an existing infection may be heavily influenced by host behaviours, such as microhabitat selection and thermoregulation, that briefly increase body temperatures to those that are detrimental to the parasite. Thus, management interventions incorporating environmental manipulation could aid in protecting some frog populations from chytridiomycosis-related declines (Scheele et al. 2014; Roznik et al. 2015a; Garner et al. 2016), although variability in the heat tolerance of different Bd strains could limit the applicability of this type of intervention to only some of the regions where Bd occurs. Providing canopy openings that facilitate frog basking, *via* small-scale removal of trees or large branches overhanging critical habitat (e.g., streams) has been proposed as a simple, non-invasive management strategy for riverine and other host species (Scheele et al. 2014; Roznik et al. 2015a). Artificial heat sources have also been recommended as an alternative to habitat modification where other types of environmental manipulation are not possible (Scheele et al. 2014). Our results, combined with evidence that shade reduction is linked to decreased infection risk (Raffel et al. 2010; Becker and Zamudio 2011; Becker et al. 2012; Roznik et al. 2015a; Scheele et al. 2015a) suggest that these interventions could be highly effective at reducing burdens of Bd and could therefore improve survival in populations with endemic infection. This management approach could be particularly applicable to translocation or reintroduction sites for critically endangered species (Garner et al. 2016).

5.6 Highlights

- We exposed Bd-infected frogs and Bd cultures to daily heat pulses mimicking median body temperatures of rainforest frogs or constant cool temperatures (control).
- Compared to control frogs, frogs that experienced heat pulses developed infections more slowly, were less likely to exceed lethal infection intensities, and were more likely to clear infections.
- Cultured Bd grew more slowly when exposed to heat pulses than in constant-temperature control treatments, suggesting that mild heat pulses have direct negative effects on Bd growth.
- Bd is highly responsive to simplified heat spikes representing median body temperatures of rainforest frogs and this can strongly influence the course of Bd infections.

Chapter 6 Experimental evidence that field body temperatures influence disease dynamics in an ectotherm

Sasha E. Greenspan, Elizabeth A. Roznik, Lexie Edwards, Richard Duffy, Deborah S. Bower, David A. Pike, Lin Schwarzkopf, Ross A. Alford

Citation for data in Tropical Data Hub (embargoed until publication): Greenspan, S. (2017). *Batrachochytrium dendrobatidis* growth data for Chapter 6 of PhD thesis: Thermal thresholds in the amphibian disease chytridiomycosis. James Cook University. [Data Files]

<http://dx.doi.org/10.4225/28/5a0cf51034a1c>

DOI: [10.4225/28/5a0cf51034a1c](https://doi.org/10.4225/28/5a0cf51034a1c)

Contributions: SEG, EAR, DSB, DAP, LS, and RAA co-developed the study. EAR, LE, RD, and DAP carried out the field work. SEG carried out the lab work. SEG carried out the statistical analyses with assistance from RAA. SEG drafted the manuscript and developed the figures and tables. All authors provided editorial input on the manuscript.

6.1 Abstract

Body temperature is a critical aspect of the ecology of ectotherms, and its influence on physiological processes should be studied at the level of the individual animal. Behaviorally elevating body temperature can influence the progression and outcome of infections by enhancing host immunity, inhibiting growth or viability of parasites, or a combination of these. We examined the body temperatures of individual green-eyed tree frogs (*Litoria serrata*), a stream-associated frog of the Australian Wet Tropics, in relation to patterns of prevalence of the frog parasite *Batrachochytrium dendrobatidis* (Bd). Many studies have noted that prevalence of Bd tends to be highest in cooler conditions, consistent with the observation that growth performance of Bd is low at temperatures higher than 25°C, but there are few data linking the temporal patterns of body temperatures experienced by individual frogs in the field to disease dynamics. We recorded the body temperatures of 79 wild green-eyed tree frogs every 15 min for up to 11 d. We compared these regimes by site, season, and elevation, and measured the growth of Bd *in vitro* in environmental chambers replicating a subset of the individual regimes from different elevations and seasons. Daily field body temperatures of frogs often exceeded air temperatures, suggesting that they thermoregulate. In warmer summer upland and winter lowland tracking periods, daily air temperatures reached 20–25°C and most frogs elevated body temperatures above 25°C regularly. In contrast, in cooler winter upland tracking periods, daily air temperatures reached 15–20°C, and most frogs did not elevate body temperatures above 25°C. Our laboratory trial revealed that Bd growth is highly responsive to the fluctuating body temperatures of individual frogs, and highlights the importance of considering individual variation in estimates of disease risk, in addition to population averages. For the first time, our study links population-level seasonal and elevational patterns in infection prevalence to host body temperature at the scale of the individual frog.

6.2 Introduction

The body temperatures of ectotherms fluctuate diurnally, seasonally, and annually (Feder and Lynch 1982). These fluctuations are influenced by environmental temperatures, but ectotherms also use behavioral thermoregulation to optimize physiological processes as the thermal environment changes (Sunday et al. 2014). Thermoregulatory behaviors include moving between sun and shade, altering posture and orientation to the sun, and regulating activity times (Stevenson 1985; Sunday et al. 2014) and these behaviors can accelerate digestion (Lillywhite et al. 1973; Freed 1980; Sinsch 1989; Witters and Sievert 2001; Lambrinos and Kleier 2003), growth (Lillywhite et al. 1973; Sinsch 1989), and reproductive processes (Muths and Corn 1997; Figueiredo et al. 2001), and mitigate infections (Richards-Zawacki 2010). The classic model of ectothermic thermoregulation relates the extent of thermoregulating to energetic costs and benefits (Huey and Slatkin 1976), but subsequent extensions of this model suggest that thermoregulation may offer fitness benefits even when energetic costs are high (Gilchrist 1995; Nadeau 2005; Herczeg 2006), especially in extreme environments (Vickers et al. 2011). In addition to influencing basic macroecological patterns in ectotherms, behavioral thermoregulation is linked to increasingly severe environmental problems such as anthropogenic global warming and emerging infectious diseases.

Behaviorally elevating body temperature can influence the progression and outcome of infections in ectotherms by enhancing host immunity, inhibiting growth or viability of parasites, or a combination of these. For example, grasshoppers *Melanoplus sanguinipes* inoculated with the fungus *Beauveria bassiana* were less likely to become diseased when allowed to bask than when basking was not possible (Inglis et al. 1996), likely because thermoregulation reduced virulence and spore production of the fungus (Springate and Thomas 2005). Similarly, increasing the body temperature of snakes increased the effectiveness of their immune response against helminth infections (Deakins 1980). Raising body temperatures above normal setpoints (behavioral fever) is also a common response to infection in invertebrate and vertebrate ectothermic hosts (Reynolds 1977; Inglis et al. 1996; Merchant et al. 2007; Richards-Zawacki 2010).

The disease chytridiomycosis, caused by the chytrid fungus *Batrachochytrium dendrobatidis* (Bd), has caused declines or extinctions of nearly 400 amphibian species since the 1970s (Lips 2016). Temperature can strongly affect the course and outcome of infections by Bd. In pure culture, optimal short-term growth of Bd occurs at 13-25°C (reviewed by Stevenson et al. 2013). Within this range, the fungus can adapt physiologically to optimize

growth under predictable daily temperature fluctuations (Raffel et al. 2013) and exhibits the fastest exponential growth rates when fluctuating temperature regimes reach the warmest optimal temperatures (Stevenson et al. 2014). At below-optimal temperatures, the fungus grows slowly but may still be virulent by trading off slower growth rates for increased fecundity (Woodhams et al. 2008; Stevenson et al. 2013) and zoospore longevity (Voyles et al. 2012). The lethal thermal maximum of Bd in constant-temperature environments is 26–29°C, depending on the isolate (Stevenson et al. 2013). In the laboratory, Bd survives but generally performs poorly in response to fluctuating temperature regimes with daily heat spikes above its lethal maximum (Daskin et al. 2011; Greenspan et al. 2017).

In the Wet Tropics region of Queensland, Australia, Bd has been linked to population declines of at least eight frog species (McDonald and Alford 1999; Alford 2010). Populations of some species disappeared from upland rainforests (> 400 m) but persisted in lowland rainforests (McDonald and Alford 1999; Alford 2010). In species that have since recovered or recolonized the uplands and are now distributed at a range of elevations, the prevalence of Bd still tends to be highest at high elevations and at cooler times of year (McDonald et al. 2005; Woodhams and Alford 2005; Llewelyn et al. 2010; Sapsford et al. 2013). These seasonal and elevational patterns in Bd prevalence are logical, given the strong thermal sensitivity of the fungus, and support the hypothesis that host body temperatures have direct effects on Bd dynamics in the field. However, studies to date are limited to population-level considerations of host temperatures or studies that measured single, instantaneous temperatures of individuals rather than detailed, semi-continuous thermal regimens of individuals. For instance, probability of infection at field sites in the Wet Tropics decreased with increasing proportions of instantaneous frog body temperatures above 25°C (Roznik 2013; Rowley and Alford 2013) and Bd infections developed more slowly in frogs exposed to heat spikes representing the median conditions experienced by populations of the Wet Tropics species *Litoria serrata* than in frogs exposed to constant cool temperatures (Greenspan et al. 2017). While these studies examined the effects of samples of host temperatures and population median thermal regimes, they did not examine the effects of the exact temperature regimes experienced by individual animals. The importance of replicating actual temperature regimes, rather than average temperatures or sampled distributions of temperatures, is becoming clearer as more studies have focused on how temperature regimes affect disease progression. For example, temperature fluctuations can lead to mortality in habitats in which mean temperatures appear ideal (Vickers and Schwarzkopf 2016). Understanding the influence on Bd

growth of individual temperature regimes experienced by frogs at different elevations will clarify how some frog populations persist when mean temperatures in their environments are within the range that is ideal for Bd growth (Bower et al. 2017).

Our goals in the present study were to collect detailed data describing the thermal regimes experienced in nature at a variety of sites, elevations, and seasons by *Litoria serrata*, a stream-associated frog of the Australian Wet Tropics, and to establish hypotheses relating these regimes to patterns of Bd prevalence in the Wet Tropics. We then aimed to measure patterns of growth of Bd *in vitro* in environmental chambers that replicated a subset of individual frog thermal regimes from different elevations and seasons, and to determine whether these patterns were consistent with our hypotheses.

6.3 Methods

Radio-tracking frogs

We selected *L. serrata* for our tracking project because this species is a rainforest endemic that experienced declines from chytridiomycosis and now persists in endemic association with Bd at a range of elevations (McKnight et al. in press). Using automated radio-telemetry, we recorded the body temperatures of 79 male *L. serrata* every 15 min for five to 11 consecutive days at four sites spanning a range of seasons and elevations. Twenty-five frogs were monitored in summer (wet season) at high elevation (800m). The high elevation summer site was Birthday Creek in Paluma Range National Park (4–14 December 2014; 18.980°S, 146.168°E, 800 m; N = 25). Twenty-five frogs were monitored in winter (dry season) at low elevation (20–100 m; Roznik 2013). The low-elevation sites were Kirrama Creek #1 in Girramay National Park (4–18 July 2011; 18.203°S, 145.886°E, 100 m; N = 11) and Stoney Creek in Djiru National Park (12–25 August 2011; 17.920°S, 146.069°E, 20 m; N = 14). Twenty-nine frogs were monitored in winter (dry season) at high elevation (750–800 m)(Roznik 2013). The high elevation winter sites were Birthday Creek in Paluma Range National Park (19 July–1 August 2011; 18.980°S, 146.168°E, 800 m; N = 15) and Windin Creek in Wooroonooran National Park (26 August–8 September 2011; 17.365°S, 145.717°E, 750 m; N = 14). At each site, we captured frogs along a 400-m stream transect.

To record frog body temperatures, we attached a temperature-sensitive radio-transmitter (Model A2414; Advanced Telemetry Systems, Isanti, MN) to each frog, using a waistband made of silicone tubing and cotton thread. The pulse rate of the signal emitted by each transmitter varied with temperature. We recorded the pulse rate of each transmitter

every 15 minutes with an automated data-logging receiver (Model SRX400A; Lotek Wireless, Newmarket, ON, Canada). We converted the pulse rates to temperatures with calibration curves provided for each transmitter by the manufacturer. We recorded air and water (stream) temperatures with waterproofed temperature dataloggers (Roznik and Alford 2012) at each site.

Bd growth trial

We measured growth of *Bd* cultures exposed to three individual frog thermal regimes. The regimes were selected from the set of individual frog temperature regimes described above. To select individual frog thermal regimes, we prioritized regimes with temperature spikes $>25^{\circ}\text{C}$, since not only have few previous studies measured *Bd* performance in response to temperature variability but even fewer have included heat spikes outside the thermal optimum range of *Bd*. This limited the study to regimes selected from summer-upland and winter-lowland data, as no winter-upland regimes included temperatures above 25°C . One regime (hereafter 'summer-upland') was selected from the upland frogs monitored in summer and this regime was representative of the body temperatures of most frogs in the summer upland tracking period (Fig. 6.1a; regime selected from group pictured in Fig. 6.2b). In the winter lowland tracking period at Stoney Creek, most frogs followed one of two thermal patterns and we selected one regime that represented each of these patterns. One pattern (hereafter 'winter-lowland-moderate') was for frogs to consistently experience mild heat spikes of a similar intensity as upland frogs in summer (Fig. 6.1b; regime selected from group pictured in Fig. 6.2g). The other pattern (hereafter 'winter-lowland-extreme') was for frogs to experience mostly mild heat spikes with intermittent heat spikes that were more intense. (Fig. 6.1c; regime selected from group pictured in Fig. 6.2h). To maximize our ability to interpret differences in *Bd* growth between treatments, we selected regimes that could be compared by a key attribute relevant to *Bd* growth (described in more detail below; summer-upland and winter-lowland-moderate primarily differed in the occurrence of temperatures $<20^{\circ}\text{C}$; winter-lowland-moderate and winter-lowland-extreme primarily differed in occurrence of intermittent temperature spikes $>29^{\circ}\text{C}$). For thermal regimes shorter than the length of the laboratory trial (10 d), we set the regimes to run on repeat in temperature-controlled chambers (see below). We also filled in occasional missing values for 15-minute temperature intervals in the temperature regimes with values calculated using maximum entropy interpolation (Dowse and Ringo 1987; Dowse 2009).

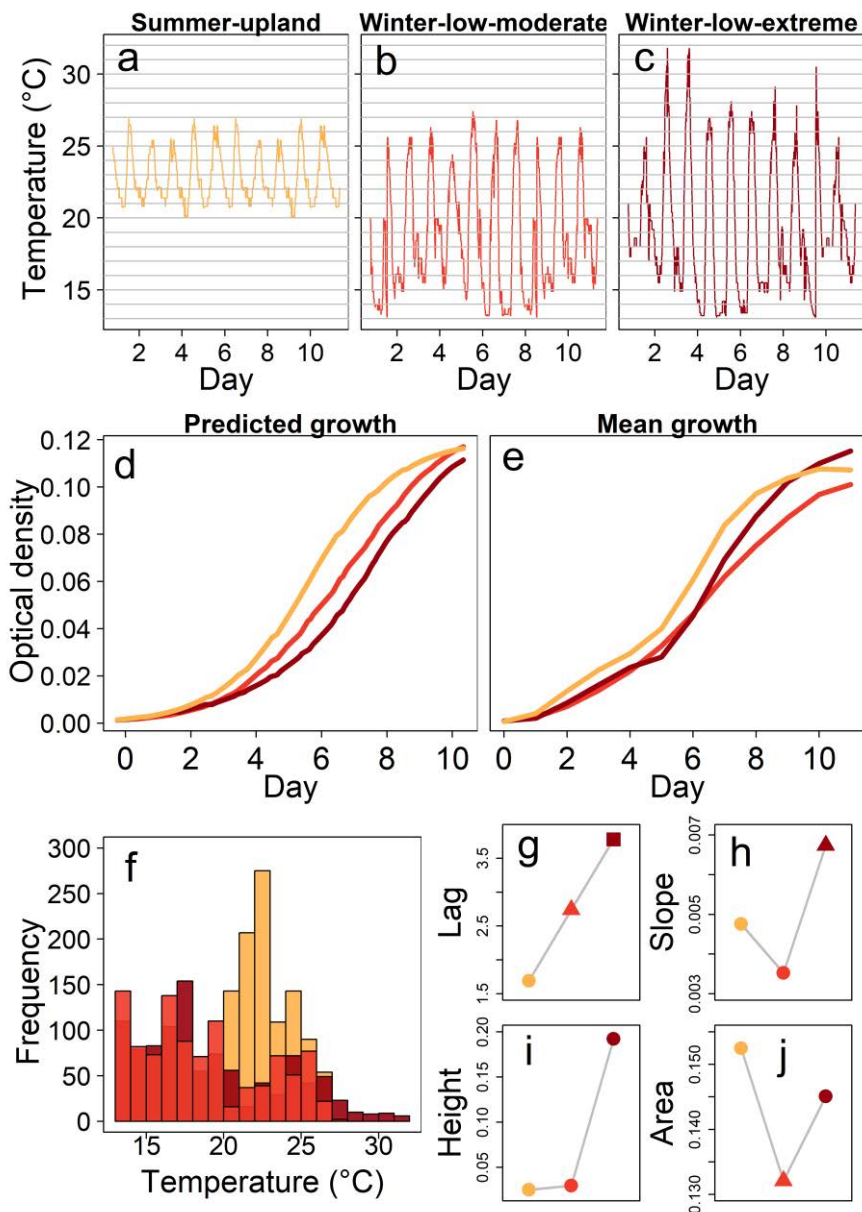


Figure 6.1 *In vitro* *Bd* growth trial. (a–c) Temperature treatments. (d) Predicted growth for each treatment. (e) Average observed growth for each treatment. (f) Frequencies of temperatures for each treatment. (g–j) Characteristics of *Bd* population growth curves for each treatment. Growth curve parameters were (g) lag duration (time preceding the exponential growth phase), (h) maximum slope of curve (representative of the maximum rate of exponential growth), and two measures of total growth: (i) maximum height of the curve and (j) area under the curve. Each symbol represents the least square mean of the population growth parameter calculated with linear mixed effects models. Different symbols indicate statistically significant pairwise differences determined with general linear hypothesis tests.

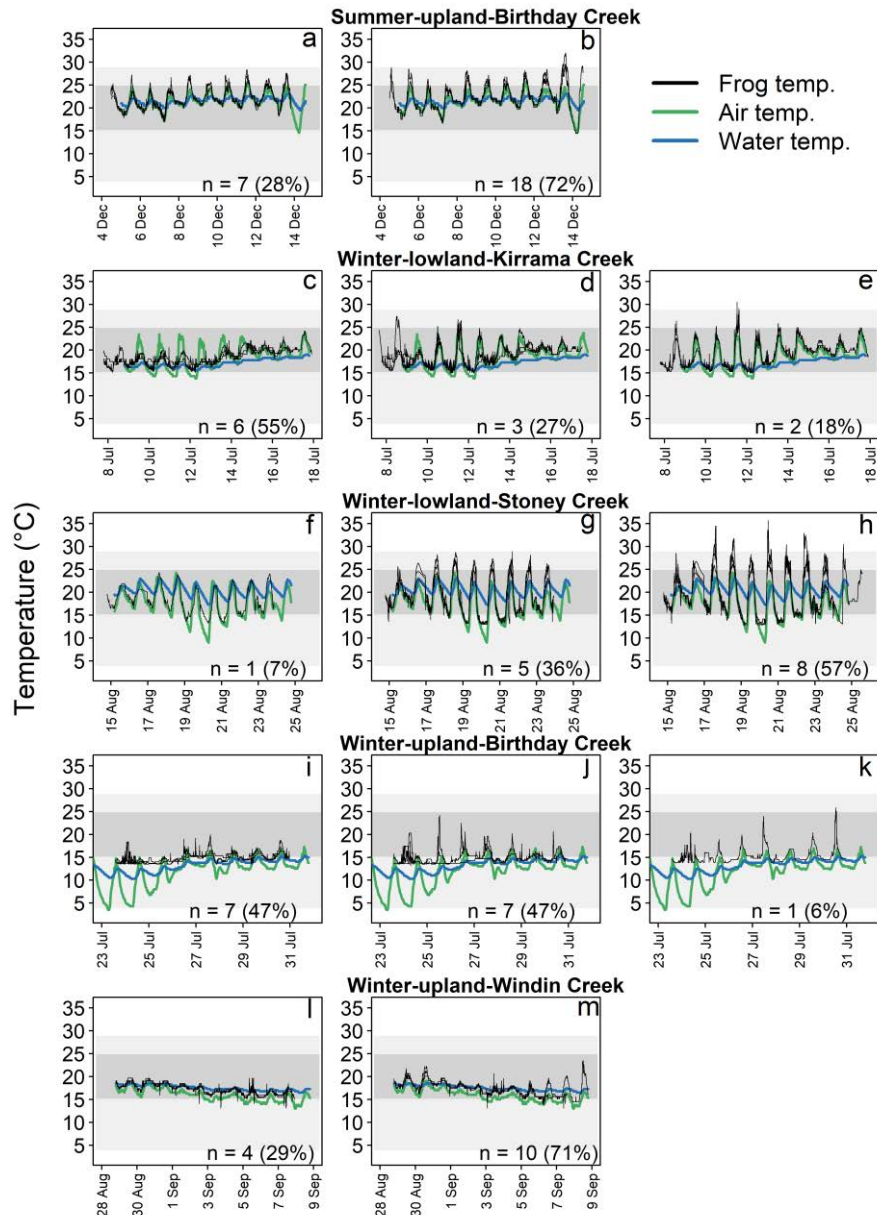


Figure 6.2 Representative temperature regimes for *Litoria serrata* recorded with temperature-sensitive radio-transmitters in the Australian Wet Tropics. Regimes are grouped by season, elevation, and tracking period. Within tracking periods, preliminary non-metric multidimensional scaling analyses ordinated the thermal regimes by maximum temperature, so for the purposes of describing variation in the individual thermal regimes that we recorded, we grouped regimes according to four temperature categories relevant to Bd growth: maximum temperature 15.1–20°C, 20.1–25°C, 25.1–29°C, and >29°C. Each plot corresponds to a line in Table 6.1. Up to three representative regimes are displayed for each group and the total sample size of each group is given at the bottom right of each plot. Gray polygons delineate the temperature categories relevant to Bd growth, with darker shades indicating

higher growth rates. Green (air temperature) and blue (water temperature) represent ambient conditions recorded with waterproofed temperature dataloggers (Roznik and Alford 2012) at each site.

The summer-upland regime (recorded in December at Birthday Creek) had relatively consistent peak daily temperatures, exceeding 25°C every day for a minimum of 15 min per day, a median of 1 h per day, and up to 5 h per day (Fig. 6.1a). Peak daily temperatures were 25.4–26.9°C, with minimum daily temperatures of 20.1–20.8°C and an overall median of 22.1°C (Fig. 6.1a). The winter-lowland regimes (recorded in August at Stoney Creek) had more extreme daily temperature fluctuations than the summer-upland regime, primarily due to lower minimum temperatures (Fig. 6.1b, c). The winter-lowland-moderate regime had relatively consistent daily peak temperatures, exceeding 25°C on 9 of 10 days for a minimum of 15 minutes per day, a median of 45 min per day, and up to 5.5 h per day (Fig. 6.1b). Peak daily peak temperatures (24.4–27.4°C) were only slightly more variable than the summer-upland regime, with lower minimum daily temperatures of 13.1–15.5°C and a lower overall median of 17.8°C (Fig. 6.1b). For the winter-lowland-extreme regime, we removed the second day of the original regime (pictured in Fig. 6.2h) because this day had several hours of interpolated temperatures. Compared to the winter-lowland-moderate regime, the winter-lowland-extreme regime had similar minimum daily temperatures (13.1–17.0°C), a similar overall median temperature (18.0°C), and similar peaks above 25°C, exceeding 25°C every day for a minimum of 15 minutes per day, a median of 45 min per day, and up to 6 h per day, but reached 31.8°C both on day 2 and day 3, with two peaks above 29°C on day 2 lasting 45 min and 1.75 h, respectively, and one peak above 29°C on day 3 lasting 2.25 h (Fig. 6.1c). The regime also briefly exceeded 29°C on day 7 (15 min) and day 9 (30 min; Fig. 6.1c). On days that did not exceed 29°C, peak temperatures were 25.6–28.1°C (Fig. 6.1c).

We used published population growth curves for Bd (Stevenson et al. 2013) to predict patterns of Bd growth under the three temperature regimes (Fig. 6.1d). Stevenson et al. (2013) documented population growth at constant 13°C, 15°C, 17°C, 19°C, 21°C, 23°C, 25°C, 26°C, 27°C, and 28°C for the Bd isolate Paluma-Lgenimaculata #2 [tadpole]-2010-CO, which originated from a larval *L. serrata* (our study species) at Birthday Creek (one of our study sites). For each constant-temperature growth curve, we used the grofit package in Program R (Kahm et al. 2010) to fit the curve to a set of conventional, parametric growth functions (logistic, Gompertz, modified Gompertz, and Richards) and a model-free spline function, select the best-fitting function according to Akaike's information criterion, and estimate parameters of the best-fitting growth function (Kahm et al. 2010; R core Team 2015). The parameters were lag duration (time preceding the exponential growth phase), maximum slope of the curve (representative of the maximum rate of exponential growth), and two measures of total

growth: maximum height of the curve and area under the curve (Kahm et al. 2010). We set all parameters to zero growth at temperatures $\geq 28^{\circ}\text{C}$ since Stevenson et al. (2013) found that Bd did not grow and eventually died when constantly exposed to these temperatures. We used linear interpolation to estimate parameters for temperatures not tested by Stevenson et al. (2013). Using substitution, we solved the version of the logistic equation used by grofit to provide a recursion equation:

$$X_{t+1} = \frac{b}{\frac{1 + (b - 1)X_t}{A}}$$

where X_t is the density of the Bd culture at time t , A is the asymptotic density, and b is the growth rate parameter. We then calculated X_t for each 1-min interval of each day of the *in vitro* trial, where A , the asymptotic maximum density, was estimated as the maximum density that would be reached at a constant temperature that equalled the mean of all 1-minute temperature readings over the course of the experiment. The parameter b was set each minute to the value it would have in an experiment run at that constant temperature throughout its course. This approach should yield a close approximation to the way Bd would actually grow under a fluctuating thermal regime, since its growth should accelerate and decelerate in response to the ambient temperature, although it may integrate temperature over a period longer than one minute. We plotted X_t to visualize predicted growth for each temperature regime (Fig. 6.1d).

For the trial, we used the Bd isolate Paluma-Lseratta-2012-RW-1. This isolate is maintained at the College of Public Health, Medical, and Veterinary Sciences, James Cook University. It originated from an adult *L. serrata* that was collected from Birthday Creek and died in captivity. The isolate was cryo-archived after two passages in nutrient broth. We revived aliquots of this isolate and cultured it in tryptone/gelatin hydrolysate/lactose (TGhL) broth in 25-cm³ tissue culture flasks, passaging it seven times before the trial and maintaining cultures at 22°C.

To obtain zoospores for each trial, we added cultured broth to Petri dishes containing TGhL broth in 1% agar. Plates were partially dried in a laminar flow cabinet, incubated at 21°C for four days, and then maintained alternatingly at 4°C and 21°C to sustain growth and zoospore production. We then added up to 5 ml of deionized (DI) water to the dishes to form

a zoospore suspension. We combined the liquid contents of each dish and calculated the concentration of zoospores with a hemocytometer (Neubauer Improved Bright-line).

We conducted the trial in tissue-culture-treated 96-well plates comprising 12 columns of eight wells. We added TGhL broth to the zoospore suspension to produce a final zoospore concentration of 2.5×10^5 zoospores per ml. We pipetted 100 μ l of the zoospore suspension into even-numbered columns and 100 μ l of TGhL broth into odd-numbered columns in each plate. We excluded 36 peripheral wells from analyses to avoid well position effects, leaving 30 wells containing the zoospore suspension and 30 wells containing TGhL broth that were included in analyses.

Seven replicate temperature-controlled chambers (Greenspan et al. 2016) were programmed to perform each of the three temperature regimes, for a total of 21 chambers, each containing one inoculated 96-well plate. The chambers were arranged in a blocked design, such that there were seven spatial blocks, each containing one chamber following each of the three temperature treatments. The location of each temperature treatment within each block was determined randomly. When the thermal regimes changed over 15 minutes by more than 0.1°C (the accuracy resolution of the temperature sensors in the chambers), the operational code for the chambers interpolated intermediate temperature steps each minute to allow for smooth temperature transitions to better approximate body temperature transitions in nature (Greenspan et al. 2016). The chambers reliably produced the frog body temperature regimes with a near-perfect 1:1 fit between target and observed temperatures during the trial period ($y = 1.0002x + 0.2135$; $R^2 = 0.9952$; 95% confidence interval for slope = 0.99997–1.00045; 95% confidence interval for intercept = 0.20849–0.21844). The observed temperatures remained within 1°C of the corresponding target temperatures for 97.9% of the trial period. The average difference between pairs of target and observed temperatures was $0.22^\circ\text{C} \pm 0.28^\circ\text{C}$ (SD). We rotated plates 180° daily to account for any small temperature gradients in the chambers. We quantified Bd growth by measuring the optical density of each well daily for 10 d (2–3 Bd generations) using a Multiskan Ascent 96/384 plate reader (MTX Lab Systems Inc., Vienna, Virginia, USA) at an absorbance of 492 nm. We then used the daily measurements of optical density to construct population growth curves for each well. We calculated daily optical density values by subtracting the average optical density of the wells containing only TGhL broth in the corresponding plate from the optical density of each well containing Bd (Stevenson et al. 2013).

For the growth curve represented by each well, we used *grofit* to estimate parameters of the curve as described above (Kahm et al. 2010). We then tested for effects of temperature treatment on each of the four growth curve parameters using linear mixed effects models (lmer function in lme4 package in Program R; Bates et al. 2015; R Core Team 2015), including replicate (1–7) as a random effect. When models indicated statistically significant differences in a parameter among treatments, we calculated least-squared means of the parameter for each treatment and performed pairwise comparisons of least-squared means (lsmeans function in lsmeans package; Lenth 2016) using general linear hypothesis tests (glht function in multcomp package; Hothorn et al. 2008).

6.4 Results

Frog body temperature variation in nature

At all elevations and in all seasons, frog temperature regimes fluctuated diurnally (Fig. 6.2). Within each tracking period, some frogs had body temperatures that followed air and water temperatures closely (Fig. 6.2a, c, f, i, l), whereas other frogs had body temperatures that exceeded ambient conditions daily during the warmest times of day (e.g., Fig. 6.2h). A common pattern was for frogs to follow air temperatures more closely during the day and water temperatures more closely at night. In the summer upland and winter lowland tracking periods, daily air temperatures reached 20–25°C and most frogs at Birthday Creek and Stoney Creek exceeded 25°C on a daily basis. In contrast, in the winter upland tracking periods, daily air temperatures reached 15–20°C and frogs generally maintained body temperatures less than 25°C. Preliminary non-metric multidimensional scaling analyses (metaMDS function in the vegan package in Program R; distance = 'euclidean'; Oksanen et al. 2016) for each site and season ordinated the thermal regimes by maximum temperature, so for the purposes of describing variation in the individual thermal regimes that we recorded, we grouped regimes according to four temperature categories relevant to Bd growth: maximum temperature 15.1–20°C, 20.1–25°C, 25.1–29°C, and >29°C.

Frogs tracked at high elevation in summer had the highest minimum (13.8–19.5°C) and median (21.2–22.4°C) body temperatures of the frogs we tracked (Fig. 6.2a, b; Table 6.1) and could be clustered into two groups based on maximum temperatures. The body temperatures of seven upland frogs in summer (28%) reached maximum temperatures of 27.3–28.7°C, exceeding 25°C nearly daily, typically for 30 min to 2 h, and up to 7.5 h at a time (Fig. 6.2a; Table 6.1). The body temperatures of 18 upland frogs in summer (72%) reached higher

maximum temperatures of 29.2–34.9°C but exceeded 30°C rarely (Fig. 6.2b; Table 6.1). The body temperatures of these frogs exceeded 25°C typically for 30 min–5.75 h and up to 10.25 h at a time and exceeded 29°C typically for 15 min–2.75 h and up to 6 h at a time (Table 6.1).

Frogs tracked at low elevation in winter had lower minimum (12.7–16.3°C) and median (18.0–19.3°C) body temperatures than those tracked in summer at high elevation (Fig. 6.2c-h; Table 6.1) and could be clustered into six groups based on site and maximum temperatures. At Kirrama Creek, the body temperatures of six frogs (55%) reached maximum temperatures of 21.0–24.2°C (Fig. 6.2c) and three frogs (27%) reached maximum temperatures of 25.5–27.4°C typically for 15–45 min and up to 2.25 h at a time (Fig. 6.2d; Table 6.1). Two frogs (18%) rarely reached 29.1–30.5°C for 15 minutes (Fig. 6.2e). The body temperatures of frogs tracked at Stoney Creek fluctuated more heavily than those at Kirrama Creek. One frog (7%) reached 24.4°C (Fig. 6.2f), five frogs (36%) reached 27.4–28.9°C, exceeding 25°C nearly daily, typically for 30 min–8.25 h and up to 12.5 h at a time (Fig. 6.2g), and eight frogs (57%) reached 29.4–35.7°C on one to three consecutive days, typically exceeding 29°C for 15–45 min and up to 4.25 h at a time (Fig. 6.2h).

Frogs tracked at high elevation in winter had the lowest median (14.3–18.1°C) body temperatures of the frogs we tracked and minimum body temperatures that were similar to the lowland frogs in winter (13.1–15.3°C; Fig. 6.2i-m; Table 6.1). The upland frogs in winter could be clustered into five groups based on site and maximum temperatures. Frogs tracked in winter (July) at Birthday Creek included seven frogs (47%) that reached 17.5–20.0°C (Fig. 6.2i), seven frogs (47%) that intermittently reached 20.1–24.2°C (Fig. 6.2j) and one frog that reached 25.9°C for 15 min on one tracking day (Fig. 6.2k; Table 6.1). At Windin Creek, four frogs (29%) reached 19.1–19.7°C (Fig. 6.2l) and ten frogs (71%) reached 20.1–23.5°C (Fig. 6.2m; Table 6.1).

Table 6.1 Summary of body temperature regimes of *Litoria serrata* in the Australian Wet Tropics.

Season (month)	Elevation	Site	Fig.	N (%)	Min. temp (°C)	Median temp (°C)	Max. temp (°C)	Median h > 25°C	Max. h > 25°C	Median h > 29°C	Max. h > 29°C
Summer (Dec.)	High (800m)	Birthday	2a	7/25 (28%)	16.9-17.3	21.6-22.4	27.3-28.7	0.50-2.00	3.75-7.50		
			2b	18/25 (72%)	13.8-19.5	21.2-22.4	29.2-34.9	0.63-5.75	3.50-10.25	0.25-2.75	0.25-6.00
Winter (Jul.)	Low (100m)	Kirrama	2c	6/11 (55%)	15.0-16.3	17.5-18.8	21.0-24.2				
			2d	3/11 (27%)	14.9-15.1	18.7-19.0	25.5-27.4	0.25-0.75	0.25-2.25		
			2e	2/11 (18%)	15.0-15.2	19.2-19.5	29.1-30.5	0.25-0.50	1.00-1.25	0.25	0.25
Winter (Aug.)	Low (20m)	Stoney	2f	1/14 (7%)	13.3	18.4	24.4				
			2g	5/14 (36%)	12.9-13.2	17.8-18.9	27.4-28.9	0.63-8.25	5.00-12.50		
			2h	8/14 (57%)	12.7-13.2	18.0-18.9	29.4-35.7	0.50-4.25	5.00-13.50	0.25-0.75	0.25-4.25
Winter (Jul.)	High (800m)	Birthday	2i	7/15 (47%)	13.3-13.6	14.5-14.8	17.5-20.0				
			2j	7/15 (47%)	13.2-13.6	14.3-14.8	20.1-24.2				
			2k	1/15 (6%)	13.8	14.8	25.9	0.25	0.25		
Winter (Aug.-Sep.)	High (750 m)	Windin	2l	4/14 (29%)	13.1-15.0	17.1-17.4	19.1-19.7				
			2m	10/14 (71%)	13.1-15.3	17.0-18.1	20.1-23.5				

Performance of Bd in individual frog temperature regimes

For the *in vitro* trial, we predicted that cultured Bd exposed to the summer-upland regime would grow fastest, the winter-lowland-moderate regime would exhibit intermediate growth, and the winter-lowland-extreme regime would grow slowest (Fig. 6.1d). In the trial, temperature treatments influenced initial lag times in Bd growth ($p < 0.001$), growth rates (maximum slope; $p = 0.024$), and total growth (area under the curve; $p < 0.001$), but not always in the ways we predicted (Fig. 6.1e). Bd growth curves for the summer-upland and winter-lowland-moderate treatments generally matched our predictions, with significantly shorter lag periods ($p < 0.001$; Fig. 6.1g) and significantly greater total growth ($p < 0.001$; Fig. 6.1j) in the summer-upland treatment. The winter-lowland-extreme treatment had significantly longer lag periods than those for the moderate winter treatment ($p < 0.001$), as we predicted (Fig. 6.1g). Counter to our predictions, however, these growth curves plateaued between days 4 and 5 and then increased sharply at significantly faster rates than in the moderate winter treatment ($p = 0.019$; Fig. 6.1h), ultimately exceeding the moderate winter treatment in total area ($p = 0.002$) and total height, although we did not detect statistically significant differences in growth curve heights between treatments ($p = 0.239$; Fig. 6.1i).

6.5 Discussion

In each season and elevation in which we radio-tracked *L. serrata* in the Australian Wet Tropics, the field body temperatures of at least some individuals exceeded air temperatures, raising the possibility that *L. serrata* thermoregulate actively. It is plausible that body temperatures exceeded air temperatures due to thermoregulation, considering that *L. serrata* has high resistance to evaporative water loss (Roznik and Alford 2014) and has ample opportunities in its habitat to absorb solar radiation or to contact sun-warmed rocks or vegetation (Roznik 2013), especially in areas with low canopy cover (Roznik et al. 2015a). In the summer upland and winter lowland tracking periods, diurnal air temperatures reached 20–25°C and most frogs experienced body temperatures above 25°C (temperatures that lower the performance of Bd) on a regular basis. In contrast, in the winter upland tracking periods, daily air temperatures reached 15–20°C and most frogs appeared unable to elevate body temperatures above 25°C. These results are consistent with the previous finding that prevalence of Bd in the Wet Tropics tends to be highest in winter at elevations above 400 m (McDonald and Alford 1999), but for the first time, our study links population-level seasonal and elevational patterns in infection prevalence to detailed host body temperature regimes at

the scale of the individual frog. The fine resolution of field body temperatures in our dataset may also serve as a valuable baseline for studies of organismal responses to anthropogenic climate change in the Australian Wet Tropics.

Although our data suggested that frogs thermoregulated in all tracking periods, body temperature regimes differed widely among individual frogs within tracking periods, and were differentiated most distinctly by maximum daily temperatures. Within each tracking period, some frog temperature regimes followed ambient conditions while others diverged substantially from ambient conditions, sometimes even reaching $>10^{\circ}$ higher than air temperatures during the warmest times of day. This finding suggests that, within populations, individual *L. serrata* differ in microhabitat selection or behaviors that influence body temperature, and highlights the importance of considering individual variation, in addition to population averages, in estimates of disease risk. Variability in thermoregulatory behavior may, at least in part, be explained by energy and fitness tradeoffs consistent with thermoregulation (Huey and Slatkin 1976; Herczeg 2006; Vickers et al. 2011) but disease can make these predictions more complex. For instance, on one hand, frogs could select warmer body temperatures primarily to optimize physiological processes, leading to a reduced probability of Bd infection (Roznik 2013; Rowley and Alford 2013) as a secondary fitness benefit. On the other hand, infected frogs could seek out warmer body temperatures than uninfected frogs, in response to the infections (Richards-Zawacki 2010). A useful avenue for future research is to determine whether Bd infection status or intensity contribute to the among-individual variation that we observed in thermal regimes. Another open question is the degree to which the host immune system is affected by variation in field body temperature occurring at fine time scales of minutes, hours, or days versus coarse time scales of weeks or months.

Our *in vitro* experiment is the first to measure growth of Bd under the complex temperature regimes experienced by individual frogs in the wild. The fungus initially grew exponentially in all treatments even when exposed to short, daily exposures to temperatures $>25^{\circ}\text{C}$, consistent with previous studies in which Bd survived *in vitro* after daily, 1-h exposures to 33°C (Daskin et al. 2011) and daily 1 to 7-h exposures to 26°C and 29°C , and in which experimentally inoculated frogs remained infected with Bd for at least several weeks when they experienced daily 26°C or 29°C heat spikes (Greenspan et al. 2017). This finding indicates that Bd can probably survive in hosts in the temperature regimes we tested, even though

temperatures >25°C lead to dormancy or mortality of Bd in constant-temperature environments (Stevenson et al. 2013).

As we predicted, Bd exposed to the summer upland regime exhibited consistently higher growth rates than under the moderate winter lowland regime. This outcome can be explained by the high frequencies of temperatures between 20–25°C (which are at the upper end of the optimal temperature range for growth of Bd) in the summer upland treatment (Fig. 1f), in line with the previous finding that Bd exhibited the fastest exponential growth rates when fluctuating temperature regimes reached the highest temperatures within the range optimal for Bd (Stevenson et al. 2014). That Bd grew better in our upland treatment than in the moderate lowland treatment is consistent with field patterns in which Bd prevalence tends to be higher at high elevations than at low elevations (McDonald and Alford 1999). Within high elevations, Bd prevalence is generally higher, survival rates are lower, and rates of loss of Bd infection are lower in winter (Sapsford et al. 2015), but summer thermal regimes may contribute strongly to the persistence of infections between winters. Our trial suggests that in uplands in summer, frog body temperatures may hover just below a virulence tipping point for Bd that is exceeded when temperatures drop in winter.

Some aspects of Bd performance in the extreme winter lowland treatment were consistent with our predictions. Growth in this treatment lagged the most in initial growth, slowed greatly at day 4–5 following the 31.8°C temperature spikes on days 2 and 3, and resumed exponential growth after day 5. This outcome was consistent with the previous findings that lag periods in Bd growth curves were longer in temperature treatments with daily heat spikes compared to constant cool temperatures (Greenspan et al. 2017) and that Bd failed to grow for two weeks at 28°C but commenced exponential growth after 9 d when transferred to 23°C (Stevenson et al. 2013). On the other hand, our study differed from Stevenson (et al. 2013) as we found that both depression and recovery of Bd following high-intensity but short-term temperature stress, which is representative of conditions in nature, may occur quickly but not instantaneously, suggesting that Bd growth rates respond to integrated temperature on the scale of days rather than minutes. Understanding the time scale at which Bd responds to temperature is helpful for predicting the course of infections that may progress over weeks or months in nature. Also, in contrast to the longer and hotter heat spikes on days 2 and 3 (maximum of 31.8°C for 45 min–2.25 h), the shorter and less intense heat spikes on days 7 (maximum of 29.1 for 15 min) and 9 (maximum of 30.5 for 30 min) did not appear to hamper Bd growth, suggesting the existence of a combined heat

intensity and duration threshold at which heat interferes with physiological processes, such as growth, of Bd.

Other aspects of Bd performance under the extreme winter lowland treatment were not consistent with our predictions. The slope of the recovery phase after day 5 was much steeper than we predicted, and there are several possible explanations. First, this might indicate a trade-off in which the organism responded to temperature stress by investing more resources into growth and reproduction in anticipation of continued stress at the expense of other life-history traits, in a similar way to the observation that Bd trades off slow growth for increased fecundity at temperatures below 15°C (Woodhams et al. 2008). Alternatively, the near plateau on days 4 and 5 indicates that fungal growth slowed and nutrients in the media were being consumed slowly, so these cultures probably had more available nutrients later in the experiment than those with consistent growth throughout the experiment. In addition, after day 5, there was a relatively large population base from which the culture could resume exponential growth. These factors could explain the markedly acute growth trajectory of the second growth phase in the extreme winter lowland treatment. *In vivo*, development of Bd colonies is presumably limited by factors such as the size of skin cells and the ability of zoospores to find suitable encystment sites (Berger et al. 2005a), which could prevent explosive growth in colonies recovering from heat stress. Our findings reinforce the importance of considering host factors in addition to parasite factors when predicting the effects of temperature on disease dynamics, especially as research on Bd-temperature interactions shifts towards more realistic temperature treatments. As a whole, our study reveals that Bd is highly responsive to the body temperatures of individual frogs and highlights the importance of understanding individual host behaviors in predicting climate-dependent disease dynamics at the level of populations and species.

6.6 Highlights

- We examined the body temperatures of individual frogs of the Australian Wet Tropics in relation to patterns of prevalence of Bd in this region.
- We measured growth of Bd exposed to individual frog thermal regimes.
- In warmer summer upland and winter lowland tracking periods, daily air temperatures reached 20–25°C and most frogs elevated body temperatures above 25°C regularly. In contrast, in cooler winter upland tracking periods, daily air temperatures reached 15–20°C, and most frogs did not elevate body temperatures above 25°C.
- Our results link the observation that prevalence of Bd, a cold-tolerant fungus, tends to be highest in winter at elevations > 400 m to frog body temperatures at the scale of the individual frog.
- Our laboratory trial revealed that Bd growth is highly responsive to the fluctuating body temperatures of individual frogs, and highlights the importance of considering individual variation in estimates of disease risk, in addition to population averages.

Chapter 7 General summary

Collectively, the research in my thesis demonstrates the complexity and importance of different aspects of temperature variability on interactions between frogs and the globally significant disease chytridiomycosis.

Chapter 3 provides a possible mechanistic explanation for observations that amphibians are more susceptible to Bd infection following temperature decreases compared to temperature increases. Cold-acclimated frogs treated with a dose of Bd and a temperature increase had active immune systems before and after treatment, whereas hot-acclimated frogs treated with a dose of Bd and a temperature decrease had active immune systems only after treatment and had higher Bd burdens than the cold-acclimated frogs. Our findings indicate that infection with Bd may have caused fewer changes to the immune system in the cold-acclimated frogs, because they had already adjusted immune parameters in response to stressful climatic conditions (cold). Although it is generally accepted that cold temperatures are immunosuppressive to amphibians, this study demonstrates that this may be an oversimplification of the interactions between temperature and immunity in ectotherms. We demonstrate that making physiological adjustments to cope with cold temperatures (acclimating) may actually prime the cellular immune system for some of the challenges of Bd infection. Our data suggest that frogs facing increases in temperature may be better poised to confront infections than those facing decreases in temperature. These findings underscore the concern raised by Raffel et al. (Raffel et al. 2013) that increases in the frequency of heat waves predicted under climate change will by definition be followed by increases in the frequency of temperature drops (back to 'normal' temperatures) which are associated with impaired immunity. A useful avenue for future study will be more in-depth immune profiling at fluctuating frog body temperatures, particularly when more is known about the components of the immune system that are protective against Bd.

Chapter 4 demonstrates that Bd infections can increase the heat sensitivity of frogs, consistent with 58% (11/19) of previous studies that tested host thermal responses to parasites, including data for parasitized amphibians, fish, and mollusks. Acclimation to realistic daily heat pulses raised the heat tolerance of infected frogs but not by enough to account for reductions in heat tolerance from infection. This suggests that for populations of some species, even as thermal tolerances are adjusted to long-term increases in temperature from climate change, this may not be sufficient to protect animals from the thermal consequences of parasitism. In addition, these results highlight the importance of incorporating biologically

meaningful acclimation temperature regimes into the design of ecological experiments. Our results raise the concern that increased heat sensitivity from infections may discourage protective thermoregulatory behaviors in frogs, even at temperatures below critical thermal maxima, tipping the balance in favor of the parasite. While gradual increases in average temperatures could favor the hosts of some parasites, such as cool-loving fungi, our study illustrates that we may currently be unable to predict the combined effects of infections and climate change on host populations. Of particular concern are unpredictable heat waves that are long enough to impose thermal stress on hosts but are too short to be therapeutic, for example by ridding hosts of heat-intolerant parasites, or to allow for thermal acclimation. Further studies are needed to determine the physiological and evolutionary causes of reduced thermal tolerance from infection, the synergistic effects of infection and temperature on fitness at non-critical temperatures, and the capacity for heat hardening and resistance adaptation in common parasites.

Chapters 5 and 6 demonstrate that brief, diurnal temperature spikes mimicking conditions in rainforests strongly influence growth of *Bd* and the progression of *Bd* infections. In Chapter 5, we exposed *Bd*-infected frogs to daily heat pulses representing median conditions experienced by *Litoria serrata*. Compared to control frogs exposed to constant cool temperatures, frogs that experienced daily 26°C heat spikes developed infections more slowly and exceeded lethal infection intensities more slowly. These effects were stronger when frogs experienced 29°C heat pulses and, unlike frogs exposed to 26°C heat spikes, most frogs that experienced 29°C heat spikes eventually cleared their infections. Thus, the 29°C treatment appeared to exceed a threshold at which the rate of *Bd* growth was either insufficient to maintain fungal populations within hosts, or the host immune system outpaced the population growth of the fungus, resulting in eventual elimination of infections, or both. This experiment indicated that *Bd* is highly responsive to simplified heat spikes representing median body temperatures of *Litoria serrata* and provided much incentive to test responses of the fungus to even more realistic patterns of body temperature spikes.

In Chapter 6, our temperature treatments were more realistic because they replicated the field temperature regimes of individual frogs, which allowed us to further hone in on temperature-mediated virulence thresholds for *Bd*. *Bd* exhibited a high rate of growth when it was exposed to an upland frog temperature regime recorded in summer, suggesting that in uplands in summer, frog body temperatures may hover just below a virulence tipping point for *Bd* that is exceeded when temperatures drop in winter, causing seasonal disease patterns. In

addition, temperature spikes that reached 31.8°C on only two consecutive days strongly inhibited growth of Bd cultures temporarily; growth lagged for the two days following the heat spikes, but then recovered. This finding suggests that both depression and recovery of Bd following high-intensity but short-term temperature stress, which is representative of conditions in nature, may occur quickly but not instantaneously, helping to clarify the time scale at which Bd responds to temperature. Considering that Bd is a relatively small organism with relatively few cells and a relatively short life cycle, it is possible that this fungus could integrate temperature on an extremely short time scale such as minute to minute. At the opposite end of the spectrum, if the fungus was not responsive to temperature on such a short time scale, it could instead perform as if it was in a constant temperature treatment based on the average temperature that it experiences over days or weeks. Our results suggest that Bd responds to temperature integrated on the scale of days, which is intermediate between these two extremes. Also, in contrast to longer and hotter heat spikes (maximum of 31.8°C for 45 min–2.25 h on two consecutive days), shorter and less intense heat spikes (maximum of 29.1°C for 15 min and maximum of 30.5°C for 30 min on isolated days) did not appear to hamper Bd growth, suggesting the existence of a combined heat intensity and duration threshold at which heat interferes with physiological processes, such as growth, of Bd. Understanding how Bd responds to and recovers from different types of heat spikes is helpful for predicting the course of infections that may progress amid changing temperatures over a period of weeks or months in nature. It was clear from our examination of individual frog temperature regimes in different seasons and elevations that population-level seasonal and elevational patterns in Bd infection prevalence can be traced to the thermal regimes experienced by individual frogs. Additional research is needed to determine whether Bd infection status or intensity contribute to the among-individual variation that we observed in thermal regimes. Another open question is the degree to which the host immune system is affected by variation in field body temperature occurring at fine time scales of minutes, hours, or days versus coarse time scales of weeks or months.

Together, the results of this thesis highlight the importance of incorporating realistic, fluctuating temperatures into experiments investigating host-pathogen interactions. Even in habitats in which *average* environmental temperatures may be suitable for pathogen growth and reproduction, infection risk or the outcome of an existing infection may be heavily influenced by the real temperatures experienced by individual animals. Considering that Bd is highly responsive to the body temperatures of individual frogs, environmental manipulation

could be a useful management intervention in some situations (Scheele et al. 2014; Roznik et al. 2015a; Garner et al. 2016). Providing canopy openings that facilitate frog basking, *via* small-scale removal of trees or large branches overhanging critical habitat (e.g., streams) has been proposed as a simple, non-invasive management strategy for riverine and other host species (Scheele et al. 2014; Roznik et al. 2015a). Artificial heat sources have also been recommended as an alternative to habitat modification where other types of environmental manipulation are not possible (Scheele et al. 2014). Our results, combined with evidence that shade reduction is linked to decreased infection risk (Raffel et al. 2010; Becker and Zamudio 2011; Becker et al. 2012; Roznik et al. 2015a; Scheele et al. 2015a) suggest that these interventions could be highly effective at reducing burdens of Bd and could therefore improve survival in populations with endemic infection. This management approach could be particularly applicable to translocation or reintroduction sites for critically endangered species (Garner et al. 2016).

References

- Agnew P, Koella JC, Michalakis Y (2000) Host life history responses to parasitism. *Microbes Infect* 2:891–896.
- Alford RA (2010) Declines and the global status of amphibians. In: Sparling DW, Lindner G, Bishop CA, Krest SK (eds) *Ecotoxicology of Amphibians and Reptiles*, 2nd edn. SETAC Press, USA, pp 13–46.
- An D, Waldman B (2016) Enhanced call effort in Japanese tree frogs infected by amphibian chytrid fungus. *Biol Lett* 12:20160018.
- Andre SE, Parker J, Briggs CJ (2008) Effect of temperature on host response to *Batrachochytrium dendrobatidis* infection in the mountain yellow-legged frog (*Rana muscosa*). *J Wildl Dis* 44:716–720.
- Arikan H, Cicek K (2014) Haematology of amphibians and reptiles: a review. *North West J Zool* 10:190–209.
- Bai C, Liu X, Fisher MC, Garner TWJ, Li Y (2012) Global and endemic Asian lineages of the emerging pathogenic fungus *Batrachochytrium dendrobatidis* widely infect amphibians in China. *Divers Distrib* 18:307–318.
- Bataille A, Cashins SD, Grogan L, Skerratt LF, Hunter D, Mcfadden M, Scheele B, Brannelly LA, Macris A, Harlow PS, Bell S, Berger L, Waldman B (2015) Susceptibility of amphibians to chytridiomycosis is associated with MHC class II conformation. *Proc B* 282:20143127.
- Bataille A, Fong JJ, Cha M, Wogan GOU, Baek HJ, Lee H, Min M-S, Waldman B (2013) Genetic evidence for a high diversity and wide distribution of endemic strains of the pathogenic chytrid fungus *Batrachochytrium dendrobatidis* in wild Asian amphibians. *Mol Ecol* 22:4196–4209.
- Bates AE, Leiterer F, Wiedeback ML, Poulin R (2011) Parasitized snails take the heat: a case of host manipulation? *Oecologia* 167:613–621.
- Bates D, Mächler M, Bolker B, Walker S (2015) Fitting linear mixed-effects models using lme4. *J Stat Softw* 67:1–48.
- Becker CG, Rodriguez D, Longo A V, Talaba AL, Zamudio KR (2012) Disease risk in temperate amphibian populations is higher at closed-canopy sites. *PLoS One* 7:e48205.
- Becker CG, Zamudio KR (2011) Tropical amphibian populations experience higher disease risk in natural habitats. *Proc Natl Acad Sci U S A* 108:9893–9898.
- Bellard C, Genovesi P, Jeschke JM (2016) Global patterns in threats to vertebrates by biological invasions. *Proc R Soc B Biol Sci* 283:20152454.

- Bennett MF, Daigle KR (1983) Temperature, stress and the distribution of leukocytes in red-spotted newts, *Notophthalmus viridescens*. *J Comp Physiol A* 153:81–83.
- Berger L, Hyatt AD, Speare R, Longcore JE (2005a) Life cycle stages of the amphibian chytrid *Batrachochytrium dendrobatidis*. *Dis Aquat Organ* 68:51–63.
- Berger L, Speare R, Daszak P, Green DE, Cunningham AA, Goggin CL, Slocombe R, Ragan MA, Hyatt AD, McDonald KR, Hines HB, Lips KR, Marantelli G, Parkes H (1998) Chytridiomycosis causes amphibian mortality associated with population declines in the rain forests of Australia and Central America. *Proc Natl Acad Sci USA* 95:9031–9036.
- Berger L, Speare R, Hines HB, Marantelli G, Hyatt AD, McDonald KR, Skerratt LF, Olsen V, Clarke JM, Gillespie G, Mahony M, Sheppard M, Williams C, Tyler MJ (2004) Effect of season and temperature on mortality in amphibians due to chytridiomycosis. *Aust Vet J* 82:434–439.
- Berger L, Speare R, Skerratt LF (2005b) Distribution of *Batrachochytrium dendrobatidis* and pathology in the skin of green tree frogs *Litoria caerulea* with severe chytridiomycosis. *Dis Aquat Organ* 68:65–70.
- Bernardo J, Spotila JR (2006) Physiological constraints on organismal response to global warming: mechanistic insights from clinally varying populations and implications for assessing endangerment. *Biol Lett* 2:135–139.
- Blair WF (1964) Isolating mechanisms and interspecies interactions in anuran amphibians. *Q Rev Biol* 39:334–344.
- Bonaccorso E, Guayasamin JM, Méndez D, Speare R (2003) Chytridiomycosis as a possible cause of population declines in *Atelopus cruciger* (Anura: Bufonidae). *Herpetol Rev* 34:331–333.
- Bonneaud C, Mazuc J, Gonzalez G, Haussy C, Chastel O, Faivre B, Sorci G (2003) Assessing the cost of mounting an immune response. *Am Nat* 161:367–379.
- Bosch J, Martínez-Solano I, García-Paris M (2001) Evidence of a chytrid fungus infection involved in the decline of the common midwife toad (*Alytes obstetricans*) in protected areas of central Spain. *Biol Conserv* 97:331–337.
- Bower DS, Mengersen K, Alford RA, Schwarzkopf L (2017) Using a Bayesian network to clarify areas requiring research in a host-pathogen system. *Conserv Biol* Early view.
- Boyle DG, Boyle DB, Olsen V, Morgan JAT, Hyatt AD (2004) Rapid quantitative detection of chytridiomycosis (*Batrachochytrium dendrobatidis*) in amphibian samples using real-time Taqman PCR assay. *Dis Aquat Organ* 60:141–148.
- Brannelly LA, Richards-Zawacki CL, Pessier AP (2012) Clinical trials with Itraconazole as a

- treatment for chytrid fungal infections in amphibians. *Dis Aquat Organ* 101:95–104.
- Brannelly LA, Webb RJ, Skerratt LF, Berger L (2016) Effects of chytridiomycosis on hematopoietic tissue in the spleen, kidney and bone marrow in three diverse amphibian species. *Pathog Dis* 74:1–10.
- Brannelly L, Hunter D, Lenger D, Scheele B, Grogan L, Webb R, Skerratt L, Berger L (2015) Disease ecology during the breeding season in the endangered *Litoria verreauxii alpina* and management implications. In: Ecological Society of Australia Annual Conference. Adelaide, p 117–118.
- Brem FMR, Lips KR (2008) *Batrachochytrium dendrobatidis* infection patterns among Panamanian amphibian species, habitats and elevations during epizootic and enzootic stages. *Dis Aquat Organ* 81:189–202.
- Briggs CJ, Knapp RA, Vredenburg VT (2010) Enzootic and epizootic dynamics of the chytrid fungal pathogen of amphibians. *Proc Natl Acad Sci* 107:9695–9700.
- Brook BW, Sodhi NS, Bradshaw CJA (2008) Synergies among extinction drivers under global change. *Trends Ecol Evol* 23:453–460.
- Burdon JJ (1987) *Diseases and plant population biology*. Cambridge University Press, Cambridge.
- Cabañes FJ, Sutton DA, Guarro J (2014) *Chrysosporium*-related fungi and reptiles: a fatal attraction. *PLoS Pathog* 10:e1004367.
- Cade W (1984) Effects of fly parasitoids on nightly calling duration in field crickets. *Can J Zool* 62:226–228.
- Campbell CR, Voyles J, Cook DI, Dinudom A (2012) Frog skin epithelium: electrolyte transport and chytridiomycosis. *Int J Biochem Cell Biol* 44:431–434.
- Carey C, Bruzgul JE, Livo LJ, Walling ML, Kuehl KA, Dixon BF, Pessier AP, Alford RA, Rogers KB (2006) Experimental exposures of boreal toads (*Bufo boreas*) to a pathogenic chytrid fungus (*Batrachochytrium dendrobatidis*). *Ecohealth* 3:5–21.
- Carey C, Cohen N, Rollins-Smith L (1999) Amphibian declines: an immunological perspective. *Dev Comp Immunol* 23:459–472.
- Carilli JE, Norris RD, Black B, Walsh SM, Mcfield M (2010) Century-scale records of coral growth rates indicate that local stressors reduce coral thermal tolerance threshold. *Glob Chang Biol* 16:1247–1257.
- Carver S, Bell BD, Waldman B (2010) Does chytridiomycosis disrupt amphibian skin function? *Copeia* 2010:487–495.

- Catenazzi A, Lehr E, Rodriguez LO, Vredenburg VT (2011) *Batrachochytrium dendrobatidis* and the collapse of anuran species richness and abundance in the upper Manu National Park, southeastern Peru. *Conserv Biol* 25:382–391.
- Catenazzi A, Lehr E, Vredenburg V (2014) Thermal physiology, disease, and amphibian declines on the eastern slopes of the Andes. *Conserv Biol* 28:509–517.
- Chatfield M, Richards-Zawacki C (2011) Elevated temperature as a treatment for *Batrachochytrium dendrobatidis* infection in captive frogs. *Dis Aquat Organ* 94:235–238.
- Chown SL, Jumbam KR, Sorensen JG, Terblanche JS (2009) Phenotypic variance, plasticity and heritability estimates of critical thermal limits depend on methodological context. *Funct Ecol* 23:133–140.
- Clark TD, Sandblom E, Jutfelt F (2013) Aerobic scope measurements of fishes in an era of climate change: respirometry, relevance and recommendations. *J Exp Biol* 216:2771–2782.
- Claver JA, Quaglia AIE (2009) Comparative morphology, development, and function of blood cells in nonmammalian vertebrates. *J Exot Pet Med* 18:87–97.
- Cleveland WS, Grosse E, Shyu WM (1992) Local regression models. Chapter 8 of *Statistical Models in S*. eds J.M. Chambers and T.J. Hastie, Wadsworth & Brooks/Cole.
- Cocroft R, Ryan M (1995) Patterns of advertisement call evolution in toads and chorus frogs. *Anim Behav* 49:283–303.
- Cooper EL, Wright RK, Klempau AE, Smith CT (1992) Hibernation alters the frog's immune system. *Cryobiology* 29:616–631.
- Cox DR (1972) Regression models and life-tables. *J R Stat Soc Ser B* 34:187–220.
- Dabbert C, Lochmiller R, Teeter R (1997) Effects of acute thermal stress on the immune system of the northern bobwhite (*Colinus virginianus*). *Auk* 114:103–109.
- Dahanukar N, Krutha K, Paingankar MS, Padhye AD, Modak N, Molur S (2013) Endemic asian chytrid strain infection in threatened and endemic anurans of the northern western Ghats, India. *PLoS One* 8:1–8.
- Daskin JH, Alford RA, Puschendorf R (2011) Short-term exposure to warm microhabitats could explain amphibian persistence with *Batrachochytrium dendrobatidis*. *PLoS One* 6:e26215.
- Daszak P, Cunningham AA, Hyatt AD (2003) Infectious disease and amphibian population declines. *Divers Distrib* 9:141–150.
- Davies NB, Halliday TR (1978) Deep croaks and fighting assessment in toads *Bufo bufo*. *Nature* 274:683–685.

- Davis A, Durso A (2009) White blood cell differentials of northern cricket frogs (*Acris c. crepitans*) with a compilation of published values from other amphibians. *Herpetologica* 65:260–267.
- Davis AK, Keel MK, Ferreira A, Maerz JC (2009) Effects of chytridiomycosis on circulating white blood cell distributions of bullfrog larvae (*Rana catesbeiana*). *Comp Clin Path* 19:49–55.
- Davis AK, Maerz JC (2008) Comparison of hematological stress indicators in recently captured and captive paedomorphic mole salamanders, *Ambystoma talpoideum*. *Copeia* 2008:613–617.
- Davis AK, Maney DL, Maerz JC (2008) The use of leukocyte profiles to measure stress in vertebrates: a review for ecologists. *Funct Ecol* 22:760–772.
- Deakins DE (1980) Helminth diagnosis and treatment in captive reptiles. In: Murphy JB, Collins JT (eds) *Perspectives in Biophysical Ecology. Contributions to Herpetology No. 1*. Society for the Study of Amphibians and Reptiles, Lawrence, Kansas, p 443–473.
- Deutsch CA, Tewksbury JJ, Huey RB, Sheldon KS, Ghalambor CK, Haak DC, Martin PR (2008) Impacts of climate warming on terrestrial ectotherms across latitude. *Proc Natl Acad Sci U S A* 105:6668–72.
- Dhabhar F, Miller A, Stein M, McEwen B, Spencer R (1994) Diurnal and acute stress-induced changes in distribution of peripheral blood leukocyte subpopulations. *Brain Behav Immun* 8:66–79.
- Dhabhar FS, Miller AH, McEwen BS, Spencer RL (1995) Effects of stress on immune cell distribution. Dynamics and hormonal mechanisms. *J Immunol* 154:5511–5527.
- Dowse HB (2009) Analyses for physiological and behavioral rhythmicity. In: Johnson ML, Brand L (eds) *Methods in Enzymology, Computer Methods, Part A*. Elsevier Inc. Academic Press, Burlington, p 141–174.
- Dowse HB, Ringo JM (1987) Further evidence that the circadian clock in *Drosophila* is a population of coupled ultradian oscillators. *J Biol Rhythms* 2:65–76.
- Duarte H, Tejedo M, Katzenberger M, Marangoni F, Baldo D, Beltrán JF, Martí DA, Richter-Boix A, Gonzalez-Voyer A (2012) Can amphibians take the heat? Vulnerability to climate warming in subtropical and temperate larval amphibian communities. *Glob Chang Biol* 18:412–421.
- Easterling DR (2000) Climate extremes: observations, modeling, and impacts. *Science* 289:2068–2074.
- Ern R, Huong DTT, Phuong NT, Madsen PT, Wang T, Bayley M (2015) Some like it hot: thermal

tolerance and oxygen supply capacity in two eurythermal crustaceans. *Sci Rep* 5:10743.

Farrer RA, Weinert LA, Bielby J, Garner TWJ, Balloux F, Clare F, Bosch J, Cunningham AA, Weldon C, du Preez LH, Anderson L, Pond SLK, Shahar-Golan R, Henk DA, Fisher MC (2011) Multiple emergences of genetically diverse amphibian-infecting chytrids include a globalized hypervirulent recombinant lineage. *Proc Natl Acad Sci* 108:18732–18736.

Feder ME, Burggren WW (eds) (1992) *Environmental physiology of the amphibians*. University of Chicago Press, Chicago

Feder ME, Lynch JF (1982) Effects of latitude, season, elevation, and microhabitat on field body temperatures of neotropical and temperate zone salamanders. *Ecology* 63:1657–1664.

Fellers GM, Bradford DF, Pratt D, Wood LL (2007) Demise of repatriated populations of mountain yellow-legged frogs (*Rana muscosa*) in the Sierra Nevada of California. *Herpetol Conserv Biol* 2:5–21.

Fellers GM, Green DE, Longcore JE, Gatten Jr RE (2001) Oral chytridiomycosis in the mountain yellow-legged frog (*Rana muscosa*). *Copeia* 2001:945–953.

Felton A, Alford RA (2006) Multiple mate choice criteria and the importance of age for male mating success in the microhylid frog, *Cophixalus ornatus*. *Behav Ecol Sociobiol* 59:786–795.

Figueiredo M, Lima S, Agostinho C, Da Costa Baeta F, Weigert S (2001) Acclimatized incubators for environmental experiments with frogs, in cages. *Rev Bras Zootec* 30:1135–1142.

Fisher M, Gow N, Gurr S (2016) Tackling emerging fungal threats to animal health, food security and ecosystem resilience. *Phil Trans R Soc Lond* 371:20160332.

Fisher MC, Henk DA, Briggs CJ, Brownstein JS, MAdoff LC, McCraw SL, Gurr SJ (2012) Emerging fungal threats to animal, plant and ecosystem health. *Nature* 484:186–194.

Forzán MJ, Heatley J, Russell KE, Horney B (2017) Clinical pathology of amphibians: a review. *Vet Clin Pathol* 46:11–33.

Freed AN (1980) An adaptive advantage of basking behavior in an anuran amphibian. *Physiol Zool* 53:433–444.

Frye FL (1991) Hematology as applied to clinical reptile medicine. In: Frye FL (ed) *Biomedical and Surgical Aspects of Captive Reptile Husbandry*. Kreiger Publishing Co., Malabar, FL, p 209–277.

Garner TWJ, Schmidt BR, Martel A, Pasmans F, Muths E, Cunningham AA, Weldon C, Fisher MC, Bosch J, Garner TWJ (2016) Mitigating amphibian chytridiomycoses in nature. *Philos Trans R Soc Lond B Biol Sci* 371:20160207.

- Gayou DC (1984) Effects of temperature on the mating call of *Hyla versicolor*. *Copeia* 1984:733–738.
- Geiger CC, Küpfer E, Schär S, Wolf S, Schmidt BR (2011) Elevated temperature clears chytrid fungus infections from tadpoles of the midwife toad, *Alytes obstetricans*. *Amphibia-Reptilia* 32:276–280.
- Gerhardt H, Doherty J (1988) Acoustic communication in the gray treefrog, *Hyla versicolor*: evolutionary and neurobiological implications. *J Comp Physiol A* 162:261–278.
- Gervasi SS, Foufopoulos J (2008) Costs of plasticity: responses to desiccation decrease post-metamorphic immune function in a pond-breeding amphibian. *Funct Ecol* 22:100–108.
- Gervasi SS, Hunt EG, Lowry M, Blaustein AR (2014) Temporal patterns in immunity, infection load and disease susceptibility: understanding the drivers of host responses in the amphibian-chytrid fungus system. *Funct Ecol* 28:569–578.
- Gilchrist GW (1995) Specialists and generalists in changing environments. I. Fitness landscapes of thermal sensitivity. *Am Nat* 146:252–270.
- Gillespie G, Hines H (1999) Status of temperate riverine frogs in south-eastern Australia. In: Campbell A (ed) *Declines and disappearances of Australian frogs*. Environment Australia, p 109–130.
- Gillespie GR, Hollis GJ (1996) Distribution and habitat of the spotted tree frog, *Litoria spenceri* Dubois (Anura: Hylidae), and an assessment of potential causes of population declines. *Wildl Res* 23:49–75.
- Goka K, Yokoyama JUN, Une Y, Kuroki T, Suzuki K, Nakahara M, Kobayashi A, Inaba S, Mizutani T, Hyatt AD (2009) Amphibian chytridiomycosis in Japan: distribution, haplotypes and possible route of entry into Japan. *Mol Ecol* 18:4757–4774.
- Greenspan SE, Bower DS, Webb RJ, Roznik EA, Stevenson LA, Berger L, Marantelli G, Pike DA, Schwarzkopf L, Alford RA (2017) Realistic heat pulses protect frogs from disease under simulated rainforest frog thermal regimes. *Funct Ecol* Early view.
- Greenspan SE, Longcore JE, Calhoun AJK (2012) Host invasion by *Batrachochytrium dendrobatidis*: fungal and epidermal ultrastructure in model anurans. *Dis Aquat Organ* 100:201–10.
- Greenspan SE, Morris W, Warburton R, Edwards L, Duffy R, Pike DA, Schwarzkopf L, Alford RA (2016) Low-cost fluctuating-temperature chamber for experimental ecology. *Methods Ecol Evol* 7:1567–1574.
- Hadji-Azimi I, Coosemans V, Canicatti C (1987) Atlas of adult *Xenopus laevis laevis* hematology.

- Dev Comp Immunol 11:807–874.
- Hamilton WD, Zuk M (1982) Heritable true fitness and bright birds: a role for parasites? Science 218:384–387.
- Hausfater G, Gerhardt HC, Klump GM (1990) Parasites and mate choice in gray treefrogs, *Hyla versicolor*. Am Zool 30:299–311.
- Heatley JJ, Johnson M (2009) Clinical technique: amphibian hematology: a practitioner's guide. J Exot Pet Med 18:14–19.
- Herczeg G (2006) Experimental support for the cost-benefit model of lizard thermoregulation. Behav Ecol Sociobiol 60:405–414.
- Hoskin CJ, Higgie M, McDonald KR, Moritz C (2005) Reinforcement drives rapid allopatric speciation. Nature 437:1353–1356.
- Howard AF V, N'Guessan R, Koenraadt CJM, Asidi A, Farenhorst M, Akogbéto M, Knols BGJ, Takken W (2011) First report of the infection of insecticide-resistant malaria vector mosquitoes with an entomopathogenic fungus under field conditions. Malar J 10:24.
- Huey RB, Slatkin M (1976) Cost and benefits of lizard thermoregulation. Q Rev Biol 51:363–384.
- Hurlbert SH (1984) Pseudoreplication and the design of ecological field experiments. Ecol Monogr 54:187–211.
- Hurlbert SH (2009) The ancient black art and transdisciplinary extent of pseudoreplication. J Comp Psychol 123:434–443.
- Inglis GD, Johnson DL, Goettel MS (1996) Effects of temperature and thermoregulation on mycosis by *Beauveria bassiana* in grasshoppers. Biol Control 7:131–139.
- IUCN (2015) IUCN Red List of Threatened Species. Version 2015.2. See www.iucnredlist.org.
- James TY, Letcher PM, Longcore JE, Mozley-Standridge SE, Porter D, Powell MJ, Griffith GW, Vilgalys R (2006) A molecular phylogeny of the flagellated fungi (Chytridiomycota) and description of a new phylum (Blastocladiomycota). Mycologia 98:860–871.
- Johnson ML, Berger L, Philips L, Speare R (2003) Fungicidal effects of chemical disinfectants, UV light, desiccation and heat on the amphibian chytrid *Batrachochytrium dendrobatidis*. Dis Aquat Organ 57:255–260.
- Joneson S, Stajich JE, Shiu SH, Rosenblum EB (2011) Genomic transition to pathogenicity in chytrid fungi. PLoS Pathog 7:e1002338.
- Kahm M, Hasenbrink G, Lichtenberg-frate H, Ludwig J, Kschischo M (2010) Grofit: fitting biological growth curves. J Stat Softw 33:1–21.

- Karasuyama H, Yamanishi Y (2014) Basophils have emerged as a key player in immunity. *Curr Opin Immunol* 31:1–7.
- Kinney VC, Heemeyer JL, Pessier AP, Lannoo MJ (2011) Seasonal pattern of *Batrachochytrium dendrobatidis* infection and mortality in *Lithobates areolatus*: affirmation of Vredenburg's "10,000 zoospore rule." *PLoS One* 6:e16708.
- Klein DA (2006) Diversity of Chytrids. In: Benckiser G, Schnell S (eds) *Biodiversity in agricultural production systems*. CRC Press, Boca Raton, p 165–187.
- Kolbe JJ, Ehrenberger JC, Moniz HA, Angilletta MJ (2014) Physiological variation among invasive populations of the brown anole (*Anolis sagrei*). *Physiol Biochem Zool* 87:92–104.
- Kowalski KT, Schubauer JP, Scott CL, Spotila JR (1978) Interspecific and seasonal differences in the temperature tolerance of stream fish. *J Therm Biol* 3:105–108.
- Kutywayo V, Karanja L, Oduor G, Nyirenda S (2006) Characterisation of a Malawian isolate of *Beauveria bassiana*, a potential control agent of coffee stem borer, *Monochamus leuconotus*. *Commun Agric Appl Biol Sci* 71:245–52.
- Lambrinos JG, Kleier CC (2003) Thermoregulation of juvenile Andean toads (*Bufo spinulosus*) at 4300 m. *J Therm Biol* 28:15–19.
- Lauckner G (1980) Diseases of Mollusca: Gastropoda. In: Kinne O (ed) *Diseases of Marine Animals. Volume 1. General Aspects, Protozoa to Gastropoda*. John Wiley & Sons, Inc., Chichester, UK, p 311–400.
- Lauckner G (1983) *Diseases of Marine Animals. Volume II. Introduction, Bivalvia to Scaphopoda*. Biologische Anstalt Helgoland, Hamburg.
- Laurance WF (2011) The world's tropical forests are already feeling the heat. *Yale Environ*. 360
- Laurance WF, McDonald KR, Speare R (1996) Epidemic disease and the catastrophic decline of Australian rain forest frogs. *Conserv Biol* 10:406–413.
- Lee F, Cheng T (1971) *Schistosoma mansoni* infection in *Biomphalaria glabrata*: alterations in heart rate and thermal tolerance in the host. *Pathology* 18:412–418.
- Lee RM, Rinne JN (1980) Critical thermal maxima of five trout species in the southwestern United States. *Trans Am Fish Soc* 109:632–635.
- Lifjeld JT, Dunn PO, Whittingham LA (2002) Short-term fluctuations in cellular immunity of tree swallows feeding nestlings. *Oecologia* 130:185–190.
- Lillywhite HB, Licht P, Chelgren P (1973) The role of behavioral thermoregulation in the growth energetics of the toad, *Bufo boreas*. *Ecology* 54:375–383.
- Lips KR (1999) Mass mortality and population declines of anurans at an upland site in western

- Panama. *Conserv Biol* 13:117–125.
- Lips KR (2016) Overview of chytrid emergence and impacts on amphibians. *Phil Trans R Soc Lond* 371:20150465.
- Liu X, Rohr JR, Li Y (2013) Climate, vegetation, introduced hosts and trade shape a global wildlife pandemic. *Proc Biol Sci* 280:20122506.
- Llewelyn J, Phillips BL, Alford RA, Schwarzkopf L, Shine R (2010) Locomotor performance in an invasive species: cane toads from the invasion front have greater endurance, but not speed, compared to conspecifics from a long-colonised area. *Oecologia* 162:343–348.
- Longcore JE, Pessier AP, Nichols DK (1999) *Batrachochytrium dendrobatidis* gen. et sp. nov., a chytrid pathogenic to amphibians. *Mycologia* 91:219–227.
- Lowe CH, Vance VJ (1955) Acclimation of the critical thermal maximum of the reptile *Urosaurus ornatus*. *Science* 122:73–74.
- Lutterschmidt WI, Hutchison VH (1997) The critical thermal maximum: history and critique. *Can J Zool* 75:1561–1574.
- Lutterschmidt WI, Schaefer JF, Fiorillo RA (2007) The ecological significance of helminth endoparasites on the physiological performance of two sympatric fishes. *Comp Parasitol* 74:194–203.
- MacGregor RGS, Richards W, Loh GL (1940) The differential leucocyte count. *J Pathol Bacteriol* 51:337–368.
- Madelaire CB, José da Silva R, Ribeiro Gomes F (2013) Calling behavior and parasite intensity in treefrogs, *Hypsiboas prasinus*. *J Herpetol* 47:450–455.
- Maniero GD, Carey C (1997) Changes in selected aspects of immune function in the leopard frog, *Rana pipiens*, associated with exposure to cold. *J Comp Physiol B Biochem Syst Environ Physiol* 167:256–263.
- Marcum R, St-Hilaire S, Murphy P, Rodnick K (2010) Effects of *Batrachochytrium dendrobatidis* infection on ion concentrations in the boreal toad *Anaxyrus (Bufo) boreas boreas*. *Dis Aquat Organ* 91:17–21.
- Margolis M (2011) *Arduino cookbook: recipes to begin, expand, and enhance your projects*, 2nd edn. O'Reilly Media, Inc.
- Martel A, Spitzen-van der Sluijs A, Blooi M, Bert W, Ducatelle R, Fisher MC, Woeltjes A, Bosman W, Chiers K, Bossuyt F, Pasmans F (2013) *Batrachochytrium salamandrivorans* sp. nov. causes lethal chytridiomycosis in amphibians. *Proc Natl Acad Sci U S A* 110:15325–9.
- Martin LB (2009) Stress and immunity in wild vertebrates: timing is everything. *Gen Comp*

- Endocrinol 163:70–76.
- Martin LB, Scheuerlein A, Wikelski M (2003) Immune activity elevates energy expenditure of house sparrows: a link between direct and indirect costs? *Proc Biol Sci* 270:153–158.
- Martin WF (1971) Mechanics of sound production in toads of the genus *Bufo*: passive elements. *J Exp Zool* 176:273–293.
- Mazzoni R, Cunningham AA, Daszak P, Apolo A, Perdomo E, Speranza G (2003) Emerging pathogen of wild amphibians in frogs (*Rana catesbeiana*) farmed for international trade. *Emerg Infect Dis* 9:995–998.
- McDaniel SJ (1969) *Littorina littorea*: lowered heat tolerance due to *Cryptocotyle lingua*. *Exp Parasitol* 25:13–5.
- McDonald K, Alford RA (1999) A review of declining frogs in northern Queensland. In: Campbell A (ed) *Declines and disappearances of Australian frogs*. Environment Australia, Canberra, p 14–22.
- McDonald KR, Mendez D, Muller R, Freeman AB, Speare R (2005) Decline in the prevalence of chytridiomycosis in frog populations in North Queensland, Australia. *Pacific Conserv Biol* 11:114–120.
- McMahon TA, Sears BF, Venesky MD, Bessler SM, Brown JM, Deutsch K, Halstead NT, Lentz G, Tenouri N, Young S, Civitello DJ, Ortega N, Fites JS, Reinert LK, Rollins-Smith LA, Raffel TR, Rohr JR (2014) Amphibians acquire resistance to live and dead fungus overcoming fungal immunosuppression. *Nature* 511:224–227.
- Meehl GA (2004) More intense, more frequent, and longer lasting heat waves in the 21st century. *Science* 305:994–997.
- Merchant M, Williams S, Trosclair PL, Eusey RM, Mills K (2007) Febrile response to infection in the American alligator (*Alligator mississippiensis*). *Comp Biochem Physiol Part A Mol Integr Physiol* 148:921–925.
- Murphy PJ, St-Hilaire S, Corn PS (2011) Temperature, hydric environment, and prior pathogen exposure alter the experimental severity of chytridiomycosis in boreal toads. *Dis. Aquat. Organ.* 95:31–42.
- Murray KA, Retallick RWR, Puschendorf R, Skerratt LF, Rosauer D, McCallum HI, Berger L, Speare R, VanDerWal J (2011) Assessing spatial patterns of disease risk to biodiversity: implications for the management of the amphibian pathogen, *Batrachochytrium dendrobatidis*. *J Appl Ecol* 48:163–173.
- Muths E, Corn P (1997) Basking by adult boreal toads (*Bufo boreas boreas*) during the breeding

- season. *J Herpetol* 31:426–428.
- Muths E, Scherer RD, Pilliod DS (2011) Compensatory effects of recruitment and survival when amphibian populations are perturbed by disease. *J Appl Ecol* 48:873–879.
- Nadeau GB-D and P (2005) The cost-benefit model of thermoregulation does not predict lizard thermoregulatory behavior. *Ecology* 86:560–566.
- Narins PM, Feng AS, Fay RR, Popper AN (eds) (2007) *Hearing and sound communication in amphibians*. Springer Science + Business Media, LLC, New York
- Nichols DK, Pessier AP, Longcore JE (1998) Cutaneous chytridiomycosis in amphibians: an emerging disease? In: *Proceedings AAZV and AAWV Joint Conference*. p 269–271.
- Nowakowski AJ, Watling JI, Whitfield SM, Todd BD, Kurz DJ, Donnelly MA (2017) Tropical amphibians in shifting thermal landscapes under land use and climate change. *Conserv Biol* 31:96–105.
- Nowakowski AJ, Whitfield SM, Eskew EA, Thompson ME, Rose JP, Caraballo BL, Kerby JL, Donnelly MA, Todd BD (2016) Infection risk decreases with increasing mismatch in host and pathogen environmental tolerances. *Ecol Lett* 19:1051–1061.
- Ockendon N, Baker DJ, Carr JA, White EC, Almond REA, Amano T, Bertram E, Bradbury RB, Bradley C, Butchart SHM, Doswald N, Foden W, Gill DJC, Green RE, Sutherland WJ, Tanner EVJ, Pearce-Higgins JW (2014) Mechanisms underpinning climatic impacts on natural populations: altered species interactions are more important than direct effects. *Glob Chang Biol* 20:2221–2229.
- Oksanen J, Blanchet F, Kindt R, Legendre P, O’hara R, Simpson G, Solymos P, Stevens M, Wagner H (2016) *vegan: community ecology package*. R package version 2.4-1. <https://CRAN.R-project.org/package=vegan>.
- Olson DH, Aanensen DM, Ronnenberg KL, Powell CI, Walker SF, Bielby J, Garner TWJ, Weaver G, Fisher MC (2013) Mapping the global emergence of *Batrachochytrium dendrobatidis*, the amphibian chytrid fungus. *PLoS One* 8:e56802.
- Parris KM, Velik-lord M, North JM a (2009) Frogs call at a higher pitch in traffic noise. *Ecol Soc* 14:25.
- Peig J, Green A (2009) New perspectives for estimating body condition from mass/length data: the scaled mass index as an alternative method. *Oikos* 118:1883–1891.
- Pessier AP, Nichols DK, Longcore JE, Fuller MS (1999) Cutaneous chytridiomycosis in poison dart frogs (*Dendrobates* spp.) and White’s tree frogs (*Litoria caerulea*). *J Vet Diagn Invest* 69:1081–1087.

- Peterson JD, Steffen JE, Reinert LK, Cobine PA, Appel A, Rollins-Smith L, Mendonça MT (2013) Host stress response is important for the pathogenesis of the deadly amphibian disease, chytridiomycosis, in *Litoria caerulea*. PLoS One 8:e62146.
- Pfennig KS, Tinsley RC (2002) Different mate preferences by parasitized and unparasitized females potentially reduces sexual selection. J Evol Biol 15:399–406.
- Phillott AD, Grogan LF, Cashins SD, McDonald KR, Berger L, Skerratt LF (2013) Chytridiomycosis and seasonal mortality of tropical stream-associated frogs 15 years after introduction of *Batrachochytrium dendrobatidis*. Conserv Biol 27:1058–1068.
- Piotrowski JS, Annis SL, Longcore JE (2004) Physiology of *Batrachochytrium dendrobatidis*, a chytrid pathogen of amphibians. Mycologia 96:9–15.
- Piovia-Scott J, Pope K, Worth S (2014) Correlates of virulence in a frog-killing fungal pathogen: evidence from a California amphibian decline. ISME J 2014:1–9.
- Polak M, Starmer WT (1998) Parasite-induced risk of mortality elevates reproductive effort in male *Drosophila*. Proc R Soc L B 265:2197–2201.
- Portner HO (2002) Climate variations and the physiological basis of temperature dependent biogeography: systemic to molecular hierarchy of thermal tolerance in animals. Comp Biochem Physiol - A Mol Integr Physiol 132:739–761.
- Powell MJ (1993) Looking at mycology with a Janus face: a glimpse at Chytridiomycetes active in the environment. Mycologia 85:1–20.
- Puschendorf R, Bolanos F (2006) Detection of *Batrachochytrium dendrobatidis* in *Eleutherodactylus fitzingeri*: effects of skin sample location and histologic stain. J Wildl Dis 42:301–306.
- Puschendorf R, Hodgson L (2013) Underestimated ranges and overlooked refuges from amphibian chytridiomycosis. Divers Distrib 2013:1–9.
- Puschendorf R, Hoskin CJ, Cashins SD, McDonald K, Skerratt LF, Vanderwal J, Alford RA (2011) Environmental refuge from disease-driven amphibian extinction. Conserv Biol 25:956–64.
- Pxytycz B, Jozkowicz A (1994) Differential effects of temperature on macrophages of ectothermic vertebrates. J Leukoc Biol 56:729–731.
- Rachowicz LJ, Vredenburg VT (2004) Transmission of *Batrachochytrium dendrobatidis* within and between amphibian life stages. Dis Aquat Organ 61:75–83.
- R Core Team (2015) R: A language and environment for statistical computing. R Foundation for Statistical Computing. Vienna, Austria. URL <https://www.R-project.org/>.
- Raffel TR, Halstead NT, McMahon TA, Davis AK, Rohr JR (2015) Temperature variability and

- moisture synergistically interact to exacerbate an epizootic disease. *Proc B* 282:20142039.
- Raffel TR, Michel PJ, Sites EW, Rohr JR (2010) What drives chytrid infections in newt populations? Associations with substrate, temperature, and shade. *Ecohealth* 7:526–536.
- Raffel TR, Rohr JR, Kiesecker JM, Hudson PJ (2006) Negative effects of changing temperature on amphibian immunity under field conditions. *Funct Ecol* 20:819–828.
- Raffel TR, Romanic JM, Halstead NT, McMahon TA, Venesky MD, Rohr JR (2013) Disease and thermal acclimation in a more variable and unpredictable climate. *Nat Clim Chang* 3:146–151.
- Rahmstorf S, Coumou D (2011) Increase of extreme events in a warming world. *Proc Natl Acad Sci* 108:17905–17909.
- Räisänen J (2002) CO₂-induced changes in interannual temperature and precipitation variability in 19 CMIP experiments. *J Clim* 15:2395–2411.
- Ramsey JP, Reinert LK, Harper LK, Woodhams DC, Rollins-Smith LA (2010) Immune defenses against *Batrachochytrium dendrobatidis*, a fungus linked to global amphibian declines, in the South African clawed frog, *Xenopus laevis*. *Infect Immun* 78:3981–3992.
- Retallick RWR, Miera V (2007) Strain differences in the amphibian chytrid *Batrachochytrium dendrobatidis* and non-permanent, sub-lethal effects of infection. *Dis Aquat Organ* 75:201–207.
- Reynolds WW (1977) Fever and antipyresis in the bluegill sunfish, *Lepomis Macrochirus*. *Comp Biochem Physiol Part C Comp Pharmacol* 57:165–167.
- Rezende EL, Tejedo M, Santos M (2011) Estimating the adaptive potential of critical thermal limits: methodological problems and evolutionary implications. *Funct Ecol* 25:111–121.
- Ribas L, Li M-S, Doddington BJ, Robert J, Seidel JA, Kroll JS, Zimmerman LB, Grassly NC, Garner TWJ, Fisher MC (2009) Expression profiling the temperature-dependent amphibian response to infection by *Batrachochytrium dendrobatidis*. *PLoS One* 4:e8408.
- Richards-Zawacki CL (2010) Thermoregulatory behaviour affects prevalence of chytrid fungal infection in a wild population of Panamanian golden frogs. *Proc Biol Sci* 277:519–28.
- Richards SJ, McDonald KR, Alford RA (1993) Declines in populations of Australia's endemic tropical rainforest frogs. *Pacific Conserv Biol* 1:66–77.
- Robertson JGM (1986) Female choice, male strategies and the role of vocalizations in the Australian frog *Uperoleia rugosa*. *Anim Behav* 34:773–784.
- Rodriguez D, Becker CG, Pupin NC, Haddad CFB, Zamudio KR (2014) Long-term endemism of

- two highly divergent lineages of the amphibian-killing fungus in the Atlantic Forest of Brazil. *Mol Ecol* 23:774–787.
- Roff DA (2002) *Life history evolution*. Sinauer Associates, Sunderland, MA.
- Rollins-Smith LA, Fites JS, Reinert LK, Shiakolas AR, Umile TP, Minbiole KPC (2015) Immunomodulatory metabolites released by the frog-killing fungus *Batrachochytrium dendrobatidis*. *Infect Immun* 83:4565–4570.
- Rollins-Smith L, Woodhams D (2012) Ecoimmunology. In: Demas G, Nelson R (eds) *Ecoimmunology*. Oxford University Press, New York, NY, p 92–143.
- Ron S, Merino A (2000) Amphibian declines in Ecuador: overview and first report of chytridiomycosis from South America. *Froglg* 42:2–3.
- Rosenblum EB, James TY, Zamudio KR, Poorten TJ, Ilut D, Rodriguez D, Eastman JM, Richards-Hrdlicka K, Joneson S, Jenkinson TS, Longcore JE, Parra Olea G, Toledo LF, Arellano ML, Medina EM, Restrepo S, Flechas SV, Berger L, Briggs CJ, Stajich JE (2013) Complex history of the amphibian-killing chytrid fungus revealed with genome resequencing data. *Proc Natl Acad Sci U S A* 110:9385–90.
- Rosenblum EB, Stajich JE, Maddox N, Eisen MB (2008) Global gene expression profiles for life stages of the deadly amphibian pathogen *Batrachochytrium dendrobatidis*. *Proc Natl Acad Sci* 105:17034–17039.
- Rowley JJJ, Alford RA (2007) Non-contact infrared thermometers can accurately measure amphibian body temperatures. *Herpetol Rev* 38:308–311.
- Rowley JJJ, Alford RA (2013) Hot bodies protect amphibians against chytrid infection in nature. *Sci Rep* 3:1515.
- Roznik EA (2013) Effects of individual behaviour on host-pathogen interactions: Australian rainforest frogs and the chytrid fungus *Batrachochytrium dendrobatidis*. PhD Thesis. James Cook University.
- Roznik EA, Alford RA (2012) Does waterproofing Thermochron iButton dataloggers influence temperature readings? *J Therm Biol* 37:260–264.
- Roznik EA, Alford RA (2014) Using pairs of physiological models to estimate temporal variation in amphibian body temperature. *J Therm Biol* 45:22–29.
- Roznik EA, Alford RA (2015) Seasonal ecology and behavior of an endangered rainforest frog (*Litoria rheocola*) threatened by disease. *PLoS One* 10:e0127851.
- Roznik EA, Sapsford SJ, Pike DA, Schwarzkopf L, Alford RA (2015a) Natural disturbance reduces disease risk in endangered rainforest frog populations. *Sci Rep* 5:13472.

- Roznik EA, Sapsford SJ, Pike DA, Schwarzkopf L, Alford RA (2015b) Condition-dependent reproductive effort in frogs infected by a widespread pathogen. *Proc B* 282:20150694.
- Rummukainen M (2012) Changes in climate and weather extremes in the 21st century. *Wiley Interdiscip Rev Clim Chang* 3:115–129.
- Santos MP, Dias LP, Ferreira PC, Pasin LAAP, Rangel DEN (2011) Cold activity and tolerance of the entomopathogenic fungus *Tolypocladium* spp. to UV-B irradiation and heat. *J Invertebr Pathol* 108:209–213.
- Sapsford SJ, Alford RA, Schwarzkopf L (2013) Elevation, temperature, and aquatic connectivity all influence the infection dynamics of the amphibian chytrid fungus in adult frogs. *PLoS One* 8:e82425.
- Sapsford SJ, Voordouw MJ, Alford RA, Schwarzkopf L (2015) Infection dynamics in frog populations with different histories of decline caused by a deadly disease. *Oecologia* 179:1099–1110.
- Schar C, Vidale PL, Luthi D, Frei C, Haberli C, Liniger MA, Appenzeller C (2004) The role of increasing temperature variability in European summer heatwaves. *Nature* 427:332–336.
- Scheele BC, Driscoll DA, Fischer J, Fletcher AW, Hanspach J, Vörös J, Hartel T (2015a) Landscape context influences chytrid fungus distribution in an endangered European amphibian. *Anim Conserv* 18:480–488.
- Scheele BC, Hunter DA, Grogan LF, Berger L, Kolby JE, Mcfadden MS, Marantelli G, Skerratt LF, Driscoll DA (2014) Interventions for reducing extinction risk in chytridiomycosis-threatened amphibians. *Conserv Biol* 28:1195–1205.
- Scheele BC, Hunter DA, Skerratt LF, Brannelly LA, Driscoll DA (2015b) Low impact of chytridiomycosis on frog recruitment enables persistence in refuges despite high adult mortality. *Biol Conserv* 182:36–43.
- Scheffers BR, Brunner RM, Ramirez SD, Shoo LP, Diesmos A, Williams SE (2013) Thermal buffering of microhabitats is a critical factor mediating warming vulnerability of frogs in the Philippine Biodiversity Hotspot. *Biotropica* 45:628–635.
- Schloegel LM, Ferreira CM, James TY, Hipolito M, Longcore JE, Hyatt AD, Yabsley M, Martins A, Mazzoni R, Davies AJ (2010) The North American bullfrog as a reservoir for the spread of *Batrachochytrium dendrobatidis* in Brazil. *Anim Conserv* 13:53–61.
- Schloegel LM, Toledo LF, Longcore JE, Greenspan SE, Vieira CA, Lee M, Zhao S, Wangen C, Ferreira CM, Hipolito M, Davies AJ, Cuomo C a, Daszak P, James TY (2012) Novel, panzootic and hybrid genotypes of amphibian chytridiomycosis associated with the

- bullfrog trade. *Mol Ecol* 21:5162–77.
- Sherman E (2008) Thermal biology of newts (*Notophthalmus viridescens*) chronically infected with a naturally occurring pathogen. *J Therm Biol* 33:27–31.
- Sinervo B, Mendez-de-la-Cruz F, Miles DB, Heulin B, Bastiaans E, Villagran-Santa Cruz M, Lara-Resendiz R, Martinez-Mendez N, Calderon-Espinosa ML, Meza-Lazaro RN, Gadsden H, Avila LJ, Morando M, De la Riva IJ, Sepulveda P V., Rocha CFD, Ibarguengoytia N, Puntriano CA, Massot M, Lepetz V, Oksanen TA, Chapple DG, Bauer AM, Branch WR, Clobert J, Sites JW (2010) Erosion of lizard diversity by climate change and altered thermal niches. *Science* 328:894–899.
- Sinsch U (1989) Behavioural thermoregulation of the Andean toad (*Bufo spinulosus*) at high altitudes. *Oecologia* 80:32–38.
- Skerratt LF, Berger L, Speare R, Cashins S, McDonald KR, Phillott AD, Hines HB, Kenyon N (2007) Spread of chytridiomycosis has caused the rapid global decline and extinction of frogs. *Ecohealth* 4:125–134.
- Somero GN (2005) Linking biogeography to physiology: evolutionary and acclimatory adjustments of thermal limits. *Front Zool* 2:1.
- Springate S, Thomas MB (2005) Thermal biology of the meadow grasshopper, *Chorthippus parallelus*, and the implications for resistance to disease. *Ecol Entomol* 30:724–732.
- Stearns SC (1992) *The evolution of life histories*. Oxford University Press, New York.
- Stevenson LA, Alford RA, Bell SC, Roznik EA, Berger L, Pike DA (2013) Variation in thermal performance of a widespread pathogen, the amphibian chytrid fungus *Batrachochytrium dendrobatidis*. *PLoS One* 8:e73830.
- Stevenson LA, Roznik EA, Alford RA, Pike DA (2014) Host-specific thermal profiles affect fitness of a widespread pathogen. *Ecol Evol* 4:4053–4064.
- Stevenson R (1985) The relative importance of behavioral and physiological adjustments controlling body temperature in terrestrial ectotherms. *Am Nat* 126:362–386.
- Stillman JH (2003) Acclimation capacity underlies susceptibility to climate change. *Science* 301:65.
- Stocker TF, Qin G-K, Plattner LV, Alexander SK, Allen NL, Bindoff F-M, Bréon J a., Church U, Cubasch S, Emori P, Forster P, Friedlingstein N, Gillett JM, Gregory DL, Hartmann E, Jansen B, Kirtman R, Knutti K, Krishna Kumar P, Lemke J, Marotzke V, Masson-Delmotte G a., Meehl II, Mokhov S, Piao V, Ramaswamy D, Randall M, Rhein M, Rojas C, Sabine D, Shindell LD, Talley LD, Vaughan DG, Xie SP (2013) Technical Summary. *Climate Change*

- 2013: The Physical Science Basis. Contribution of Working Group I to the Fifth Assessment Report of the Intergovernmental Panel on Climate Change.
- Stockwell MP, Bower DS, Bainbridge L, Clulow J, Mahony MJ (2015) Island provides a pathogen refuge within climatically suitable area. *Biodivers Conserv* 24:2583–2592.
- Stockwell MP, Garnham JI, Bower DS, Clulow J, Mahony MJ (2016) Low disease causing threshold in a frog species susceptible to chytridiomycosis. *FEMS Microbiol Lett* 363:fnw111.
- Stuart SN, Chanson JS, Cox NA, Young BE, Rodrigues ASL, Fischman DL, Waller RW (2004) Status and trends of amphibian declines and extinctions worldwide. *Science* 306:1783–1786.
- Sunday JM, Bates AE, Kearney MR, Colwell RK, Dulvy NK, Longino JT, Huey RB (2014) Thermal-safety margins and the necessity of thermoregulatory behavior across latitude and elevation. *Proc Natl Acad Sci* 111:5610–5615.
- Talley BL, Muletz CR, Vredenburg VT, Fleischer RC, Lips KR (2015) A century of *Batrachochytrium dendrobatidis* in Illinois amphibians (1888 – 1989). *Biol Conserv* 182:254–261.
- Tallmark B, Norrgren G (1976) The influence of parasitic trematodes on the ecology of *Nassarius reticulatus* (L.) in Gullmar Fjord (Sweden). *Zoon* 4:149–154.
- Van Rooij P, Martel A, Haesebrouck F, Pasmans F (2015) Amphibian chytridiomycosis: a review with focus on fungus-host interactions. *Vet Res* 46:137.
- Vaughan GE, Coble DW (1975) Sublethal effects of three ectoparasites on fish. *J Fish Biol* 7:283–294.
- Vernberg W, Vernberg F (1963) Influence of parasitism on thermal resistance of the mud-flat snail, *Nassarius obsoleta* Say. *Exp Parasitol* 332:330–332.
- Vickers M, Manicom C, Schwarzkopf L (2011) Extending the cost-benefit model of thermoregulation: high-temperature environments. *Am Nat* 177:452–61.
- Vickers M, Schwarzkopf L (2016) A random walk in the park: an individual-based null model for behavioral thermoregulation. *Am Nat* 187:481–490.
- Voyles J, Berger L, Young S, Speare R, Webb R, Warner J, Rudd D, Campbell R, Skerratt LF (2007) Electrolyte depletion and osmotic imbalance in amphibians with chytridiomycosis. *Dis Aquat Organ* 77:113–118.
- Voyles J, Johnson LR, Briggs CJ, Cashins SD, Alford R a, Berger L, Skerratt LF, Speare R, Rosenblum EB (2012) Temperature alters reproductive life history patterns in

- Batrachochytrium dendrobatidis*, a lethal pathogen associated with the global loss of amphibians. *Ecol Evol* 2:2241–2249.
- Voyles J, Young S, Berger L, Campbell C, Voyles WF, Dinudom A, Cook D, Webb R, Alford RA, Skerratt LF (2009) Pathogenesis of chytridiomycosis, a cause of catastrophic amphibian declines. *Science* 326:582–585.
- Vredenburg VT, Bingham R, Knapp R, Morgan J a T, Moritz C, Wake D (2007) Concordant molecular and phenotypic data delineate new taxonomy and conservation priorities for the endangered mountain yellow-legged frog. *J Zool* 271:361–374.
- Vredenburg VT, Knapp RA, Tunstall TS, Briggs CJ (2010) Dynamics of an emerging disease drive large-scale amphibian population extinctions. *Proc Natl Acad Sci U S A* 107:9689–9694.
- Wake DB, Vredenburg VT (2008) Are we in the midst of the sixth mass extinction? A view from the world of amphibians. *Proc Natl Acad Sci* 105:11466.
- Walker SF, Bosch J, James TY, Litvintseva AP, Oliver Valls JA, Piña S, García G, Rosa GA, Cunningham AA, Hole S (2008) Invasive pathogens threaten species recovery programs. *Curr Biol* 18:R853–R854.
- Wardziak T, Luquet E, Plenet S, Léna JP, Oxarango L, Joly P (2013) Impact of both desiccation and exposure to an emergent skin pathogen on transepidermal water exchange in the palmate newt *Lissotriton helveticus*. *Dis Aquat Organ* 104:215–224.
- Welbergen J a, Klose SM, Markus N, Eby P (2008) Climate change and the effects of temperature extremes on Australian flying-foxes. *Proc R Soc B Biol Sci* 275:419–425.
- Welch A, Semlitsch R, Gerhardt H (1998) Call duration as an indicator of genetic quality in male gray tree frogs. *Science* 280:1928–1930.
- Wheat D (2011) Arduino Software. *Arduino Internals* 89–97.
- Williams SE (2006) Vertebrates of the Wet Tropics rainforests of Australia: species distributions and biodiversity. Cooperative Research Centre for Tropical Rainforest Ecology and Management Report #46, Cairns.
- Winter K, Garcia M, Holtum JAM (2008) On the nature of facultative and constitutive CAM: environmental and developmental control of CAM expression during early growth of *Clusia*, *Kalanchoe*, and *Opuntia*. *J Exp Bot* 59:1829–1840.
- Witters L, Sievert L (2001) Feeding causes thermophily in the woodhouse’s toad (*Bufo woodhousii*). *J Therm Biol* 26:205–208.
- Woodhams DC, Alford RA (2005) Ecology of chytridiomycosis in rainforest stream frog assemblages of tropical Queensland. *Conserv Biol* 19:1449–1459.

- Woodhams DC, Alford RA, Briggs CJ, Johnson M, Rollins-Smith LA (2008) Life-history trade-offs influence disease in changing climates: strategies of an amphibian pathogen. *Ecology* 89:1627–1639.
- Woodhams DC, Alford RA, Marantelli G (2003) Emerging disease of amphibians cured by elevated body temperature. *Dis Aquat Organ* 55:65–67.
- Woodhams DC, Ardipradja K, Alford RA, Marantelli G, Reinert LK, Rollins-Smith LA (2007a) Resistance to chytridiomycosis varies among amphibian species and is correlated with skin peptide defenses. *Anim Conserv* 10:409–417.
- Woodhams DC, Rollins-Smith LA, Alford RA, Simon MA, Harris RN, Rollins-Smith L (2007b) Innate immune defenses of amphibian skin: antimicrobial peptides and more. *Anim Conserv* 10:425–428.
- Wright RK, Cooper EL (1981) Temperature effects on ectotherm immune responses. *Dev Comp Immunol* 5:117–122.
- Yeh S-W, Kug J-S, Dewitte B, Kwon M-H, Kirtman BP, Jin F-F (2009) El Niño in a changing climate. *Nature* 461:511–514.
- Young S, Warner J, Speare R, Berger L, Skerratt LF, Muller R (2012) Hematologic and plasma biochemical reference intervals for health monitoring of wild Australian tree frogs. *Vet Clin Pathol* 41:478–492.
- Young S, Whitehorn P, Berger L, Skerratt LF, Speare R, Garland S, Webb R (2014) Defects in host immune function in tree frogs with chronic chytridiomycosis. *PLoS One* 9:e107284.
- Zapata AG, Varas A, Torroba M (1992) Seasonal variations in the immune system of lower vertebrates. *Immunol Today* 13:142–147.
- Zweifel R (1968) Effects of temperature, body size, and hybridization on mating calls of toads, *Bufo a. americanus* and *Bufo woodhousii fowleri*. *Copeia* 1968:269–285.

Appendix Robust calling performance in frogs infected by a deadly fungal pathogen

Sasha E. Greenspan, Elizabeth A. Roznik, Lin Schwarzkopf, Ross A. Alford, and David A. Pike

This chapter has been published in *Ecology and Evolution* by John Wiley and Sons Ltd. as an open access article under the terms of the Creative Commons Attribution License and is reproduced here with no changes.

Link to article: <http://onlinelibrary.wiley.com/doi/10.1002/ece3.2256/full>

Link to license: <https://creativecommons.org/licenses/by/4.0/>

Citation: Greenspan SE, Roznik EA, Schwarzkopf L, Alford RA, Pike DA (2016) Robust calling performance in frogs infected by a deadly fungal pathogen. *Ecology and Evolution* 6:5964–5972.

Contributions: All authors co-developed the study. SEG, EAR, and DAP carried out the field work. SEG carried out the statistical analyses with assistance from RAA. SEG drafted the manuscript and developed the figures and tables. All authors provided editorial input on the manuscript.

A.1 Abstract

Reproduction is an energetically costly behavior for many organisms, including species with mating systems in which males call to attract females. In these species, calling males can often attract more females by displaying more often, with higher intensity, or at certain frequencies. Male frogs attract females almost exclusively by calling, and we know little about how pathogens, including the globally devastating fungus, *Batrachochytrium dendrobatidis*, influence calling effort and call traits. A previous study demonstrated that the nightly probability of calling by male treefrogs *Litoria rheocola* is elevated when they are in good body condition and are infected by *B. dendrobatidis*. This suggests that infections may cause males to increase their present investment in mate attraction to compensate for potential decreases in future reproduction. However, if infection by *B. dendrobatidis* decreases the attractiveness of their calls, infected males might experience decreased reproductive success despite increases in calling effort. We examined whether calls emitted by *L. rheocola* infected by *B. dendrobatidis* differed from those of uninfected individuals in duration, pulse rate, dominant frequency, call rate, or inter-call interval, the attributes commonly linked to mate choice. We found no effects of fungal infection status or infection intensity on any call attribute. Our results indicate that infected males produce calls similar in all the qualities we measured to those of uninfected males. It is therefore likely that the calls of infected and uninfected males should be equally attractive to females. The increased nightly probability of calling previously demonstrated for infected males in good condition may therefore lead to greater reproductive success than that of uninfected males. This could reduce the effectiveness of natural selection for resistance to infection, but could increase the effectiveness of selection for infection tolerance, the ability to limit the harm caused by infection, such as reductions in body condition.

A.2 Introduction

Animals maximize their fitness by adjusting their allocation of resources throughout their lifetimes (Stearns 1992; Roff 2002). Reproduction is an energetically costly behavior for many species. Pathogen infections can thus alter reproductive investment in complex ways. Individuals carrying infections may reduce their present investment in reproduction so that they can divert energy to manage the costs of infection, for example by producing and increasing immune responses (Cade 1984; Bonneaud et al. 2003; Martin et al. 2003; Madelaire et al. 2013). For instance, male field crickets, *Gryllus integer*, call less frequently when parasitized by *Euphasiopteryx ochracea* flies (Cade 1984), and male Burmeister's treefrogs, *Hypsiboas prasinus*, decrease their calling rate with increasing helminth parasite intensity (Madelaire et al. 2013). Alternatively, infected individuals may increase their investment in reproduction to compensate for a potentially shortened lifespan (Agnew et al. 2000). For example, male *Drosophila nigrospracula* court more when parasitized by mites (*Macrocheles subbadius*; Polak and Starmer 1998).

Because male courtship behaviors are usually subject to sexual selection by females, male reproductive success is contingent not only on the quantity or frequency of reproductive behavior but also on its quality, which is evaluated by females during mate choice (Welch et al. 1998). In frogs, male advertisement calls are energetically intensive, and the spectral and temporal properties of calls that are associated with female mate choice are quantifiable, making them suitable for studies of disease-mediated changes in courtship behavior (Blair 1964; Gerhardt and Doherty 1988; Cocroft and Ryan 1995; Welch et al. 1998; Hoskin et al. 2005; An and Waldman 2016). Female frogs generally prefer frequent, long, rapidly repeated, and low-frequency calls (Gerhardt and Doherty 1988; Felton and Alford 2006; Parris et al. 2009). These attributes often reflect high investment in calling, good body condition, or large body size, all of which may be directly important or may be honest indicators of male quality (Gerhardt and Doherty 1988; Felton and Alford 2006; Parris et al. 2009). Parasite-mediated models of sexual selection predict that the calls of unhealthy males will be less attractive than those of healthy males (Hamilton and Zuk 1982). Females thus should prefer to mate with healthy males, thereby avoiding passing on genes for parasite susceptibility to their offspring. In contrast, if the sexual signals of unhealthy males are either indistinguishable from or more attractive than those of healthy males, females may pass on genes for disease susceptibility to their offspring (Pfennig and Tinsley 2002; An and Waldman 2016).

The amphibian pathogen *Batrachochytrium dendrobatidis* (hereafter Bd) has recently

become endemic in many anuran populations worldwide (Farrer et al. 2011). We understand very little about how this pathogen influences frog behavior, including energetically costly mate attraction and reproductive behavior. If the calls of infected males are as or more attractive to females than those of uninfected males, as is hypothesized in Bd-infected *Hyla japonica* (An and Waldman 2016), then these males could perpetuate infections by passing them to mates and by passing on genetic traits that render offspring susceptible to disease.

Our objective was to determine whether Bd infection alters individual call attributes commonly linked to mate choice. As a model species we used a stream-breeding rainforest frog from tropical Australia (*Litoria rheocola*) that breeds year-round and is already known to exhibit a body condition-dependent response of one aspect of male reproductive behavior (probability of calling each night) to Bd infection (Roznik et al. 2015b). In uninfected males of this species, the probability of calling each night (i.e., whether or not a frog calls on a given night) is independent of body condition (Roznik et al. 2015b). However, when males are infected by Bd, the probability of calling each night is significantly related to body condition. Specifically, infected frogs in the poorest body condition are 40% less likely to call than uninfected frogs, whereas those in the best body condition are 30% more likely to call than uninfected frogs (Roznik et al. 2015b).

The ultimate effect of these relationships on male reproductive success in *L. rheocola* is unknown, because Roznik et al. did not examine the *characteristics* of the calls emitted by each individual. Males could modulate their call attributes according to their infection status or intensity in several possible ways: infected males could 1) enhance the quality of calls, for example by calling more rapidly, producing longer calls, or producing calls at frequencies that are more attractive to females, as occurs in the seasonal-breeding *Hyla japonica* (An and Waldman 2016). However, infected males (even those in good body condition) might be unable to expend additional energy to do this, and instead 2) might not adjust their call characteristics or 3) might even produce calls of lower quality, for example by reducing their calling rate or the lengths of individual calls. We examined these possibilities using field-collected recordings of natural calling by infected and uninfected males.

A.3 Methods

Study Species and Site

The common mistfrog, *L. rheocola*, is an Endangered (IUCN 2015) treefrog that occurs in association with rocky, fast-flowing rainforest streams in northeastern Queensland,

Australia (Roznik and Alford 2015). Males call year-round, typically perching on streamside rocks and vegetation (Roznik et al. 2015b). By the mid-1990s, chytridiomycosis outbreaks had extirpated this species from high-elevation portions of its range (>400 m ASL) (Richards et al. 1993; McDonald and Alford 1999). Many populations have subsequently recovered or recolonized in these areas and currently persist with endemic-phase infections (McDonald et al. 2005; Sapsford et al. 2013; Phillott et al. 2013; Sapsford et al. 2015). We studied attributes of male advertisement calls in a recovered or recolonized population with endemic disease at Windin Creek in Wooroonooran National Park (750 m ASL; 17.365°S, 145.717°E). This shallow, fast-flowing stream varies in width (5-10 m), substrate size (small pebbles to large boulders), and structure (contains pools, runs, riffles, and waterfalls), and runs through dense tropical rainforest with abundant large trees (10 m in height), vines, epiphytes, shrubs, and herbaceous plants (Roznik and Alford 2015).

Field sampling

We surveyed 61 calling male frogs along an 800-m stream transect on 16 nights from June through September 2014. We recorded each calling male by positioning a tripod-mounted directional microphone (ME 66, Sennheiser Nordic, Helsinki, Finland) and recorder (TASCAM DR-2J, TEAC America Inc., Montebello, CA, USA) approximately 1 m from the frog for 15 min. Audio waveforms were sampled at 48 kHz with 16-bits per sample. To minimize disturbance, we used red lamps while positioning equipment and moved >10 m away from the frog while recording.

After each recording was complete, we measured the frog's body temperature using a non-contact infrared thermometer (OS425-LS, Omega Engineering Ltd, Irlam, Manchester, UK; factory calibrated and accurate to $\pm 1.0^{\circ}\text{C}$; emissivity 0.95; Rowley and Alford 2007). We then captured the frog and measured its body (snout-urostyle) length (to 1 mm) and body mass (to 0.01 g). To determine infection status (infected or uninfected) and intensity (zoospore genome equivalents), we swabbed the ventral surface and limbs twice with a sterile rayon swab, which was then processed using diagnostic real-time quantitative PCR (details below). To avoid re-sampling the same individuals, we sampled a different section of stream each night. Individuals of this species have high site fidelity and are clustered in sections of the stream with riffles (Roznik and Alford 2015), making it highly unlikely that any individual was sampled more than once.

Fieldwork was carried out under Queensland Department of Environment and

Heritage Protection permit WITK14585514 and James Cook University Animal Ethics permit A2023.

DNA extraction and PCR

DNA was extracted from swabs using a modified Chelex[®] extraction protocol (Walsh et al. 1991). Individual swabs were placed into separate 1.5 ml microcentrifuge tubes containing 3 μ L of proteinase K and 200 μ L of 5% Chelex[®] solution. Samples were incubated at 55 °C for 60 min and then at 95 °C for 15 min with periodic vortexing. Extractions were stored at -20 °C until required. Prior to PCR amplification, extractions were centrifuged at 12,000 g for 2 min and 2 μ L of supernatant from just above the Chelex[®] resin was used for PCR amplification.

The real-time quantitative PCR protocol was modified from Boyle et al. (2004). Assays were conducted using a Roche LightCycler 480 system in a 384-well format. Ten μ L reactions containing 5 μ L of 2 \times Qiagen multiplex PCR Master Mix (Qiagen), PCR primers at a concentration of 900nM, the MGB probe at 250nM, and 2 μ L of DNA were prepared in triplicate. Included in each assay plate were control reactions containing DNA from 40, 4, 0.4 and 0.04 Bd zoospore genome equivalents and controls with no DNA template. Standards were provided by the Australian Animal Health Laboratory, CSIRO. Amplification conditions were 15 min at 95°C followed by 15 s at 95°C and 1 min at 60°C for 50 cycles. Amplification profiles of each PCR were used to determine the crossing point (Cp) value using the Absolute Quantification module of the LightCycler[®] 480 software package. A standard curve was constructed from the control reactions containing 40, 4, 0.4 and 0.04 Bd zoospore genome equivalents and this was used to determine the concentration of each sample, expressed as the number of zoospore genome equivalents (ZGE).

Call attributes and statistical analysis

We measured call attributes using Raven Pro 1.5 software. To avoid measuring call attributes at times when frogs may have been disturbed by investigators, we removed the first four minutes and the last one minute of each 15-minute recording. This produced a 10-minute call sample, in which we measured attributes of the first call in each minute of the 10 minutes. Call attributes included duration (length of the call from beginning of the first pulse to end of the last pulse), pulse rate (number of pulses per second during call), dominant frequency (frequency that occurs at the highest amplitude), call rate (total number of calls in the 10-minute call sample), and inter-call interval (length of time from end of the last pulse to

beginning of the first pulse in the subsequent call). These attributes are routinely used in studies of communication and female mate choice in anurans (Blair 1964; Cocroft and Ryan 1995; Hoskin et al. 2005). We generated spectrograms with the Hamming window, 1024-point discrete Fourier transformation, and 50% overlap.

Five of the sampled frogs each had one or two inter-call intervals that exceeded 10 s. We interpreted these values as outliers caused by momentary disturbances and excluded them from analyses. Prior to analyses, we \log_{10} -transformed inter-call interval values and infection intensity values. To obtain call attribute data for each frog for use in statistical analysis, we calculated the mean of the 8–10 measurements for each call attribute for each frog. We then modeled the effects of body temperature and body (snout-urostyle) length on each call attribute and extracted residuals from the best supported model for each attribute ($\Delta\text{AICc} < 2$). All subsequent analyses incorporated the extracted residuals, which we used as adjusted call attributes to investigate effects of infection, size-independent body condition, and infection intensity. Size-independent body condition was estimated as the residuals from a linear regression of \log_{10} -transformed body mass on square-root-transformed body length (Peig and Green 2009).

We performed a principal component analysis (PCA) to visualize the relationships among the corrected call attributes and to suggest any differences in call attributes that might exist between infected and uninfected frogs. We tested for the effects of infection status and size-independent body condition on our adjusted call attributes using multivariate analysis of covariance (MANCOVA), with infection status as a classification variable and the estimate of each frog's body condition as the covariate. To determine whether infection intensity might affect call attributes, we performed a separate canonical correlation analysis using data for infected frogs only, with adjusted call attributes as the dependent variables and \log_{10} -transformed infection intensity and body condition as independent variables. We used R software for all statistical analyses (version 3.0.3; R Core Team 2015).

A.4 Results

Thirty-six of the 61 frogs that we recorded (59%) were infected by Bd (mean infection intensity \pm SD = 22.99 ± 74.49 zoospore equivalents; maximum infection intensity = 426.7 zoospore equivalents). Overall, mating calls consisted of a series of pulses lasting 0.56 to 1.20 s (mean \pm SD = 0.87 ± 0.14 s) that were emitted at a rate of 45–76 pulses per s (mean \pm SD = 57.82 ± 7.75 pulses per s) and a dominant frequency of 2.33–3.08 kHz (mean \pm SD = 2.64 ± 0.17 kHz; Table A.1).

Model selection indicated that both body temperature and body length influenced call attributes (Table A.2, Fig. A.1) and that call duration, pulse rate, call rate, and inter-call interval were largely mediated by temperature (Fig. A.1a–d). Call duration decreased and pulse rate increased with increasing body temperature (Fig. A.1a, b). Similarly, call rate increased and inter-call interval decreased with increasing body temperature (Fig. A.1c, d). Dominant frequency was inversely correlated with body length (Fig. A.1e).

Table A.1 Call attributes, body temperatures, body sizes, and body condition indexes of common mistfrogs, *Litoria rheocola*, with and without infections by the fungus *Batrachochytrium dendrobatidis*.

	Infected n = 36			Uninfected n = 25			Overall n = 61
	Minimum	Mean \pm SD	Maximum	Minimum	Mean \pm SD	Maximum	Mean \pm SD
Duration (s)	0.56	0.85 \pm 0.14	1.20	0.58	0.89 \pm 0.14	1.20	0.87 \pm 0.14
Pulse rate (pulses/s)	44.98	57.56 \pm 7.82	76.28	46.80	58.20 \pm 7.79	73.52	57.82 \pm 7.75
Dominant frequency (kHz)	2.34	2.65 \pm 0.18	3.08	2.33	2.61 \pm 0.16	2.99	2.64 \pm 0.17
Call rate (calls/10 m)	93	257.6 \pm 67.3	423	65	238 \pm 74.4	350	249.5 \pm 70.3
Inter-call interval (s)	0.89	1.57 \pm 0.62	4.09	0.99	1.67 \pm 0.79	4.08	1.61 \pm 0.69
Body temperature ($^{\circ}$ C)	11.40	15.10 \pm 1.80	18.90	11.10	15.40 \pm 1.90	18.50	15.01 \pm 1.83
Body (snout-urostyle) length (mm)	28	30.17 \pm 1.16	33	29	30.32 \pm 0.96	33	30.23 \pm 1.07
Mass (g)	1.63	1.98 \pm 0.19	2.38	1.78	2.03 \pm 0.13	2.25	2.00 \pm 0.17
Body condition index	-0.39	-0.01 \pm 0.19	0.46	-0.24	0.01 \pm 0.15	0.41	0.00 \pm 0.17

Table A.2 Candidate models of the effects of frog body temperature and body (snout-urostyle) length on the advertisement call attributes of common mistfrogs, *Litoria rheocola*.

Response	Predictors	AICc	Δ AICc	Weight	Adjusted R ²
Duration	Temperature	-67.3	0.00	0.710	0.000
	Temperature, Length	-65.2	2.12	0.245	0.000
	Intercept only	-60.9	6.43	0.028	0.000
	Length	-59.8	7.51	0.017	0.000
Pulse rate	Temperature	409.0	0.00	0.636	0.273
	Temperature, Length	410.1	1.12	0.363	0.286
	Intercept only	426.2	17.17	0.000	0.000
	Length	428.4	19.37	0.000	0.000
Dominant frequency	Length	800.8	0.00	0.567	0.092
	Temperature, Length	802.3	1.54	0.263	0.103
	Intercept only	804.4	3.67	0.091	0.000
	Temperature	804.7	3.95	0.079	0.031
Call rate	Temperature	681.0	0.00	0.730	0.236
	Temperature, Length	683.0	1.99	0.269	0.240
	Intercept only	695.2	14.22	0.001	0.000
	Length	697.2	16.22	0.000	0.003
Inter-call interval	Temperature	20.3	0.00	0.756	0.543
	Temperature, Length	22.6	2.29	0.240	0.543
	Intercept only	31.4	11.04	0.003	0.000
	Length	32.9	12.56	0.001	0.031

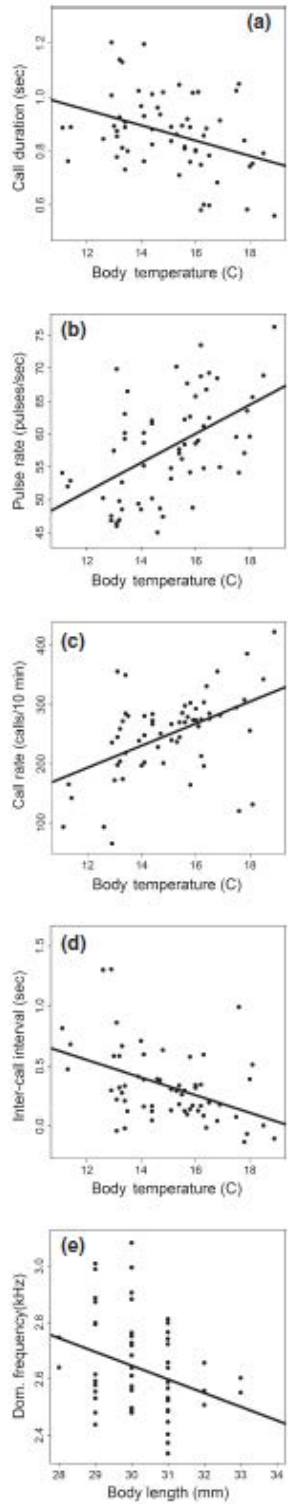


Figure A.1 Relationships between frog body temperature or frog body (snout-urostyle) length and advertisement call attributes for the common mist frog, *Litoria rheocola*. Intercall interval values were \log_{10} -transformed.

After we adjusted the calling parameters for significant effects of temperature and body length, our principal component analysis of the adjusted call attributes indicated that the first two principal components together accounted for 71% of the variability in the data (Table A.3). The analysis revealed that the temporal attributes of calls – call duration, pulse rate, call rate, and inter-call interval – were still correlated (Table A.3, Fig. A.2). The inverse correlations between call duration and pulse rate and the complex relationships between call rate, call duration, and inter-call interval make it appear that frogs alter their calls by adjusting the proportion of energetic input that lies along dimensions roughly corresponding to rate (faster pulse and/or faster emission of entire calls) and duration (length of each call, length of time between calls; Fig. A.2). In particular, it appears that higher pulse rates are balanced against shorter calls, and that longer calls are produced by decreasing the pulse rate, maintaining a relatively constant number of pulses (Fig. A.2). Higher call rate is produced by decreasing inter-call interval. Even with the effect of body length removed, dominant frequency varies relatively independently of the other call characteristics (Fig. A.2).

We found no significant difference in adjusted call characteristics between infected and uninfected animals; in the PCA, both the distributions of individual points and the locations of group centroids were quite similar (Fig. A.2). This was confirmed by the results of the MANCOVA and the canonical correlation analysis (Table A.4). After accounting for the effects of body temperature and body length on the attributes of frog calls, we found no significant or substantial effect of infection status, infection intensity, or body condition (Table A.4, Fig. A.2).

Table A.3 Summary of the importance of components and axis loadings in a principal component analysis of adjusted advertisement call attributes of common mistfrogs, *Litoria rheocola*. We adjusted the data by removing the effects of frog body temperature and body (snout-urostyle) length from the data for each frog.

	PC1	PC2	PC3	PC4	PC5
Standard deviation	1.522	1.121	0.969	0.620	0.325
Proportion of variance	0.463	0.251	0.188	0.077	0.021
Cumulative proportion	0.463	0.714	0.902	0.979	1.000
Loading values					
Duration	-0.370	0.625	0.161	0.659	0.111
Inter-call interval	-0.565	-0.362	-0.208	-0.042	0.710
Pulse rate	0.466	-0.449	-0.217	0.721	0.122
Dominant frequency	-0.106	-0.397	0.906	0.098	-0.016
Call rate	0.561	0.345	0.249	-0.189	0.684

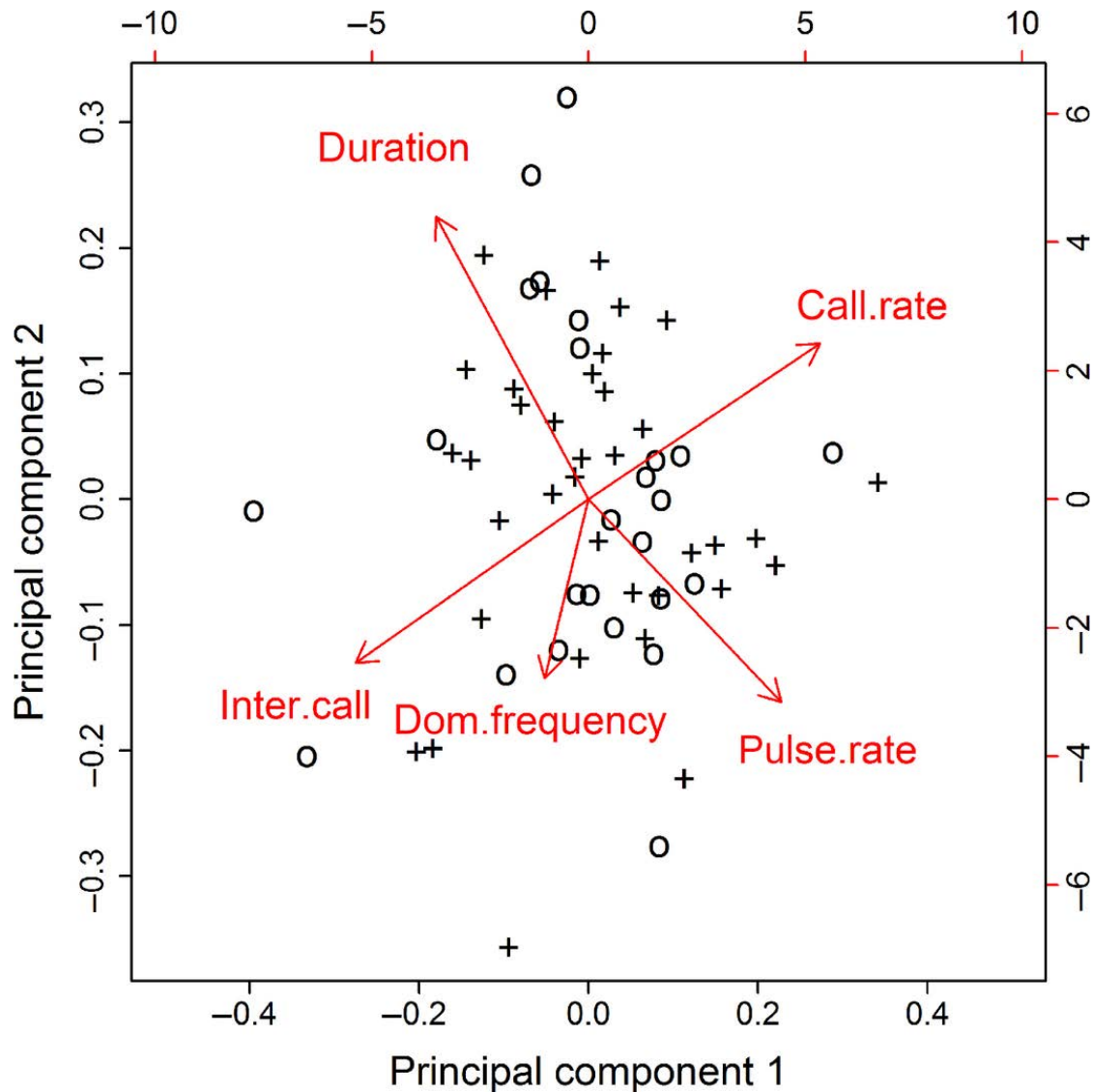


Figure A.2 Biplot showing the relationships between adjusted advertisement call attributes of common mistfrogs, *Litoria rheocola*, and illustrating the location of each individual data point in principal component space. We adjusted the data by removing the effects of frog body temperature and body (snout-urostyle) length from the data for each frog. Principal components 1 and 2 accounted for 70% of the variability in call attribute data (Table 3). The length and direction of each arrow correspond to the loading of each adjusted call attribute on the first two principal axes (Table 4). Symbols indicate frog infection status (infected [+]) or uninfected [o]). Interspersion of the symbols suggests that infected and uninfected frogs do not differ in call attributes commonly linked to mate choice.

Table A.4 Summary of multivariate analysis of covariance and canonical correlation analysis of the effects of *Batrachochytrium dendrobatidis* infections on adjusted advertisement call attributes of common mistfrogs, *Litoria rheocola*. We adjusted the data by removing the effects of frog body temperature and body (snout-urostyle) length from the data for each frog. The adjusted call attributes included in each analysis as dependent variables were call duration, pulse rate, dominant frequency, call rate, and inter-call interval.

Main effect	Predictors	Wilk's λ	df	F	P
Infection status	Infection status	0.907	5,53	1.092	0.376
	Body condition	0.994	5,53	0.068	0.997
	Infection status \times body condition	0.952	5,53	0.531	0.752
Infection intensity	Infection intensity	0.814	5,28	1.278	0.301
	Body condition	0.945	5,28	0.327	0.892
	Infection intensity \times body condition	0.763	5,28	1.744	0.157

A.5 Discussion

Body temperature explained much of the observed variation in call duration, pulse rate, call rate, and inter-call interval, independent of frog infection status. We observed a general trend of increasing pulse rate and decreasing call duration with increasing frog body temperatures (Fig. A.1a, b). Similarly, we observed an increase in call rate and a decrease in inter-call interval with increasing frog body temperatures (Fig. A.1c, d). Physiological rates, including those associated with vocalizations (Zweifel 1968; Gayou 1984; Narins et al. 2007), are positively correlated with temperature in anurans because they are ectotherms (Feder and Burggren 1992). It follows that call duration is typically negatively correlated with temperature (Zweifel 1968; Gayou 1984; Narins et al. 2006) because a call will be shorter if a given number of pulses are closer together in time (Gayou 1984). In the same way, the interval between calls will be shorter if there are more calls in a given length of time. The inverse relationship between the dominant frequency of calls and frog body length (Fig. A.1e) was expected given that body size is the primary determinant of dominant frequency (Zweifel 1968; Martin 1971; Davies and Halliday 1978; Robertson 1986).

After accounting for the effects of temperature and body length on call characteristics, we found no significant influence of Bd infection status or intensity on the call duration, pulse rate, dominant frequency, call rate, or inter-call interval of the rainforest frog *Litoria rheocola*. These results are similar to findings that dominant frequency and call duration were not related to helminth parasite load in the treefrogs *Hyla versicolor* (Hausfater et al. 1990) and *Hypsiboas prasinus* (Madaire et al. 2013), but differ from recent findings in Bd-infected *Hyla japonica*, which called more rapidly and had longer calls than uninfected frogs (An and Waldman 2016), suggesting that behavioural responses of frogs to infection by Bd differ among species. Overall, our results suggest that for *L. rheocola*: 1) lightly infected males produce calls with sounds that should be, on average, as attractive to females as the calls of uninfected males (see duration, pulse rate and dominant frequency in Table A.1); and 2) on the nights that they call, lightly infected males produce, on average, equal numbers of calls compared to uninfected males (see call rate and inter-call interval in Table A.1).

Because none of the standard aspects of call quality differed between infected and uninfected males, the changes that Bd infection produces in the nightly probability of calling of *L. rheocola* (i.e., more likely to call on a given night when in good condition and less likely to call on a given night when in poor condition; Roznik et al. 2015b) should lead to changes in mating opportunities. Our results, together with those reported by Roznik et al. (Roznik et al. 2015b), thus suggest that infected males in

poor body condition are likely to mate less often than uninfected males, while infected males in good body condition should mate more often than uninfected males. Whether this pattern leads to changes in the success of matings, and ultimately in offspring production, may depend on how Bd infection affects other aspects of male and female reproductive behavior and physiology (e.g., effects of infection on gametogenesis)(Brannelly et al. 2015).

How infection alters male calling effort clearly differs among species and may depend on species or environmental context, such as susceptibility to Bd and the duration of the breeding season. An and Waldman (2016) recently documented increases in three of ten call quality parameters tested in nine male *H. japonica* lightly infected (15–43 zoospore equivalents) with Bd (compared to 33 uninfected individuals). *H. japonica* is not known to suffer morbidity and mortality from this pathogen, unlike our species *L. rheocola*, which is susceptible to Bd and has undergone population declines, but is currently persisting with endemic infections. The costs of fighting infection may therefore be greater for *L. rheocola* than for *H. japonica*, leaving less energy available to *L. rheocola* for increasing call quality. In addition, *H. japonica* breeds during a distinct summer period, which gives males a smaller temporal window to successfully call and attract mates. By contrast, our tropical species breeds throughout the year, which provides males with a much longer temporal window during which they must balance call quality with reproductive endurance (Roznik et al. 2015b), and in which calling on more nights is likely to lead to increased opportunities for mating.

Increases in recruitment, which could reflect either increased survival to adulthood or increased reproduction, have been proposed as a population-regulating process in Bd-infected populations of *L. rheocola* (Phillott et al. 2013; Sapsford et al. 2015), *L. verreauxii alpina* (Scheele et al. 2015b), and *Anaxyrus boreas* (Muths et al. 2011) with low adult survival. Our results, combined with those of Roznik et al. (Roznik et al. 2015b) demonstrate that infected male *L. rheocola* in good body condition call on more nights, emitting calls that should be as attractive to females as those of uninfected males. Whether this results in compensatory increases in recruitment is uncertain; it would only do so if male reproductive effort is limiting. If male reproductive effort is not limiting, however, there may be no effect, or a negative effect caused by increased transmission of Bd infections to females during amplexus (Rachowicz and Vredenburg 2004).

Although models of parasite-mediated sexual selection suggest that females should discriminate against infected males based on changes in their courtship signals or behaviour, this may not be possible for female *L. rheocola*, since infected male *L. rheocola* did not alter any of the measured aspects of the quality of their advertisement calls. Based only on the characteristics of mating calls, we would expect

that the reproductive success of resistant males that remain uninfected and susceptible males that are infected should be similar, thus reducing the effects of natural selection for resistance to infection in this system. In this species, however, the probability of calling on any given night depends on both infection status and body condition (Roznik et al. 2015b). Infected males in relatively good body condition are more likely to call each night than are uninfected males, while both these classes of individuals are more likely to call each night than are infected males in poor condition (Roznik et al. 2015b). It is thus likely that infected males in good body condition have greater success in attracting mates than do uninfected males because they call on more nights. Any genes that favor increased tolerance of infection (i.e., ability to limit the harm caused by infection, such as reductions in body condition) may thus be favored by natural selection in this system. The presence of a behavioral strategy for maximizing individual male reproductive success in the face of infection may thus have altered the course of natural selection following the emergence of chytridiomycosis in *L. rheocola*. Similar effects may make the evolutionary responses of other species to the emergence of novel diseases difficult to predict.